การเคลือบผิวอนุภาคขนาดละเอียดด้วยโพลิเมอร์โดยอาศัยเทคโนโลยีคาร์บอนไดออกไซด์เหนือวิกฤตร่วมกับตัวทำละลายเอทานอล

นายเบญจพล คงสมบัติ

วิทยานิพนธ์นี้เป็นส่วนหนึ่งของการศึกษาตามหลักสูตรปริญญาวิศวกรรมศาสตรดุษฎีบัณฑิต
สาขาวิชาวิศวกรรมเคมี ภาควิชาวิศวกรรมเคมี
คณะวิศวกรรมศาสตร์ จุฬาลงกรณ์มหาวิทยาลัย
ปีการศึกษา 2552

POLYMER COATING OF FINE PARTICLES USING SUPERCRITICAL CARBON DIOXIDE TECHNOLOGY WITH ETHANOL COSOLVENT

Mr. Benjapol Kongsombut

A Dissertation Submitted in Partial Fulfillment of the Requirements
for the Degree of Doctor of Engineering Program in Chemical Engineering
Department of Chemical Engineering
Faculty of Engineering
Chulalongkorn University
Academic year 2009

Thesis Title	POLYMER COATING OF FINE PARTICLES USING SUPERCRITICAL CARBON DIOXIDE TECHNOLOGY WITH ETHANOL COSOLVENT
By	Mr. Benjapol Kongsombut
Field of Study	Chemical Engineering
Thesis Advisor	Associate Professor Tawatchai Charinpanitkul, D.Eng.
Thesis Co-Advisor	Professor Atsushi Tsutsumi, D.Eng.

Accepted by the Faculty of Engineering, Chulalongkorn University in Partial Fulfillment of the Requirements for the Doctoral Degree

..... Dean of the Faculty of Engineering
(Associate Professor Boonsom Lerdhirunwong, Dr.Ing.)

THESIS COMMITTEE

..... Chairman
(Professor Wiwut Tanthapanichakoon, Ph.D.)

..... Thesis Advisor
(Associate Professor Tawatchai Charinpanitkul, D.Eng.)

..... Thesis Co-Advisor
(Professor Atsushi Tsutsumi, D.Eng.)

..... Examiner
(Associate Professor Prasert Pavasant, Ph.D.)

..... Examiner
(Assistant Professor Sorada Kanokpanont, Ph.D.)

..... Examiner
(Assistant Professor Nattaporn Tonanont, D.Eng.)

..... External Member
(Associate Professor Poj Kulvanich, Ph.D.)

เบญจพล คงสมบัติ : การเคลือบผิว อนุภาคขนาดละเอียด ด้วยโพลิเมอร์ โดยอาศัยเทคโนโลยีคาร์บอนไดออกไซด์เหนือวิกฤตร่วมกับตัวทำละลายเอทานอล (POLYMER COATING OF FINE PARTICLES USING SUPER-CRITICAL CARBON DIOXIDE TECHNOLOGY WITH ETHANOL COSOLVENT) อ. ที่ปรึกษาวิทยานิพนธ์หลัก : รศ.ดร.ธวัชชัย ชรินพาณิชกุล, อ. ที่ปรึกษาวิทยานิพนธ์ร่วม : ศ.ดร.อะซึชิ ซึซึมิ, 169 หน้า.

การเคลือบผิวอนุภาคยาด้วยโพลิเมอร์ เป็นเทคนิคที่ใช้เพื่อควบคุมการปลดปล่อยยาจากอนุภาคซึ่งช่วยให้การรักษามีประสิทธิภาพยิ่งขึ้น เนื่องจากความเข้มข้นของยาอยู่ในระดับคงที่และต่อเนื่องตลอดเวลา ในงานวิจัยนี้ ได้ทำการศึกษาวิธีการเคลือบผิวอนุภาคระดับไมโครเมตรและนาโนเมตรด้วยโพลิเมอร์ชนิดย่อยสลายได้ทางชีวภาพคือ โพลีแลคติกโคไกลคอลิกแอซิด หรือ พีแอลจีเอ เพื่อผลิตเป็นระบบนำส่งยาแบบนำวิถีชนิดควบคุมการปลดปล่อย อาทิ ไมโครแคปซูล และนาโนสเฟียร์ ในกระบวนการนี้ได้ประยุกต์ใช้คาร์บอนไดออกไซด์เหนือวิกฤตร่วมกับเอทานอล ทำหน้าที่ เป็นตัวทำละลายสำหรับพีแอลจีเอ แทนการใช้ตัวทำละลายอินทรีย์ชนิดของเหลว ดังนั้น กระบวนการนี้จึงไม่ทำให้เกิดของเสียที่เป็นพิษต่อสิ่งแวดล้อม อีกทั้งยังช่วยป้องกันการเสื่อมสภาพของยา อันเนื่องมาจากการสัมผัสโดยตรงกับความร้อน และตัวทำละลายอินทรีย์ที่มีฤทธิ์รุนแรง

การเคลือบผิวด้วยวิธีนี้นั้นอาศัย เทคนิคการขยายตัวอย่างรวดเร็วของสารละลายและสารแขวนลอยเหนือวิกฤตในการผลิตอนุภาคพีแอลจีเอเพื่อใช้เคลือบลงบนอนุภาคจำลองยาคือ อนุภาคซิลิกาและอนุภาคไททาเนียมไดออกไซด์ ที่มีขนาดอนุภาคเฉลี่ย 1.4 ไมครอนและ 70 นาโนเมตรตามลำดับ โดยเตรียมสารแขวนลอยอนุภาคจำลองยาดังกล่าวในสารละลายของพีแอลจีเอซึ่งละลายอยู่ในตัวทำละลายผสมเหนือวิกฤตของคาร์บอนไดออกไซด์และเอทานอลที่ความดัน 250 บรรยากาศและอุณหภูมิ 40 องศาเซลเซียส และความเข้มข้นของเอทานอลระหว่าง 0 - 23.8 เปอร์เซ็นต์โดยน้ำหนัก จากนั้นปล่อยให้สารละลายและสารแขวนลอยเหนือวิกฤตที่เตรียมได้ขยายตัวสู่สภาวะบรรยากาศ ผ่านทางหัวฉีดที่มีขนาดเส้นผ่านศูนย์กลางระหว่าง 0.1 และ 0.3 มิลลิเมตร จากการวิเคราะห์ด้วยเทคนิคไมโครสโคปพบว่า ขนาดของอนุภาคพีแอลจีเอที่ผลิตได้มีขนาดเฉลี่ยอยู่ระหว่าง 55 – 330 นาโนเมตร โดยอนุภาคมีขนาดขึ้นอยู่กับความเข้มข้นของเอทานอลที่ใช้ ความเข้มข้นของพีแอลจีเอในสารละลายเหนือวิกฤตแปรผันตามความเข้มข้นของเอทานอล โดยมีค่าประมาณ 0.15 เปอร์เซ็นต์โดยน้ำหนักเมื่อใช้เอทานอลที่ความเข้มข้นสูงสุด จากผลการทดลองพบว่า อนุภาคซิลิกาและไททาเนียมไดออกไซด์ซึ่งผ่านกระบวนการนี้ ถูกเคลือบผิวด้วยชั้นของพีแอลจีเอที่มีความหนาของชั้นเคลือบโดยประมาณ 10 – 100 นาโนเมตร ซึ่งเกิดขึ้นทั้งในลักษณะที่เป็นอนุภาคเดี่ยวและอนุภาคซึ่งเกาะกันเป็นกลุ่มก้อน

ภาควิชา .....วิศวกรรมเคมี.....ลายมือชื่อนิสิต .....

สาขาวิชา .... วิศวกรรมเคมี..... ลายมือชื่อ อ.ที่ปรึกษาวิทยานิพนธ์หลัก.....

ปีการศึกษา ...2552 .....ลายมือชื่อ อ.ที่ปรึกษาวิทยานิพนธ์ร่วม.....

4571812521 : MAJOR CHEMICAL ENGINEERING
KEYWORDS : PARTICLE COATING / PLGA / SUPERCRITICAL CARBON DIOXIDE

BENJAPOL KONGSOMBUT : POLYMER COATING OF FINE PARTICLES USING SUPERCRITICAL CARBON DIOXIDE TECHNOLOGY WITH ETHANOL COSOLVENT. THESIS ADVISOR : ASSOC. PROF. TAWATCHAI CHARINPANITKUL, D.Eng., THESIS CO-ADVISOR : PROF. ATSUSHI TSUTSUMI, D.Eng., 169 pp.

For the improvement of therapeutic effectiveness, coating of drug particles with polymer has been used widely in pharmacy and medicine for controlled-release applications. The polymer coating could help improve the circulation of drug and maintain the concentration of therapeutic agents in the blood vessels. In this research, coating of microsize and nanosize powders with a polymer has been investigated for the production of controlled-release particulate drug delivery systems, such as microcapsules and nanospheres. Poly($_{D,L}$-lactide-co-glycolide) or PLGA, as polymer and 1.4-micron silica (SiO_2) and 70-nm titanium dioxide (TiO_2) powders as core particles were employed as the coating model for the investigation. As a benign alternative to toxic organic liquid solvents, a supercritical fluid (SCF) mixture of carbon dioxide (CO_2) mixed with ethanol cosolvent, was used to dissolve PLGA in the preparation of coating solution. With the use of SCF solvent, disposals of environmentally hazardous wastes from the process and denaturation of therapeutic agents in the product could be avoided.

Rapid expansion of supercritical solution (RESS) process was utilized to produce polymer particles, which can be used for coating, as well as to generate polymer-coated microsize or nanosize particles. PLGA was dissolved in supercritical carbon dioxide (SC-CO_2) to form a supercritical solution at 25 MPa and 313 K. Ethanol, up to 23.8 wt.%, was added to SC-CO_2 to enhance the PLGA solubility. The charged amount of PLGA in SC-CO_2 with 23.8 wt.% ethanol was approximately 0.15 wt.% of the supercritical solution. The RESS process was performed by spraying supercritical solution through a capillary nozzle to ambient air, leading to precipitation of well-dispersed PLGA particles. The average particle size of the precipitated PLGA particles ranges from 55 to 330 nm, depending on the ethanol concentration. For particle coating, SiO_2 and TiO_2 core powders were suspended in the supercritical solution before performing the expansion. The precipitation of PLGA particles accompanying with deposition of the precipitated particles on the core particle surface, solvent evaporation and disintegration of agglomeration of the core particles resulted in formation of coated particles in the form of both individual particles and agglomerates. The thickness of the coating layer was non-uniform but could be estimated to be around 10 to 100 nm.

Department : .....Chemical Engineering.... Student's Signature .....

Field of Study : ....Chemical Engineering.... Advisor's Signature .....

Academic Year : ...2009..... Co-Advisor's Signature .....

ACKNOWLEDGEMENTS

First and foremost, I would like to express my deep sense of gratitude to *Assoc. Prof. Tawatchai Charinpanitkul* for his belief in my capabilities and his relentless encouragement. I have gone through different learning phases, scientific as well as personal, as a researcher under his guidance. I am also grateful for his kind concern and help beyond my study. I appreciate his enthusiasm, which helped me to expedite the Ph.D. work and complete it on time.

I am also very grateful to *Prof. Atsushi Tsutsumi* for being my supervisor for the one-year period of study in Japan. The freedom given by him was a vital tool for me to shape myself as an independent researcher.

Also, I would like to acknowledge *Prof. Wiwut Tanthapanichakoon* for his fruitful discussions and suggestions on the modeling work. I learned a lot from both his academic excellence and character nobleness.

I gratefully thank *Prof. Wiwut Tanthapanichakoon*, *Assoc. Prof. Tawatchai Charinpanitkul, Assoc. Prof. Prasert Pavasant, Assoc. Prof. Poj Kulvanich, Assist. Prof. Sorada Kanokpanont* and *Assist. Prof. Nattaporn Tonanont* for their useful comments and for taking time out of their tight schedules to serve on my thesis committee.

I would like to acknowledge valuable suggestions from *Dr. Wei Chen* and *Dr. Masahiro Ikeda* at Tsutsumi laboratory that provided a platform to build up this research. I also wish to acknowledge *Mr. H. Tsunakawa* of the High Voltage Electron Microscope Laboratory for his technical guidance and assistance on SEM and TEM analysis, which is an inseparable part of this thesis.

Working in Japan with a different language and culture was not easy. Though the acquaintance time was a little long, I could somehow manage to cope up with it. I am very thankful to *Miss Yukie Tanaka* and *Dr. Haiyan Lin* for their kind help on putting me up in the first weeks to get me started working at Tsutsumi laboratory. I would also like to thank *Dr. Waraporn Soksawatmaekhin* and all the members of *Thai Students' Association in Chiba* for their hospitality, and wonderful experience during the working period in Japan.

Apart from the scientific knowledge, the financial support also played an important role in this Ph.D. work. This research would have not been possible without the financial support of the *Thailand Research Fund (TRF)* through the Royal Golden Jubilee (RGJ) Ph.D. program. I am very grateful to the *Association of International Education, Japan (AIEJ)* for partial financial support to do research at Tsutsumi Laboratory, the University of Tokyo, for one year (October 2003-September 2004). Also, partial financial support from the *University-Industry collaborative project of Chulalongkorn University*, the *Centenial Fund of Chulalongkorn University* to Center of Excellence in Particle Technology (CEPT) and the *New Energy and Industrial Technology Development Organization (NEDO)* is acknowledged.

In the small world of CEPT, I enjoyed working with all members. My most sincere thanks are due to *Ms. Pusanisa Patharachotesawate* for her timely help on official works, and to all members for their warm collaborations and kindness.

Finally, I want to express my deep thanks to my family members, *Ms. Jarurat Chuleerux* and all of my friends for their love, encouragement and constant support in climbing another step in my life in the right direction.

CONTENTS

CHAPTER Page

CHAPTER Page

CHAPTER Page

LIST OF TABLES

Page

Page

LIST OF FIGURES

Page

Page

Page

ABBREVIATIONS

C_1-C_5	Constants
CFC	Chlorofluorocarbon
CO_2	Carbon dioxide
$\overline{d}_p$	Average diameter
EOS	Equation of state
f	Fugacity
g	Radial distribution function
ΔG_{mix}	Gibbs free energy
GAS	Gas anti-solvent
GRAS	Generally regarded as safe
ΔH_{mix}	Change of enthalpy on mixing
k	Binary interaction parameter
k_B	Boltzman constant
L/D	Length-to-diameter ratio
Li	Mixing length
m	Mass
M_w	Molecular weight
n	Number of mole
P_c	Critical pressure
PGA	Poly(glycolic acid)
PGSS	Particles from gas saturated solution
PLA	Poly(lactic acid)
PLGA	Poly($_{D,L}$-lactic-co-glycolic acid)
PR	Peng-Robinson
PT	Patel-Teja
Q	Quadrupole moment
r	Size parameter
R	Gas constant
RESS	Rapid expansion of supercritical solution
RESS-N	Rapid expansion of supercritical solution with a non-solvent
S	Supersaturation ratio
ΔS_{mix}	Change of entropy on mixing
SAS	Supercritical anti-Solvent
SC-CO_2	Supercritical carbon dioxide
SCF	Supercritical fluid
SEDS	Solution enhanced dispersion by supercritical fluid

SEM	Scanning electron microscopy
SiO_2	Silica
SRK	Soave-Redlich-Kwong
T	Temperature (absolute)
T_c	Critical temperature (absolute)
TEM	Transmission electron microscopy
TiO_2	Titanium dioxide or titania
ΔU_{mix}	Change of internal energy on mixing
V	Volume of mixture
VOC	Volatile organic compound
w	Mass fraction (binary system)
W	Mass fraction (ternary system)
wt.	Weight
x, y	Mole fraction
z	Number of different pairs between components
α	Polarizability
φ	fugacity coefficient
ϕ	Close packed volume fraction
ρ	Density
ρ_c	Critical density
μ	Dipole moment
π^*	Dipolarity/polarizability; solvent-strength parameter
Γ	Intermolecular pair-potential energy
γ	Intermolecular radius
v	Molar volume
ω	Interchange energy
χ	Interaction parameter

Subscripts

c	Critical
eq	Equilibrium or saturated condition
g	Glass transition
i,j	Component
$\sqcup$	Reduced
*	Characteristic

CHAPTER I

SUPERCRITICAL CARBON DIOXIDE AS A PROCESS SOLVENT FOR PHARMACEUTICAL POLYMERS

1.1 Introduction

Polymers are used extensively in pharmaceutical applications, both in medical devices and in drug delivery systems. In the field of drug delivery, polymers represent an important constituent of pharmaceutical dosage forms, e.g. solid dosage forms, disperse systems and biodegradable particulate systems. Pharmaceutical applications of polymers range diversely from being filler materials and binders in drug tablets to agents for controlling viscosity and flowability in liquid drugs. In addition, polymers can be used for coating drugs to mask the unpleasant taste of drug, to increase drug stability, to provide prevention of side effect of drug and to modify drug release characteristics (Jones, 2004).

Various synthetic and natural polymers are extensively used in pharmaceutical applications. Processing of pharmaceutical polymers is not an easy task as most of them are highly viscous and have a high molecular weight. To dissolve and reduce the viscosity of these polymers, conventional methods frequently require the use of volatile organic compounds (VOCs) and chlorofluorocarbons (CFCs) as process solvents. Nevertheless, VOCs and CFCs are generally known to be toxic to humans and environmentally hazardous. Using VOCs and CFCs in pharmaceutical processes may be subjected to some drawbacks, e.g. alteration of structure of therapeutic agent, presence of residual solvent in the product, and emissions of a large amount of the

solvents from large-scale manufacturing into the environment. All these drawbacks have already motivated chemical engineers and chemists in pharmaceutical industries to look for new and cleaner solvents.

One of promising alternatives is the use of supercritical fluids (SCFs). A SCF is defined as a substance under supercritical conditions, that is, above its critical pressure and temperature. **Figure 1.1** illustrates a pressure-temperature diagram of a substance indicating the supercritical region. The critical pressure (P_c) is the pressure which causes the gas to become a liquid at the critical temperature. Above the critical temperature (T_c), a liquid phase will not appear no matter how much the pressure is increased. The density of a substance at the critical point (C) is called the critical density (ρ_c). The critical temperatures, pressures, and densities of some common solvents are listed in **Table 1.1**.

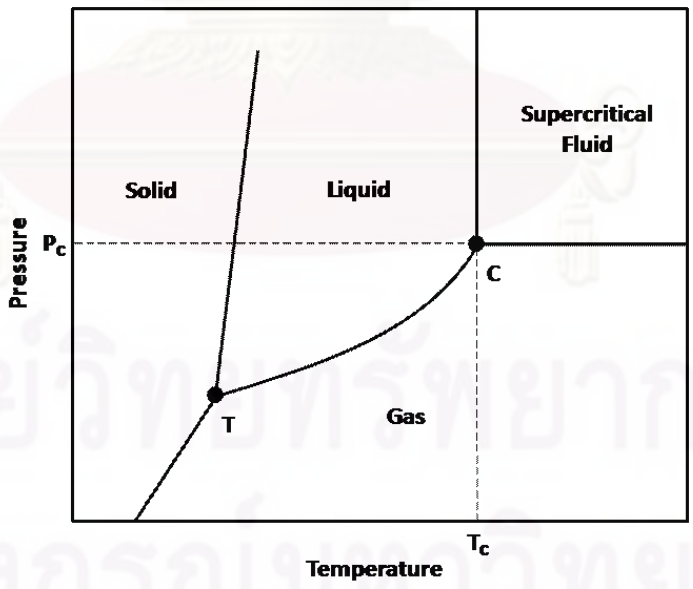

Figure 1.1 A phase diagram of a substance approaching the supercritical phase

Table 1.1 Critical properties of selected solvents (Mchugh and Krukonis, 1994)

Solvent	Critical Temperature (T_c; °C)	Critical Pressure (P_c; bar)	Critical Density (ρ_c; g/ml)
Ammonia	132.5	113.5	0.24
Benzene	129.0	48.9	0.30
n-Butane	152.0	38.0	0.23
Carbon dioxide	31.1	73.8	0.45
Chlorotrifluoromethane	28.9	39.5	0.58
Ethane	32.2	48.9	0.20
Ethanol	243.4	63.8	0.28
Ethylene	9.3	50.4	0.22
Isopropanol	235.3	47.6	0.27
Methanol	240.5	79.9	0.27
n-Propane	96.8	42.6	0.22
Propylene	91.9	46.2	0.23
Toluene	318.6	41.1	0.29
Water	374.2	221.2	0.34

A SCF exists in a homogeneous fluid phase possessing properties between those of gases and liquids, e.g. liquid-like solvent properties and gas-like viscosity, thermal conductivity and diffusivity. It is commonly accepted that the solvent power of a SCF is mainly related to its density in the critical point region. A high density implies a strong solvent power. The important unique property of a SCF is that its solvent power can be tuned by regulating its pressure or temperature. As demonstrated in **Figure 1.2**, a small change in the pressure or temperature of a SCF generally causes a large change in its density and thus its solvent power. This feature is beneficial for

pharmaceutical solubilization, polymer plasticization, separation and extraction or organic solvents or impurities (Brunner, 2004). Even though the density of SCFs increases with pressure and becomes liquid-like, the viscosity and diffusivity remain between liquid-like and gas-like values. The gas-like properties of SCFs significantly enhance mass transfer that promotes selectivity for extractions and reactions. Additionally, SCFs have a very low surface tension, which allows efficient penetration into microporous materials. As a result, extraction of natural products can be expected to be more efficiently processed with SCFs than with conventional liquid solvents (Rantakyla, 2004). The combination of these unique properties makes SCFs excellent for use as solvents or reaction mediums. A comparison of properties of liquid, gas and SCF solvents is presented in **Table 1.2**

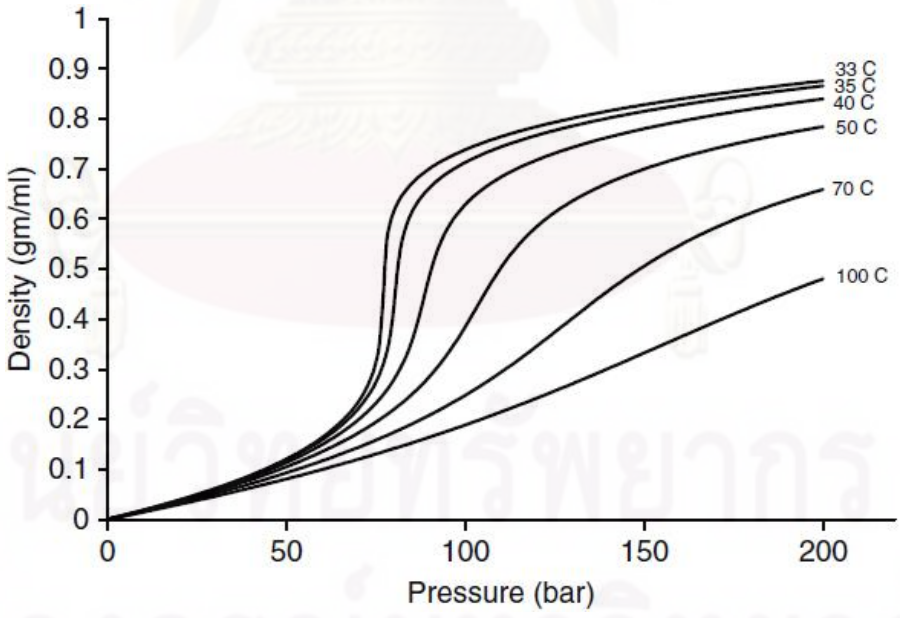

Figure 1.2 Variation of SCF density with pressure (the fluid is CO_2. Redrawn from Gupta and Shim (2007) and Brennecke and Eckert (1989))

Table 1.2 Selected properties of liquids, gases and supercritical fluids (Mchugh and Krukonis, 1994)

Properties	Liquid	Supercritical Fluid	Gas
Density (kg/m^3)	1,000	200 – 800	1
Viscosity (mPa.s)	0.5 – 1.0	0.05 – 0.1	0.01
Diffusivity (cm^2/s)	10^{-5}	$10^{-4} – 10^{-3}$	0.1

Various compounds can be used as SCF solvents. However, light hydrocarbons, water and carbon dioxide (CO_2) are among the most received attention compounds. Low molecular weight gases, such as CO_2 and ethane, and polar compounds such as trifluoromethane have received great attention for extraction purpose. Ethane is the choice of solvent for solid hydrocarbons, whereas chlorotrifluoromethane is a good solvent for all solids except non-polar hydrocarbons (Rantakyla, 2004). With the ability to act both as electron donor and acceptor, CO_2 is a good solvent for non-polar and some polar compounds with low molecular weight, but a poor solvent for polar and most high molecular weight compounds (Hyatt, 1984). Alternatively, rare gases such as krypton and xenon, although they are favorable for some purposes, are seldom used for economic reasons.

Despite the beneficial features described above, SCFs should not be considered as universal solvents. An overview of **Table 1.1** indicates that the critical temperature of a compound depends on the polarity of the compound. For examples, the critical temperatures of non-polar gases such as carbon dioxide or ethane are below 50°C, whereas for polar compounds such as methanol or water, the critical temperature is well above 200°C. For many fluids, the transition into supercritical state occurs at

high temperatures, which are generally not permissible for pharmaceuticals. It is usually desirable that the critical temperature of the solvent is below 100°C or as low as room temperature to prevent degradation or denaturation of therapeutic agents (Laitinen, 2000). In addition, the solvent must be non-toxic to allow safety use for human due to possible solvent contamination in the product. These requirements point towards CO_2 as a suitable solvent for supercritical processing of pharmaceuticals.

Table 1.3 Selected properties of carbon dioxide

Chemical formula	CO_2 (O=C=O)
Molecular weight	44.01
Normal boiling point	-78.5°C
Latent heat of vaporization	571.3 kJ/kg
Specific gravity (gas)	1.539 (1 for air)
Specific heat (gas)	0.85 kJ/kg · °C
Density (gas)	1.9769 kg/m^3
Triple point temperature	-56.6°C
Triple point pressure	5.17 bar
Critical temperature	31.1°C
Critical pressure	73.8 bar

1.2 Supercritical Carbon Dioxide

Carbon dioxide (CO_2) is a natural gas whose its chemical structure is composed of two oxygen atoms covalently bonded to a single carbon atom. It makes up less than 1% by volume, but is an important constituent of the atmosphere. CO_2 is produced by

the respiration of animals, decomposition of organic matters and through human activities such as burning of fossil fuels, coal and wood. It is colorless, odorless, versatile and a promising alternative to VOC- and CFC-based solvents. The main properties of CO_2 are summarized in **Table 1.3**.

CO_2 is the most commonly used solvent in industrial practice for several reasons. Compared with VOC- and CFC-based liquid solvents (Aaltonen and Rantakyla, 1991; Dixon and Johnston, 1997):

- CO_2 is non-toxic, non-flammable, non-reactive, non-corrosive and available in a large amount as a by-product from ammonia and ethanol industries and refineries.
- CO_2 can be easily removed by simple depressurization. It does not leave any solvent residue in the product after processing.
- CO_2 is inexpensive. It is the second least expensive solvent after water. Although highly pure CO_2 is not economical, it is comparable in price with highly pure organic solvents.
- CO_2 possesses no disposal problems and fewer hazards than VOCs and CFCs. It does not create a problem with respect to the green house effect as it is being conserved during the processes.

Compared with all liquid solvents (Rantakyla, 2004):

- The high and large scale of diffusivity, low viscosity and low surface tension of CO_2 is expected to reduce time consumption for mass-transfer controlled processes, such as separations, extractions and reactions.
- The solvent power of CO_2 depends strongly on pressure and temperature. Thus, the solute can precipitate from the CO_2 by a pressure reduction.

This separation becomes a gas-liquid or gas-solid separation; therefore fractionation of large amounts of dilute liquid solutions in the downstream phase can be avoided.

- The separation of CO_2 from the mixtures is an energy efficient process. The heat of vaporization of CO_2 needed for the separation is much smaller than that needed to evaporate most liquid solvents.
- Product fractionation and purification can be carried out directly from the mixtures without changing solvents. This can be done in a series of separator vessels arranged in descending pressure/temperature order or in countercurrent contactors.
- Product crystallization can be carried out directly from CO_2 by allowing the mixtures expand into a lower pressure or ambient air. Formation of ultrafine particles with a small size distribution can be performed in this way.
- CO_2 creates a non-oxidizing atmosphere for products throughout the process.

However, CO_2 is not ideal in all respects. For examples, mixtures of CO_2 and water are corrosive, and CO_2 is not inert with respect to primary and secondary aliphatic amine solutes because both react with CO_2 to yield carbonates (Giddings, 1989). In addition to the benefits stated above, CO_2 provides particular advantages in the pharmaceutical industries due to the facts that:

- The supercritical conditions of CO_2 are easily attainable. CO_2 becomes a SCF when it is heated above 31.1°C and simultaneously compressed above 73.8 bar. Under these conditions, denaturation of pharmaceutical

compounds and polymers can be avoided.

- CO_2 is a Generally Regarded As Safe (GRAS) solvent that leaves no trace in the product. This is probably the most important pharmaceutical advantage of CO_2.

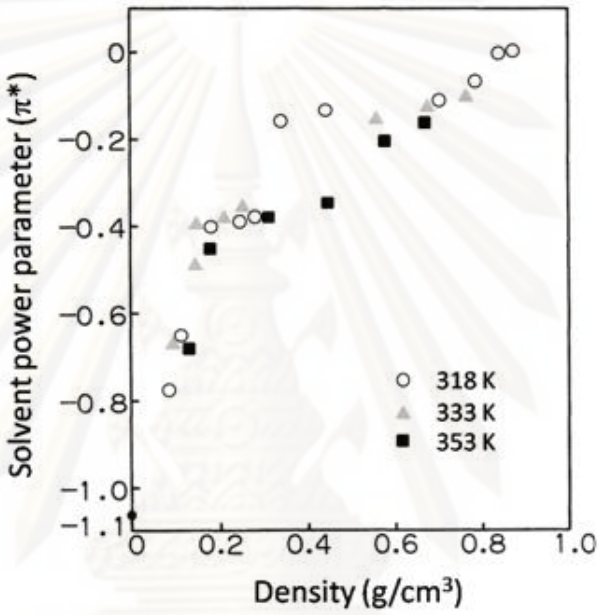

Figure 1.3 Effect of density on solvent power (π^*) of SC-CO_2 (Redrawn from Ikushima et al., 1991)

Supercritical and liquid CO_2 can both be used as solvents. In contrast to liquid CO_2, the solvent power of SC-CO_2 is highly dependent on its temperature and pressure. At low pressure, the density of SC-CO_2 decreases dramatically with an increase in temperature, whereas changes in temperature have much less effect on the density at high pressure. Thus, to a first approximation, density, not pressure, is proportional to the solvent power of SC-CO_2. Based upon solubility measurements in the range from ambient conditions up to 1000 bar and 100°C, the solvent power of

SC-CO_2 increases with density at a given temperature, and increases with temperature at a given density (Smith et al., 1987; Ikushima et al., 1991; Taylor, 1996). The density dependence of the solvent power can be observed through the relationship between the density and the dipolarity/polarizability (π^*), a solvent-strength parameter, of SC-CO_2 in **Figure 1.3**.

The environmentally benign nature of CO_2 is known as a result of high bonding stability in its molecule. CO_2 has a symmetrical molecular structure without a lone pair on the central atom. Thus, it is a good solvent for hydrocarbons and non-polar solids with low molecular weight, but a poor solvent for polar and most high molecular weight compounds (Hyatt, 1984). The solubility of a compound in SC-CO_2 strongly depends on the chemical groups available in the compound molecules, e.g. aromatic hydrocarbons, phenols, aromatic carboxylic acids, pyrones and lipids (Werling and Debenedetti, 1999). As the number of carbon atoms increases and following the introduction of polar functional groups, the solubility decreases dramatically with pressure up to 40 MPa. This feature provides the possibilities for fractionating extraction of complex carbon compounds. An excellent summary on the solvent behavior of SC-CO_2 has been given by Stahl et al. (1980):

- Hydrocarbons and other typically lipophilic organic compounds of relatively low polarity, e.g. esters, ethers, lactones and epoxides, are dissoluble in the lower pressure range, i.e. 7-10 MPa.
- The introduction of strongly polar functional groups (e.g. -OH, -COOH) decreases solubility. In the range of benzene derivatives, substances with three phenolic hydroxyls are still soluble, as are compounds with one

carboxyl and two hydroxyl groups. Substances in this range that decreases solubility are those with one carboxyl and three or more hydroxyl groups.

- More strongly polar substances, e.g. sugars and amino acids, are not soluble in the range up to 40 MPa.
- Fractionation occurs in the pressure gradient when there are greater differences in the commencement of boiling or sublimation, i.e. in the volatility, and/or marked differences in the polarity of the substances (dielectric constant value). The fractionation effects are most marked in the range where there is a sharp rise in the density and dielectric constant of fluid carbon dioxide.

It is commonly accepted that adding small amounts of polar compounds (called cosolvents, entrainers or modifiers) to CO_2 can enhance the solubility of polar and non-polar solutes in SC-CO_2. Water and short-chain alcohols are usually the most acceptable cosolvents in industrial practice. Some reviews of solid solubilities in SC-CO_2 have been published by several research groups (Hyatt, 1984; Gupta and Shim, 2007).

1.3 Solubility of Polymers in SC-CO_2

The knowledge of polymer solubility in SC-CO_2 is crucial for the success of a polymer-SC-CO_2 process. The solubility represents the amount of the polymer that can be dissolved in the SC-CO_2 at equilibrium conditions. Comprehensive attention is paid to where the polymer is dissolved in SC-CO_2 in order to define the processing window.

1.3.1 Thermodynamic Fundamentals of Polymer-SC-CO_2 mixtures

The fundamental principles of molecular and classical thermodynamics can be used to provide a theoretical approach to model the thermodynamic properties and the solubility behavior of polymer-SC-CO_2 mixtures. In addition, they provide a rational methodology for choosing cosolvents to enhance the polymer solubility in SC-CO_2 and to reduce pressure and temperature thresholds for obtaining a homogeneous phase between the components.

For a binary mixture of CO_2 in contact with a polymer, the Gibbs free energy (ΔG_{mix}) is given by:

$$\Delta G_{mix} = \Delta H_{mix} - T\Delta S_{mix} \qquad (1.1)$$

where ΔH_{mix} and ΔS_{mix} are the change of enthalpy and entropy, respectively, on mixing. To form a stable solution of the polymer in SC-CO_2 at a given temperature and pressure, the Gibbs free energy must be negative and minimum (Prausnitz et al., 1986). Enthalpic interactions strongly depend on the mixture density and on the polymer-polymer, CO_2-CO_2 and polymer-CO_2 interaction energies. ΔS_{mix} depends on both the combinatorial entropy of mixing and the non-combinatorial contribution associated with the volume change on mixing. The combinatorial entropy always favors the mixing. Alternatively, the non-combinatorial contribution can have a negative impact on the mixing if the polymer-polymer interactions are very strong (Patterson, 1982).

At the supercritical conditions, the change in the internal energy on mixing (ΔU_{mix}) can give a reasonable approximation to the change of the enthalpy of mixing, which is shown in **Equation (1.2)**:

$$\Delta H_{mix} \approx \Delta U_{mix} = \frac{2\pi\rho}{k_B T}\sum_{i,j} x_i x_j \int \Gamma_{ij} g_{ij} \gamma^2 d\gamma \qquad (1.2)$$

where subscripts *i* and *j* refer to the polymer and the CO_2 components, x_i and x_j are mole fractions of the components, Γ_{ij} is the intermolecular pair-potential energy of the components, the electrostatic attractive part of the potential energy between the molecules, which is a function of temperature (T) and the intermolecular radius, the distance between molecules of the components, (γ), ρ is the solution density, which is a function of temperature and pressure, g_{ij} is the radial distribution function, which is dependent of γ, ρ and T, and k_B is the Boltzmann constant (Lee, 1988).

In general, a polymer chain can be understood as several repeating units connected to one another. Thus, the solution of polymer in SC-CO_2 should not be characterized by a mixture of repeating units of the polymer randomly distributed among the CO_2 molecules. Since a high value of enthalpy of mixing indicates a strong interaction between the solute and the solvent molecules, and thus a high solubility of the solute in the solvent, some important information on the solubility behavior of the polymer in SC-CO_2 are derived from the interpretation of **Equation (1.2)**:

- The solubility of the polymer in SC-CO_2 can be considered roughly proportional to its density.

- An enhancement of the polymer solubility can be achieved by an increase in density through increasing the solution pressure.
- Increasing the density by an addition of a dense liquid cosolvent to SC-CO_2 also can result in enhanced polymer solubility.

The dissolution of the polymer in a SCF solvent is essential to satisfy the energetic criteria. It is required that the polymer-solvent interactions predominate over the polymer-polymer and the solvent-solvent interactions. The disparity in the interaction energies between the components in the solution can be overcome partly by hydrostatic pressure. A useful parameter to describe the balance of the interaction energies is the interchange energy (ω), which is defined as following equation:

$$\omega = z\left[\Gamma_{ij} - \frac{1}{2}\left(\Gamma_{ii} + \Gamma_{jj}\right)\right] \tag{1.3}$$

where z is the number of different pairs in the solution and Γ is the intermolecular pair-potential energy. By making assumption of freely tumbling small molecules in the solution, Γ is given roughly by:

$$\Gamma_{ij} \approx -\left[C_1\frac{\alpha_i\alpha_j}{r^6} + C_2\frac{\mu_i^2\mu_j^2}{r^6kT} + C_3\frac{\mu_i^2Q_i^2}{r^8kT} + C_4\frac{\mu_j^2Q_i^2}{r^8kT} + C_5\frac{Q_i^2Q_j^2}{r^{10}kT} + complex\ \ formation\right] \tag{1.4}$$

where α, μ, Q are the polarizability, dipole moment, and quadrupole moment of the components, and C_1, C_2, C_3, C_4 and C_5 are constants. As indicated in **Equation (1.2)**, the enthalpy of mixing is a directly proportional function of the intermolecular pair-potential energy. Thus, the interpretation of **Equation (1.4)** can give some additional information on the solubility behavior of the polymer in SC-CO_2 system:

- The first term on the right of the equation accounts for non-polar dispersion interactions, which depend only on the polarizability of the polymer and CO_2, not on temperature. CO_2 is therefore not expected to be a good solvent at high operating temperatures.
- Due to the symmetry of its molecular structure, CO_2 has no dipole moment, but a substantial quadrupole moment (-4.3×10^{-26} $erg^{1/2}cm^{5/2}$). The second and the third to fifth terms represent dipolar interactions and quadrupolar interactions, respectively, which are inversely proportional to temperature. At high temperatures, the second term cancels out; which means any polar molecules behave as non-polar molecules. If the temperature is sufficiently high, the CO_2-CO_2 quadrupolar interactions can be considered negligible relative to the polemer-CO_2 non-polar dispersion interactions. Consequently, it may be possible to dissolve non-polar polymers in SC-CO_2 at elevated temperatures.
- The dipolar interactions usually predominate over the quadrupolar interactions, especially at low temperatures where polar interactions are the most dominant. Thus, most polar polymers are dissolved very limitedly in SC-CO_2.

- The complex formation is associated with specific interactions such as formation of hydrogen bonds and complexes. With a small dielectric constant, CO_2 has a low capability to form a hydrogen bond. However, CO_2 still can form weak acceptor-donor complexes. For example, when a polymer containing carbonyl groups is in contact with CO_2, the carbonyl oxygen atom acts as an electron donor and the carbon atom of CO_2 acts as an electron acceptor. The strength of such interactions is known to be very sensitive to temperature.

In addition, there are some other observations concerning the polymer solubility in SC-CO_2. These observations are general and apply also to liquid solvents:

- The polymer solubility in a given solvent depends on difference in the free volume between the polymer and the solvent (Patterson, 1982). For this reason, polymers with a high free volume fraction such as glassy and highly branched polymers tend to be favorable for dissolving in CO_2.
- The polymer solubility in SC-CO_2 drops to near zero at temperatures below the melting temperature (Sun, 2002).
- The polymer solubility varies significantly with the molecular weight of polymer. The impact of molecular weight falls off sharply as the molecular weight increases above 100 kDa (Sun, 2002).

1.3.2 Literature Review

Over the past two decades, the solubilities of various polymers in SC-CO_2 have been measured extensively. The solubility data derived from these polymer-CO_2

systems have been reported in the literatures (Lucien and Foster, 2000). Though SC-CO_2 is quite soluble in many polymers, it is rather a feeble solvent for polar and high molecular weight polymers (Tom et al., 1994; Lucien and Foster, 2000). Amorphous fluoropolymers and silicones are very few examples of polymers in this group that have shown a good solubility in pure SC-CO_2 under readily achievable conditions (DeSimone et al., 1992; Hoefling et al., 1993; O'Neill et al., 1998). In general, an increase in pressure increases the solubility of a solute in a gas solvent as a result of variation in the gas density. The same law is true and applicable also to a polymer and CO_2. This means unrealistically high pressures are needed to dissolve the polar and high molecular weight polymers. In this respect, from the economic point of view the high pressure may represent a potential problem, since in the short term it translates into increased capital equipment costs and in the longer term contributes to operating costs and to overall energy consumption (Perrut, 2000).

However, studies in the molecular level of polymers with SC-CO_2 have shown that not only the solubility of a polymer in SC-CO_2 depends on the CO_2 pressure, but also varies from one polymer to another depending on the specific intermolecular interaction between CO_2 and the chemical groups available in the polymer molecules. Due to the symmetry of the molecular structure and the lack of a lone pair on the central atom, CO_2 (O=C=O) has no dipole moment, but a substantial quadrupole moment and Lewis acidity. This is a reason why relatively volatile polar compounds, such as methanol, DMSO and ethanol, are miscible with SC-CO_2 (Jennings et al., 1991; Mchugh and Krukonis, 1994). The Lewis acidity in CO_2 results from the electro-positivity of the carbon atom due to deficiency of electron density compared to the oxygen atom. Thus the electron acceptor-donor interaction is presented when

CO_2 is in contact with a polymer containing Lewis base site. The quadrupole moment and Lewis acidity have been suggested as being at least partially responsible for the polymer solubility in SC-CO_2 (Kazarian et al., 1996; Brantley et al., 1999; Kazarian and Andrew Chan, 2003).

The study of multicomponent systems is also important for the processing of high molecular weight polymers with SC-CO_2. It is well known that the addition of a chemical modifier, or cosolvent, to SC-CO_2 often leads to an enhancement in the solubility of a polymer. Compared to binary systems (a polymer in contact with SC-CO_2), effects of cosolvent on the solubility enhancement in excess of 10 could be achieved from the corresponding ternary systems (a polymer, SC-CO_2 and a cosolvent) due to improved intermolecular interactions between the components in the SCF phase (Dobbs et al., 1986; Dobbs et al., 1987; Gurdial et al., 1993; Ting et al., 1993). In the ternary systems, each component behaves like a cosolvent to each other, i.e. the higher the cosolvent concentration, the greater the solubility enhancement of a component. The less soluble component would be enhanced more significantly by a greater cosolvent effect of the other component. This suggests that the polymer solubility in a polymer/SC-CO_2/cosolvent system will increase proportionally to the cosolvent concentration. This phenomenon has been observed in a number of studies (Dobbs and Johnston, 1987; Gurdial et al., 1993; Mishima et al., 1998; Mishima et al., 1999; Chafer et al., 2004). Short-chain alcohols, e.g. methanol and ethanol, and acetone are usually the most acceptable cosolvents for SC-CO_2 in industrial practice. Polymer solubilities in SC-CO_2 with or without cosolvent have been reviewed by Bartle et al. (1991) and Gupta and Shim (2007).

1.4 SC-CO_2 Plasticization of Polymers

SC-CO_2 can be considered a potential plasticizer due to its ability to reduce density and increase diffusivity of polymers (Tomasko et al., 2003). In the presence of SC-CO_2, amorphous polymers can take up a significant quantity of CO_2 causing a considerable reduction in the density and viscosity of the polymers (Goel and Beckman, 1993).

Amorphous polymers behave differently to semi-crystalline polymers. At near critical conditions, amorphous polymers absorb CO_2 to a greater extent than semi-crystalline polymers and a greater amount of plasticization is found to occur. This is because CO_2 is absorbed only into amorphous regions and not crystalline regions (Goodship and Ogur, 2004). As the concentration of CO_2 increases, sorption and swelling in amorphous polymers (or amorphous regions of semi-crystalline polymers) can cause a phase transition from glass to liquid, in corresponding to a significant reduction in the glass transition temperature of the polymers. The CO_2 concentrations in the range of 10 to 30 wt.% by can be absorbed by the polymers. Treatment of the polymers with CO_2 at concentrations of 8 to 10% can depress a glass transition temperature of 80°C to below room temperature. The amount of absorption can be increased by increases in temperature and pressure of CO_2. Plasticization of the polymer also causes an increase in crystallinity, which results in an increase in the melting temperature and induces changes in mechanical properties of the polymers, e.g. elastic modulus and creep properties (Goodship and Ogur, 2004).

Numerous recent studies have demonstrated the effectiveness of applying SC-CO_2 in the plasticization of various polymers (Bortner and Baird, 2002; Lan and Tseng, 2002; Areerat et al., 2002). Due to the small (cluster) size of SC-CO_2, the

polymers can be more easily penetrated with SC-CO_2 than do larger liquid solvents. This property allows a controlled rapid sorption of SC-CO_2 through the adjustment of temperature and pressure, which is very useful for applications such as polymer fractionation and purification, impregnation and extraction of impurities, membrane conditioning, polymerization reactions and production of particles, foams, gels and fibres.

1.5 Particle Production from SC-CO_2

Production of small size particles with desired properties is the objective of many industries. In most cases, the requirement of small particle size is accompanied by the desirability of particle size distribution that is as narrow as possible. In the pharmaceutical industry, particles of micrometer and sub-micrometer size with precisely controlled particle size are beneficial for use in formulations administered by various routes including the parenteral, inhalation, and oral modes.

Conventional methods for particle production used in the pharmaceutical industry include mechanical techniques and equilibrium controlled techniques. The mechanical methods are milling and grinding, which mostly are carried out by ball milling. The equilibrium controlled methods are recrystallization, or precipitation from solution, which can be carried out by using the temperature dependency of solubility (e.g. spray drying) or using an anti-solvent to decrease the solubility. These methods suffer from limitations in producing a desirable end product (York et al., 2004):

- Milling and grinding results in 10 to 50 μm particles with large particle size distribution. In addition, these methods are not suitable

for thermally instable and low glass transition temperature compounds due to the frictional heat generated during the processes that are likely to modify or even damage the product.

- Spray drying results in particles of micrometer or sub-micrometer size, but it exposes the product to locally high temperature.
- Recrystallization from solution by anti-solvent methods does not allow precise control of the particle size and results in high content of residual organic solvent, which must be removed.

Therefore, it is necessary in the pharmaceutical industry to look for alternative technologies, which provide micro- and submicron-size particles with a narrow particle size distribution using as small as possible quantity of organic or VOC/CFC-based solvent.

The use of near critical or SCF solvents for recrystallization have been shown to be an attractive alternative to overcome these limitations. Recrystallization from supercritical fluid is similar to the conventional recrystallization, where the crystals (particles) are obtained by slowly cooling down a saturated solution according to an optimum cooling protocol. Since high pressure is required for a SCF solvent, therefore not only temperature but also pressure can be used to trigger nucleation and growth of the crystals (particle formation). By this method, it is possible to improve particle characteristics such as size, size distribution, crystal form and morphology.

In the last decade, a number of researches on particle production using SCFs have been reported. Various methods already exist that use SCFs as a solvent or anti-solvent. These methods have been well described in the literature (Jung and Perrut, 2001) and can be categorized into three main groups:

- SCF as solvent: Rapid Expansion of Supercritical Solution (RESS).
- SCF as anti-solvent: Gas Anti-Solvent (GAS), Supercritical Anti-Solvent (SAS), and Solution Enhanced Dispersion by Supercritical Fluid (SEDS)
- SCF as solute or plasticizer: Particle from Gas-Saturated Solutions (PGSS)

1.5.1 Rapid Expansion of Supercritical Solutions (RESS)

This process is also known as Supercritical Fluid Nucleation (SFN) (Vasukumar and Bansal, 2003). RESS is based on crystallization of a solute in order to facilitate the particle production. In this process, the solute is dissolved in a SCF solvent and the resulting solution is expanded through a restrictor or an orifice. The resulting pressure drop causes the solvent power (density) of the SCF solvent to decrease rapidly, leading to large supersaturations and hence precipitation of the solute. It is possible to obtain very small and mono-disperse particles because the pressure variation is very rapid and travels at the speed of sound, leading to uniform conditions within the expanding solution.

Figure 1.4 represents a schematic illustration of the RESS process, which is operated as follows. CO_2 is pressurized and heated to attain the supercritical conditions needed for the process and passed through an extractor loaded with a solute in order to form a stable solution. Following this, the solution is allowed to expand in the expansion chamber by means of a nozzle with a typical inner diameter of 50 to 100 μm. The expansion chamber is generally at or near atmospheric pressure. The rapid depressurization leads to precipitation of the solute caused by the lowering

of the solvent power of CO_2 and therefore particles are formed. Along with the depressurization, the solution experiences a large temperature drop as well. An acceptable assumption is to consider that the depressurization is an isenthalpic process provided the variation of kinetic energy can be neglected (Wang et al., 2001). As a result, the nozzle must be heated to prevent clogging by freezing of CO_2 and the solute precipitation. After the depressurization, CO_2 turns into the gas phase and is purged out of the expansion chamber. A frit filter is placed at the exit of the expansion chamber to keep the particles formed in the expansion chamber.

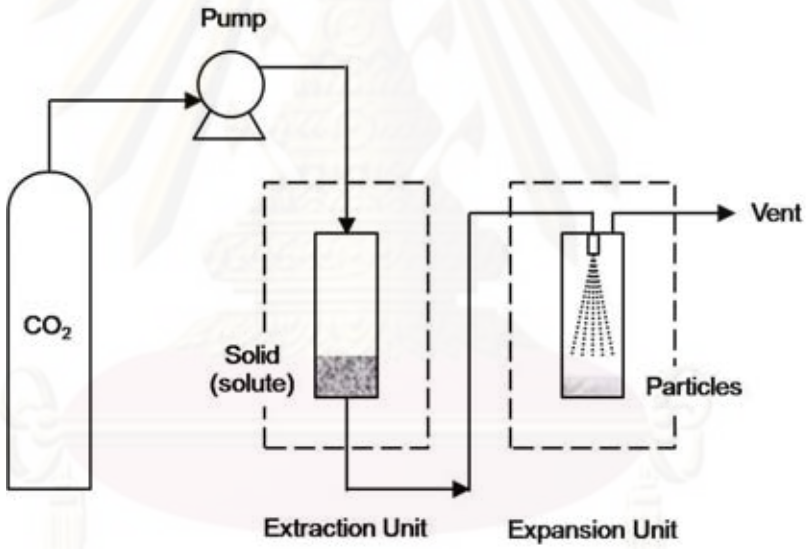

Figure 1.4 A schematic illustration of rapid expansion of supercritical solution (RESS) process.

The particle size and particle size distribution of the precipitated solute is a function of its pre-expansion solubility and expansion conditions. The pre-expansion solubility depends on the nature of the SCF solvent and the solute, operating pressure and temperature. The higher the pre-expansion solubility, the smaller the particles will

be and the narrower the particle size range (Vasukumar and Bansal, 2003). Recently, particle production by the RESS process has been reported with particle size of nanometers (Young et al., 2000; Turk et al., 2002) and in most cases micrometers and submicrometers (Berends et al., 1993; Reverchon et al., 1993; Turk, 1999; Domingo et al., 1999; Helfgen et al., 2000; Charoenchaitrakool et al., 2000), see **Table 1.4**.

Table 1.4 RESS experiments for selected materials

Materials	Solvent + Cosolvent	Pressure (MPa)	Temperature (K)	Particle size (μm)	Reference
Pharmaceuticals:					
Benzoic acid	CO_2	16-28	308-338	1-2	Berends et al., 1993
B-Carotene	C_2H_4 + toluene	31	343	0.3-20	Chang and Randolph, 1989
Caffeine	CO_2	15	369-383	3-5	Subra et al., 1998
Cholesterol	CO_2	20-30	353-422	< 0.35	Turk, 1999
Cyclosporine	CO_2	345	333	0.02-0.09	Young et al., 2000
Flavone	CO_2 + EtOH	25	308	1-5	Mishima et al., 1997
Ibuprofen	CO_2	13-19	308	< 2	Chareontrakool et al., 2000
Nabumetone	CO_2	4	323	0.02	Merrifiel and Valder, 2000
Phenatrene	CO_2	16-20	373-403	2-8	Domingo et al., 1999
Salicylic acid	CO_2	16-20	373-403	1-5	Domingo et al., 1997
Polymers:					
PGA	CO_2	-	-	10-20	Tom and Debenedetti, 1991
PLLA	CO_2 + acetone	-	-	4-25	Tom and Debenedetti, 1991
PLLA	CO_2 + HCFC	-	-	1-2	Tom et al., 1994
PMMA	CO_2 + EtOH	-	-	1.5-1.8	Matsuyama et al., 2001

While most of the studies on particle production by RESS process employed expansion into ambient or CO_2 atmosphere, some of the studies employed expansion into water (Pace et al., 1999; Young et al., 2000) suggesting that the RESS process is applicable to water-insoluble drugs. In these processes, a surfactant is added to avoid agglomeration and flocculation in order to stabilize the precipitated small particles (Yong et al., 2000).

The RESS process relies on the solvent properties of SC-CO_2. This process will be mainly efficient for compounds which are fairly soluble in SC-CO_2. For this reason, a preliminary study on the solubility of the compounds with pressure and temperature is necessary. For pharmaceutical processing, the RESS process has limited its use due to very low solubility of most pharmaceutical compounds (drugs, proteins and biodegradable polymers) in SC-CO_2 (York et al., 2004). In other words, the solute has to be able to dissolve in the SC-CO_2 at appreciable amounts in order to be viable for manufacturing (Debenedetti et al., 1993). A reasonable assumption for the production rate of pharmaceuticals would be around 10-230 g/h (Thiering et al., 2001). This quantity usually makes the RESS process unprofitable since typical pharmaceuticals (such as acetaminophen, for example) is only soluble up to 0.005486 kg/m^3 in SC-CO_2 with a density of 854.07 kg/m^3. To overcome this limitation, it is necessary in most cases to use harmful organic cosolvents in order to enhance the solubility of the target pharmaceuticals. This is primarily because the solvent power of SC-CO_2 is strongly dependent on its density, which can be adjusted by small variations of pressure and temperature as well as by addition of small amount of dense liquids (Smith et al., 1987; Ikushima et al., 1991; Taylor, 1996). However, such an addition makes the RESS process less favorable, since it loses its main advantage of being process free of organic solvent.

The benefit of RESS process is that it is fairly simple and requires only the use of one capillary nozzle for the expansion process. It is also possible to produce to encapsulate a drug in a biocompatible polymer in order to obtain a controlled-release system of the drug. Both materials (the drug and the polymer) must be dissolved in a SCF solvent. Products in the form of polymer-encapsulated drug particles or

composite particles of the drug and the polymer can be obtained depending on the relative solubility of the two materials in the SCF solvent (Debenedetti et al., 1993; Kim et al., 1996). A number of different models of the RESS process have been reported for encapsulations of drug and coatings of particles with a polymer (Young et al., 2000; Mishima et al., 2000; Chernyak et al., 2001; Franklin et al., 2001; Montero et al., 2001; Henon et al., 2002; Matsuyama et al., 2003; Tsutsumi et al., 2003).

1.5.2 Anti-Solvent Techniques

The basic principle of these techniques is to allow a solution of a solute in a primary solvent to contact SC-CO_2. The simultaneous transfers of CO_2 and the primary solvent from one phase to the other lead to supersaturation and the precipitation of the solute. Solids of compounds that are insoluble in SCF solvents can be recrystallized by means of this approach.

The anti-solvent techniques may be divided into three processes:

- Gas Anti-Solvent (GAS)
- Supercritical Anti-Solvent (SAS)
- Solution Enhanced Dispersion by Supercritical Fluid (SEDS)

Gas Anti-Solvent (GAS)

The gas anti-solvent (GAS) process uses a dense gas such as CO_2 as an anti-solvent to precipitate out a solute from a solution. For the success of this process, CO_2 needs to be significantly miscible with the solvent and the solute needs to be insoluble with CO_2 at the operating pressure and temperature. **Figure 1.5** represents a schematic

view of the GAS process. Initially, the solution is loaded into a precipitator vessel at a certain temperature. The rapid injection of compressed CO_2 into the vessel mixes with the solution and causes a volumetric expansion of the system. Consequently, the density of the solution and the solvent power of the solvent are reduced. Due to the rapid mass transfer between the compressed CO_2 and the solvent, the mixing is very fast and results in precipitation of small and uniform particles.

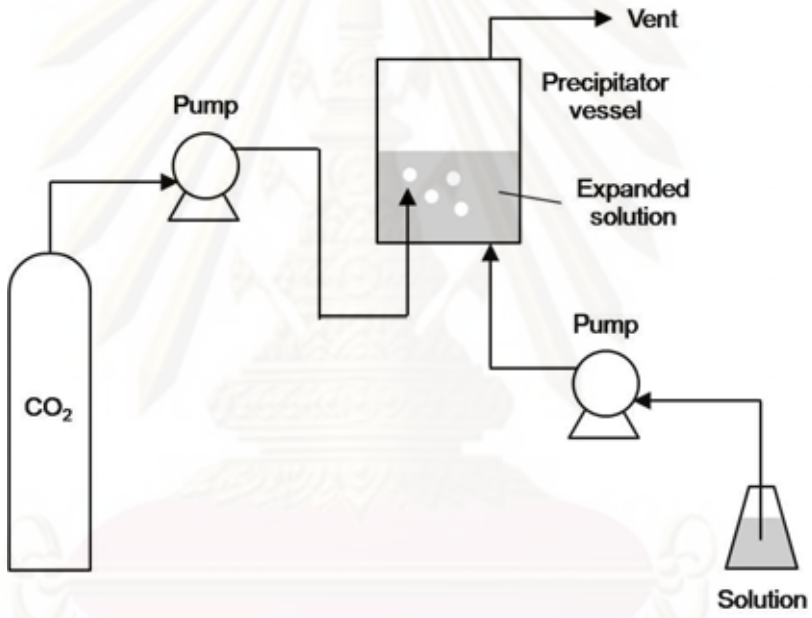

Figure 1.5 A schematic illustration of the gas anti-solvent (GAS) process

The GAS process has been shown to maintain the biomolecular activity of proteins, which means that the process is suitable for sensitive biomolecules (Winters et al., 1999; Thiering et al., 2001). It is more adaptable than the RESS process since it does not rely on the solubility of the target compound in compressed CO_2. Particle productions of various drug and polymer compounds that are not soluble significantly in pure CO_2 have been demonstrated with the GAS process (Randolph et al., 1993;

Thiering et al., 2000; Berends et al., 1996; Fusaro et al., 2004; Cocero and Ferrero, 2002). A few attempts have been made to encapsulate drugs in biodegradable polymers using GAS processes because of the difficulty in controlling the time scales of precipitation of the drugs and the polymers (Elvassore et al., 2001; Koushik and Kompella, 2004). **Table 1.5** summarizes GAS experiments found in literatures.

Table 1.5 GAS experiments for selected materials

Materials	Solvent	Pressure (MPa)	Temperature (K)	Particle size (μm)	Reference
Pharmaceuticals:					
ACP	DMSO	0.8-1.2	298-333	0.1-1	Pallado et al., 2001
Carbamezepine	Acetone	0.7	313	31	Moneghini et al., 2001
Cholesterol	Acetone	-	-	> 50	Liu et al., 2002
Cu2(indomethacin)	DMF	0.58	298-313	15	Warwick et al., 2000
ρ-HBA	Methanol	-	298-318	1	Thiering et al., 1998
HYAFF-11	DMSO	1	308-323	0.35	Bertucco et al., 1996
Insulin	EtOH	-	-	0.05-0.03	Thiering et al., 2000
Lysozyme	DMSO	-	-	0.05-0.2	Thiering et al., 2000
Myglobin	DMSO	-	-	0.03-0.4	Thiering et al., 2000
Paracetamol	Acetone	-	-	90-250	Fusaro et al., 2005
Sulfothiazole	EtOH	0.55-0.58	298	1500-4000	Kitamura et al., 1997
Drug	EtOH	-	278-323	0.24-10	Muller et al., 2000
Polymers:					
PLLA	DCM	-	-	0.5-3	Randolph et al., 1993
PMMA	Acetone	-	-	-	Coenen et al., 2003

Compared to the RESS process, the main advantages of the GAS process are (York et al., 2004):

- Lower pressure levels. Most applications reported involve pressures less than 10 MPa.
- Wider range of compounds that can be processed, especially including many polar pharmaceutical compounds that cannot be processed by RESS.

- Greater number of process parameters to control particle size and morphology.

On the other hand, the disadvantages of the GAS process in comparison to the RESS process are (York et al., 2004):

- The use of a primary organic solvent can result in a small amount of residual solvent remaining in the final product, which can be a serious concern in pharmaceutical processing.
- The continuous addition of a compressed gas can result in wider particle size distribution due to variations of supersaturation ratio in the expanded solution.
- Lower levels of supersaturation ratio are reached in the GASS process; therefore particles obtained from the GAS process are generally larger than those obtained from the RESS process.
- Since particles are formed in a liquid phase, an additional step of drying is required with an appreciable time in order to purge out the liquid solvent.
- Scaling up of the GAS process is not an easy task since the pressure conditions are temporary.

Supercritical Anti-Solvent (SAS)

SAS is also known as aerosol solvent extraction system (ASES) or precipitation with compressed anti-solvent (PCA). This process is a semi-continuous process in which a specially designed nozzle is used to spray a solution with a product into SC-CO_2 in a pressurized vessel. The solution is dispersed into the SC-CO_2 to improve

mixing and enhance mass transfer. A schematic diagram of the SAS process is shown in **Figure 1.6**.

Similar to the GAS process, the CO_2 needs to be miscible with the solvent in order to precipitate the product. To have the ability to control the particle size and morphology, the dispersion of the solution into SC-CO_2 to induce particle precipitation must be in a controlled-fashion. For this reason, different nozzle configurations have been designed as well as addition of ultrasound vibration at the nozzle tip to enhance the mixing and diffusion of CO_2 into the solution (Subramaniam et al., 1997; Jarmer et al., 2003; Chattopadhyay and Gupta, 2001). It is also possible to mix CO_2 and the solution inside a small volume before spraying into the pressurized vessel. The ease of changing the system configuration to adjust the particle characteristics makes the SAS process very attractive.

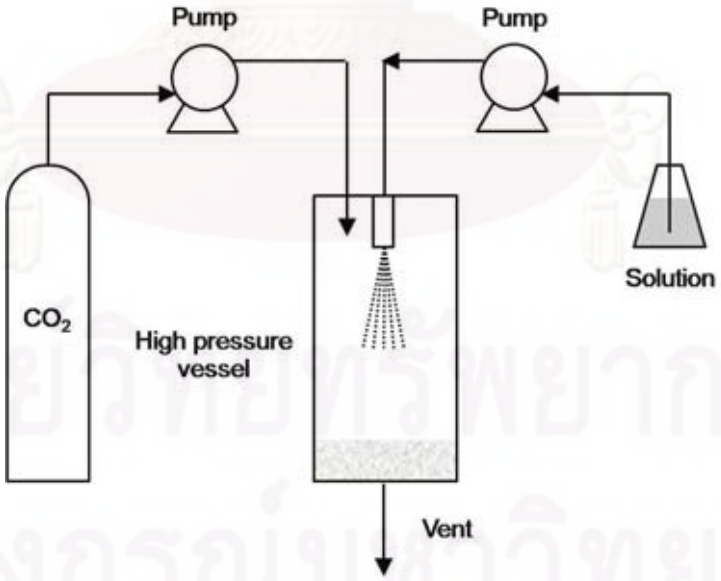

Figure 1.6 A schematic illustration of the supercritical anti-solvent (SAS) process.

Table 1.6 SAS experiments for selected materials

Materials	Solvent	Pressure (MPa)	Temperature (K)	Particle size (μm)	Reference
Pharmaceuticals:					
Amoxyllin	NMP	-	-	0.2-12	Reverchon et al., 2000
Cholesterol	DCM	-	-	1-15	Domingo et al., 1997
Insulin	DMSO	-	-	1-5	Winters et al., 1996
Lysozyme	DMSO	-	-	1-5	Winters et al., 1996
Sulfathiazole	Acetone	-	-	> 750	Yeo et al., 2003
Tetracycline	NMP	-	-	0.15-0.8	Reverchon et al., 1999
Trypsin	DMSO	-	-	1-5	Winters et al., 1996
Polymers:					
Dextran	DMSO	-	-	0.125-0.15	Reverchon et al., 2000
HPMA	DMSO	-	-	0.1-0.2	Reverchon et al., 2000
HYAFF-11	DMSO	-	-	15-20	Benedetti et al., 1997
PLLA	DCM	-	-	1-2	Reverchon et al., 2000

In comparison to the GAS process, the SAS process seems to be better in producing particles due to the following advantages:

- Smaller and more uniform particles are obtained in the SAS process, as a result of improved mixing between CO_2 and the solution (Jung and Perrut, 2001; Thiering et al., 2001; Fusaro et al., 2005).
- The SAS process is an attractive manufacturing process due to its semi-continuous nature that allows for large production rates of product without stopping the system.
- Since the solvent is constantly extracted and removed from the vessel during the process, the SAS process does not require more time consuming drying associated with the GAS process (Thiering et al., 2001).

- Less agglomeration of the precipitated particles can be obtained by the SAS process due to less amount of the solvent presented inside the vessel during the process.

Compared to conventional organic-solvent based processes, both GAS and SAS processes are milder for processing drugs in preventing drug degradation and loss of activity for biomolecules (Winters et al., 1996).

The SAS process has been used in processing different materials including pigment powders (Hong et al., 2000), semiconductor precursors (Reverchon et al., 1998), and inorganic crystals (Yeo et al., 2000). Particle designs with the SAS process have been widely studied for many pharmaceutical compounds with varying results in particle size and morphology (Wubbolts et al., 1999; Reverchon et al., 2000; Reverchon et al., 2002; Subra et al., 2005; Bustami et al., 2000). A particular focus for single component precipitation is in controlling polymer morphology and shape for use in controlled release applications (Reverchon et al., 1999; Reverchon et al., 2000; Pérez de Diego et al., 2005). Encapsulations of drug with a polymer have been demonstrated possible by changing the nozzle design or by adding multiple injection nozzles (Bleich and Mueller, 1996; Young et al., 1999; Elvassore et al., 2001). Examples of pharmaceuticals materials successfully treated with the SAS process are listed in **Table 1.6**.

Solution Enhanced Dispersion by Supercritical Fluids (SEDS)

The SEDS process is based on the idea of the SAS process. With a change in the nozzle design, the mixing of the solution is enhanced, which allows for better control in forming particles. Similar to the SAS process, the material of interest does not need

to be dissolved in SC-CO_2 and the solvent can be purged out continuously during the process. The nozzle is designed utilizing the geometry of a coaxial tube to simultaneously deliver the solution and SC-CO_2. **Figure 1.7** shows an example configuration of the nozzle used in SEDS process (Chang, 2006).

Prior to spraying the solution (solvent + material of interest) into the pressurized vessel through the nozzle, the solution mixes rapidly with SC-CO_2 by means of the coaxial tube in a small volume area called the mixing length (L_i). The mixing is enhanced within the mixing length and simultaneously particles are precipitated from the solution just before spraying into the vessel. Such a design makes it possible for better control of process parameters such as pressure, temperature and flow rate inside the small mixing area (Hanna and York, 1994; Hanna and York, 1995).

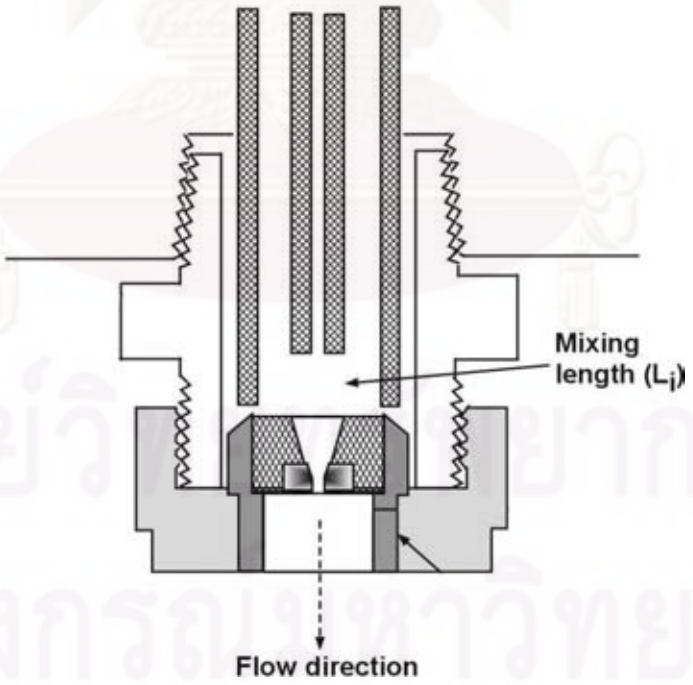

Figure 1.7 A schematic view of typical coaxial tube nozzle used in SEDS process (Chang, 2006)

The SEDS process is similar to other anti-solvent processes that its operating conditions are mild and suitable for processing sensitive pharmaceutical compounds. The process is also versatile due to the benefit that the coaxial tube can be arranged in different configurations for controlling for particle formations or encapsulations (Ghaderi et al., 2000; Tu et al., 2002). By varying process parameters such as pressure, temperature, flow rate and solubility of the solution, controlled particle size and morphology of the product can be obtained for many drugs and polymers (Ghaderi et al., 1999; Ghaderi et al., 2000; Rehman et al., 2001; Velaga et al., 2002). Examples are given in **Table 1.7**.

Table 1.7 SEDS experiments for selected materials

Materials	Solvent	Pressure (MPa)	Temperature (K)	Particle size (μm)	Reference
Pharmaceuticals:					
Acetaminophen	EtOH	8-25	313-353	5-20	Bristow et al., 2001
Insulin	Water, EtOH	-	-	0.05-0.5	Bustami et al., 2000
Lactose	MeOH	15-30	323-363	3-10.5	Palakodaty et al., 1998
Lysozyme	EtOH	20	328	0.78	Sloan et al., 1998
Salmeterol	Acetone, EtOH	25-30	318-363	4-19	Hanna and York, 1998
Sulfathiazole	Acetone, MeOH	20	353-393	2-20	Kordikowski et al., 2001
Trypsin	EtOH	20	328	1.53	Sloan et al., 1998
Polymers:					
PCL	Acetone	-	-	25-85	Ghaderi et al., 1999
PLLA	Acetone	-	-	7-10	Ghaderi et al., 2000
PLLA	EtOH	-	-	1.1-3.6	Chen et al., 2006

1.5.3 Particles from Gas Saturated Solutions (PGSS)

In the PGSS process, SCF does not act as either solvent or anti-solvent. This process involves dissolving a SCF in molten material, then expanding the solution through a nozzle.

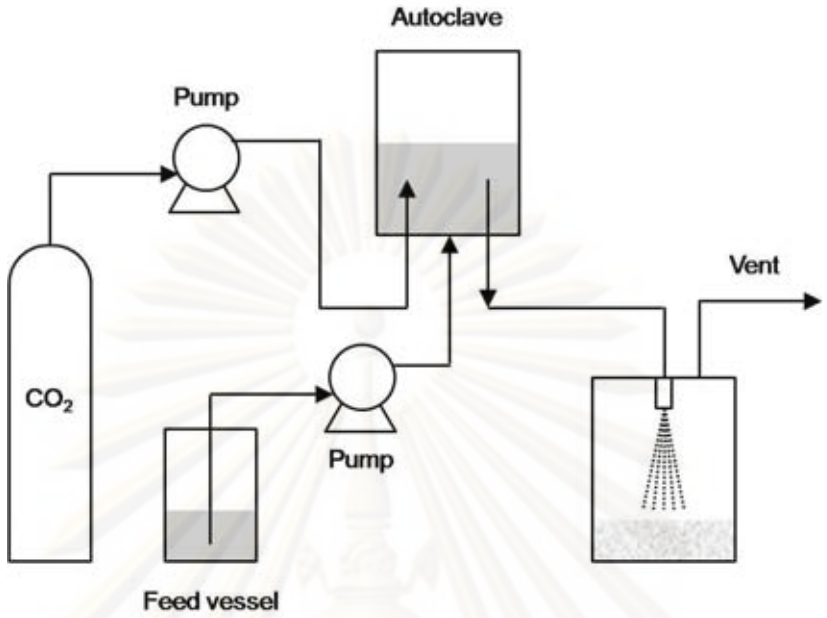

Figure 1.8 A schematic illustration of the particles from gas saturated solutions (PGSS) process

Unlike the RESS process, the PGSS process takes advantage of a much higher solubility of SC-CO_2 in molten materials or liquids than that of the materials or liquids in the SC-CO_2 at same conditions. The material of interest in the form of solid must be first melted before the SC-CO_2 is added until saturation is reached in the solution. In a typical PGSS process, the saturated solution may contain 5 to 50 wt.% of SC-CO_2 and the temperature is varied 50 K around the normal melting point of the material (York et al., 2004). The solution is then allowed to discharge through an expansion device under operating conditions that facilitate transition from SC-CO_2 to CO_2 gas and its further separation from precipitated particles. As a result of the CO_2 transition and the Joule–Thomson effect, the particle precipitation is caused by large temperature drops to below the melting point of the material. Also note that the

melting point of molten materials is decreased when exposed to compressed fluids such as SC-CO_2 (Cooper, 2000).

Figure 1.8 describes the apparatus for carrying out the PGSS process. After the material is melted in a feed vessel, it is delivered into the autoclave where CO_2 is fed from a storage tank by means of a high pressure pump. The liquid phase of the molten material is allowed to saturate with CO_2 at supercritical conditions, then sprayed into an expansion vessel through a suitable device (e.g. nozzle, capillary tube and orifice). It causes a supersaturation of CO_2 and an intense expansion of the nucleated gas bubbles leads to explosion of the molten material into fine particles. The particles are formed due to solidification by the cooling effect of the expanded gas.

The PGSS process has a number of advantages over other SCF-based particle production processes as followings (York et al., 2004):

- The operating pressure is considerably lower than in the RESS process, but of the same order of magnitude or higher than in the antisolvent processes.
- The size of apparatus for carrying out the PGSS process is smaller due to smaller amounts of CO_2 is required.
- The PGSS process requires no use of additional solvent, thus no residual solvent remains in the product. This feature makes the PGSS process favorable for processing pharmaceutical compounds.
- The PGSS process can be carried out in continuous operations, while the anti-solvent processes are operated in discontinuous or semi-continuous mode.

- For processing with polymers, the PGSS process allows operation at low temperature. The polymers can be melted at a temperature much lower than their normal melting or glass transition temperature.
- The versatility of the PGSS process makes it possible to form microspheres by means of suspensions of active molecules in a polymer or other carrier substances.
- The concept of the PGSS process is simple, since the target materials do not have to be soluble in the SC-CO_2. This feature favors the application of the PGSS process to various types of product. Polymers and sticky materials can be treated advantageously by the PGSS process.

The PGSS process has some drawbacks as well due to the following limitations (York et al., 2004):

- The particle size and particle size distribution cannot be easily controlled.
- For highly thermally sensitive materials, the operating temperature required to melt the materials may be so high that the materials may be damaged. Some pharmaceuticals may decompose before melting.

However, the balance between advantages and drawbacks of the PGSS process seems to be positive. Unlike the anti-solvent processes which mostly are still under development, the PGSS process has been patented (Mandel et al., 1996; Weidner et al., 2000) and is already used on industrial scale with capacities of some hundred kilograms per hour (York et al., 2004).

Table 1.8 PGSS experiments for selected materials

Materials	Solvent	Pressure (MPa)	Temperature (K)	Particle size (μm)	Reference
Pharmaceuticals:					
Cyclosporine A	CO_2	-	-	4.5	Tandya et al., 2006
Drug-PLGA	CO_2	-	305	-	Mandel et al., 2000
Felodipine	CO_2	20	423	42	Knez, 2000
Fenofibrate	CO_2	19	338-353	-	Kerc et al., 1999
Nifedipine	CO_2	20	443	10	Weidner et al., 2000
Nifedipine	CO_2	-	-	15-30	Reverchon et al., 2006
Nifedipine	CO_2	10-20	448-463	> 15	Sencar-Bozic et al., 1997
Polymers:					
Catalase	CO_2	-	-	-	Howdle et al., 2001
PEG	CO_2	15-25	303-363	170-500	Weidner et al., 1996
PLGA	CO_2	-	-	-	Howdle et al., 2001

Some materials of pharmaceutical interest have been treated successfully with the PGSS process both in batch and continuous modes, listed in **Table 1.8** for examples. The batch process has been used to produce powder of poly(ethylene glycol) (PEG) (Weidner et al., 1996). Conventional coating systems (e.g. acrylic coatings and low-melting polyester coatings) have been developed using a PGSS continuous process (Weidner et al., 2001).

1.5.4 Selection of a SCF Process

As has been shown in the discussion above, supercritical fluids offer a wide range of techniques to produce ultrafine particles of pharmaceutical materials with different particle sizes and morphologies. Several features make them very attractive. However, some points, such as particle recovery and process scale-up, need to be improved before applying them to industrial practice. **Table 1.9** presents a summary of these techniques.

Table 1.9 Comparison of various SCF processes

Process	Solvent	Driving force	Pressure (MPa)	Temperature (K)	Particle size (μm)	Advantages	Drawbacks
RESS	CO_2	Pressure decrease	20-30	310-400	0.2-3	Simplicity, Minimal or no use of organic solvent	Low solubility of materials, High pressure, High fluid consumption
GAS	Organic solvent	Anti-solvent effect	6-10	298-333	0.1-100	Applicable for polar compounds, Low pressure and temperature	Batch, Use of organic solvent, Wide particle size distribution
SAS	Organic solvent	Anti-solvent effect + Solvent evaporation	7-15	298-333	0.2-10	Applicable for polar compounds, Low pressure and temperature, Controlled particle size	Use of organic solvent, Separation of solvent and fluid, Semi-continuous process
SEDS	Organic solvent	Anti-solvent effect, + Solvent evaporation	10-30	308-363	0.05-10	Applicable for polar compounds, Small particles	Use of organic solvent, Separation of solvent and fluid, Semi-continuous process
PGSS	Organic solvent	Pressure decrease	8-10	323-460	15-50	Low pressure, No use of organic solvent, Low fluid consumption, Continuous process	Wide particle size distribution, High temperature

Factors affecting a decision on selection of an appropriate SCF process include the solubility of the target materials in CO_2, the solubility of CO_2 in the material, the solubility of CO_2 in a solvent and the solubility of the material in a solvent. The solvent processes such as RESS and PGSS are well-accepted given the first preference since they require minimal or no use of organic or VOC/CFC-based solvents. There is a major difference between the RESS and PGSS processes in the solubility term. In RESS, the target material is dissolved in SC-CO_2, while SC-CO_2 is dissolved in the material in PGSS. With SC-CO_2 as solvent, the RESS process is applicable only to a limited number of pharmaceutical materials due to low solubility of the materials in SC-CO_2. In that case, the PGSS process may be a better choice. However, it has yet not been tested for different classes of materials and may require some modifications.

1.6 Objective of Study

1.6.1 To develop a process for coating ultrafine particles with a polymer by using SCF technology. The developed process is intended for use in the preparation of polymeric drug delivery systems.

1.6.2 To investigate the influence of process parameters on the morphology and internal structure of the particle products.

1.7 Scope of Study

1.7.1 Coating of ultrafine particles with a polymer using SCF technology

1.7.1.1 The core particles are:

(a) Silica (SiO_2) particles with average size of 1.4 μm, and

(b) Titania (TiO_2) particles with average size of 70 nm.

1.7.1.2 The polymer is poly($_{D,L}$-lactic-co-glycolic acid) or PLGA (M.W. = 50,000–75,000; PLA:PGA = 85:15).

1.7.1.3 The process is developed on the basis of the RESS process.

1.7.1.4 The solvent is supercritical carbon dioxide (SC-CO_2).

1.7.1.5 The cosolvent is ethanol (C_2H_5OH, EtOH).

1.7.1.6 The maximum extraction pressure is 30 MPa.

1.7.1.7 The maximum extraction temperature is 313 K

1.7.1.8 The extraction time is 180 min.

1.7.2 Influence of process parameters on the morphology and internal structure of the particle products

1.7.2.1 The core-to-polymer weight ratio is 1-3.

1.7.2.2 The nozzle inside diameter is 100-300 μm.

1.7.3 Characterization of the particle products

1.7.3.1 Scanning Electron Microscopy (SEM)

1.7.3.2 Transmission Electron Microscopy (TEM)

1.7.3.3 Image-analyzing software (Image-Pro Plus version 3.0; Media Cybernetics)

1.8 Expected Benefits

1.8.1 Polymer-coated ultrafine particles will be obtained by a RESS process.

1.8.2 Comprehension of the mechanism of particle coating in the process.

1.8.3 Comprehension of the influence of process parameters on the morphology and internal structure of the particle products.

CHAPTER II

MODELING SOLUBILITY OF POLY($_{D,L}$-LACTIC-CO-GLYCOLIC ACID) IN SUPERCRITICAL CARBON DIOXIDE WITH ETHANOL AS COSOLVENT

2.1 Introduction

In SCF precipitation processes for particle production, nucleation is a very strong function of supersaturation, which depends on solubility. Solubility also can have a noticeable effect on precipitation kinetics which, in turn, yields the size and morphology of the precipitated products (Shekunov et al., 1999). Depending on the aim of the process, either a high solubility or low solubility may be desired. High solubility in SC-CO_2 is required in a process based on rapid expansion of supercritical solution (RESS) technique (Thakur and Gupta 2005). On the other hand, the anti-solvent processes, such as gas anti-solvent (GAS), supercritical anti-solvent (SAS) and solution enhanced dispersion by supercritical fluid (SEDS), require low solubility in a mixture of CO_2 and organic solvent (Chattopadhyay and Gupta, 2001; Chattopadhyay and Gupta, 2002; Thote and Gupta, 2005; Gupta and Kompella, 2006). In these cases, knowledge of solubility of the target material in SC-CO_2 is essential both for the initial feasibility study and final process design of a successful process.

However, the SCF precipitation processes have found their limitations in pharmaceutical processing, mostly due to the absent or incomplete knowledge about solubility of the material of interest in SC-CO_2. To date, there is a relatively little

knowledge about the experimental solubilities of most pharmaceutical materials in SC-CO_2 (Coimbra et al., 2006). The deficiency of experimental data is essentially due to several drawbacks in the experimental methods for the solubility measurement.

In general, the most common methods for obtaining solubility data in SCF solvents are the dynamic flow (or transpiration) and in situ spectroscopic techniques. The dynamic flow method often encountered some experimental difficulties in valve clogging and sampling of saturated mixture, which resulted in inaccurate data measurements (McHugh and Krukonis, 1994). It has been shown that the consistency of solubility measurement in the flow method is relatively low when the solubility is 10^{-4} mol fraction or lower (Ngo et al., 2001). On the other hand, the in situ spectroscopic techniques, including infrared, ultraviolet and fluorescence, require no calibration or sampling for measuring the solubility data over a wide range of concentrations, as low as 10^{-6} or 10^{-7} mol fraction (Ngo et al., 2001). However, this method has a drawback in that it requires appreciable time to reach equilibrium (as long as 10 hours when the solubility approaches 10^{-2} mol fraction) (Ngo et al., 2001). In addition, these solubility measurement methods are complex and require expensive experimental apparatuses. Huge investment and long construction and operation periods are often given to the cost of a laboratory-scale development, which may present as a major obstacle to the initial feasibility study of a SCF process. Therefore, if not completely determined experimentally, the solubility in SCF solvent must otherwise be obtained through correlations based on theoretical or empirical models applied to existing experimental data.

Prediction of the equilibrium solubilities using thermodynamic models is a reliable alternative way for obtaining the solubility data of solutes in SCFs (Hartono

et al., 2001; Guha and Madras, 2001; Madras et al., 2003; Coimbra et al. 2005). Generally, the most common thermodynamic models used for predicting solute solubility in SCF solvent are cubic equations of state (EOS). The most used models are those from van der Waals family (such as Peng-Robinson (PR), Soave-Redlich-Kwong (SRK) and Pater-Teja (PT)) and Sanchez-Lacombe lattice fluid model. Several mixing and combining rules, like classical van der Waals mixing rules, are utilized to incorporate solution model into the EOSs. Together with several solute properties, all of these models require at least one parameter exhibiting interactions between components in the solution, which, in most cases, must be determined from existing experimental solubility data.

It is important to select an appropriate EOS and mixing rules for a solubility prediction because each model cannot treat effectively the solubility of all the solutes of interest. In many cases, especially for most pharmaceutical materials, the necessary solute properties (e.g. critical properties, molar volume, sublimation pressure and Pitzer's acentric factor) are not yet available in the literature and need a prior experimental determination or prediction by several estimations. This may lead to excessive error on the results of the solubility prediction. Therefore, apart from selecting the appropriate EOS and mixing rules, an extreme caution should be made in applying these additional estimations.

2.2 Modeling of Solubility in SCF solvent with Equation of State

The general method for estimation of the solubility of a solid species (solute, 2) in a SCF phase starts with satisfying the phase equilibrium condition of equal component fugacities in the solid and SCF phases as follows:

$$f_2^{solid} = f_2^{SCF} \tag{2.1}$$

For the SCF phase, the solute mole fraction (y_2) can be written as a function of fugacity (f_2^{SCF}) and fugacity coefficient (φ_2^{SCF}):

$$y_2 = \frac{f_2^{SCF}}{\varphi_2^{SCF} P} \tag{2.2}$$

where P is the total pressure. Assuming that the SCF is not absorbed by the solid solute, the solid phase may be considered as a pure phase, and fugacity in the solid phase (f_2^{solid}) can be written as:

$$f_2^{solid} = P_2^{solid} \phi_2^{solid} \exp\left(\int_{P_2^{solid}}^{P} \frac{v_2^{solid}}{RT} dP \right) \tag{2.3}$$

where T is temperature, v_2^{solid} is the molar volume of the solid solute (m^3 / mol), P_2^{solid} is vapor pressure or sublimation pressure of the solid solute, and R is gas constant $(8.314\, J / mol \cdot K)$. For most solutes which do not possess a strong tendency of association, the values of ϕ_2^{solid} can be taken to 1 due to the low vapor pressures. In addition, due to the fact that solids are incompressible, it is reasonable to assume that the values of v_2^{solid} are independent of pressure. Hence, the solubility of a solid solute (y_2) in a SCF can be written as:

$$y_2 = \frac{P_2^{solid}}{P}\left[\frac{1}{\varphi_2^{SCF}}\exp\left(\frac{v_2^{solid}\left(P-P_2^{solid}\right)}{RT}\right)\right] \quad (2.4)$$

where the term $\frac{1}{\varphi_2^{SCF}}\exp\left(\frac{v_2^{solid}\left(P-P_2^{solid}\right)}{RT}\right)$ is called the enhancement factor and $\frac{P_2^{solid}}{P}$ is the solubility in the ideal gas. The fugacity coefficient of the solid solute in SCF phase $\left(\varphi_2^{SCF}\right)$ can be calculated from (Prausnitz et al., 1986):

$$RT\ln\varphi_2^{SCF} = \int_v^{\infty}\left[\left(\frac{\partial P}{\partial n_2}\right)_{T,v,n_1} - \frac{RT}{v}\right]dv - RT\ln\left(\frac{Pv}{RT}\right) \quad (2.5)$$

where n_2 is the number of moles of the solid solute, n_1 is the number of moles of CO_2, and v is the molar volume of the mixture. An appropriate equation of state is then used to evaluate the integration and the value of v.

2.2.1 Selection of EOS Model and Mixing Rules

SCF precipitation processes are used to micronize a number of pharmaceutical materials, which involve various types of molecules, from simple to very complex. To select a reliable and appropriate model of EOS and mixing rules that contains all the molecular information of the material, a brief comparison between commonly used models should be noted here. Most of the van der Waals family models (PR, SRK and PT) are well correlated with solubility data of simple sphere-like molecules. On the

other hand, the Sanchez-Lacombe model has been developed on the basis of a lattice fluid model for treating chain-like molecules (Colussi et al., 2006). It should be remarked that these two models are mean-field models, which means that they cannot be applied in the vicinity of the critical point with good results.

In this study, a commercial biodegradable polymer, poly($_{D,L}$-lactic-co-glycolic acid) (PLGA) and SC-CO_2 with ethanol as cosolvent are mixed to provide SCF solutions for RESS process. To the best of knowledge, data about the solubility of PLGA in a SCF solvent have not been yet available in the literature. Moreover, there is no information about a reliable mathematical model which may be used in predicting the PLGA solubility. Taking into consideration that the majority of PLGA molecules are long-chain, not sphere-like, it is therefore reasonable to use the Sanchez-Lacombe EOS to evaluate the PLGA solubilities in the SCF solvent. Together with a thermodynamically consistent expression of fugacity coefficients, proper estimations of the EOS characteristic parameters will be made in order to obtain a reliable evaluation of the PLGA solubilities. The Sanchez–Lacombe EOS has been used successfully for modeling solute solubilities in many polymer/SC-CO_2 systems (Chernyak et al., 2001; Sarah et al., 2003; Li et al., 2007)

2.2.2 **Sanchez-Lacombe EOS** (Sanchez and Lacombe, 1976)

Based on the lattice theory of Sanchez and Lacombe stated that a pure fluid can be viewed as a mixture of segments and holes which occupy the sites of a lattice, the lattice-fluid model of EOS for a pure component has the following form:

$$\tilde{P} + \tilde{\rho}^2 + \tilde{T}\left[\ln\left(1-\tilde{\rho}\right) + \left(1-\frac{1}{r}\right)\tilde{\rho}\right] = 0 \qquad (2.6)$$

where

$$\tilde{P} = \frac{P}{P*} \qquad (2.7)$$

$$\tilde{T} = \frac{T}{T*} \qquad (2.8)$$

$$\tilde{\rho} = \frac{\rho}{\rho*} \qquad (2.9)$$

$$\rho^* = \frac{M_W}{v^*} \qquad (2.10)$$

$$r = \frac{P^* v^*}{RT^*} \qquad (2.11)$$

where $\tilde{P}$, $\tilde{T}$, and $\tilde{\rho}$ are the reduced parameters, P^*, T^*, ρ^* and v^* are the characteristic pressure, temperature, density and molar volume, respectively, M_W is the molecular weight, R is the gas constant $\left(8.31451\, J \cdot mol^{-1} \cdot K^{-1}\right)$ and r is the size parameter, which represents the number of lattice sites occupied by a molecule.

In order to extend the use of this model to mixtures, the mixing rules described below are applied (Xiong and Kiran, 1994):

$$\frac{1}{v^*} = \sum_i \frac{\phi_i}{v_i^*} \qquad (2.12)$$

$$\phi_i = \frac{\frac{W_i}{\rho_i^*}}{\sum_j \frac{W_j}{\rho_j^*}} \tag{2.13}$$

$$\frac{1}{M_w} = \sum_i \frac{\phi_i}{M_{w,i}} \tag{2.14}$$

where ϕ_i , W_i and $M_{w,i}$ are respectively the close packed volume fraction, mass fraction and molecular weight of the component i . The characteristic pressure for the mixture $\left(P^*\right)$ is given by the following equations:

$$P^* = \sum_j \phi_j P_j^* - RT \sum_j \sum_{i<j} \phi_i \phi_j \chi_{ij} \tag{2.15}$$

$$\chi_{ij} = \frac{P_i^* + P_j^* - 2\left(1-k_{ij}\right)\sqrt{P_i^* P_j^*}}{RT} \tag{2.16}$$

where k_{ij} is the binary interaction parameter. The characteristic temperature for the mixture $\left(T^*\right)$ is given by the following equations:

$$T^* = \frac{P^* v_0}{R} \tag{2.17}$$

$$\frac{1}{v_0} = \sum_i \phi_i \left(\frac{P_i^*}{RT_i^*}\right) \tag{2.18}$$

2.3 Results and Discussion

The Sanchez-Lacombe EOS together with mixing rules, **Equation (2.6) – Equation (2.18)**, were used to model the phase behavior of the system CO_2 + PLGA + ethanol at upstream conditions of the RESS process. For the scope of this study, RESS experiments were performed under certain pressure and temperature conditions. A series of preliminary experiments were carried out on RESS of PLGA to check the applicability of the apparatus and to determine the range of operating pressure and temperature conditions. The experimental results suggested that the operating conditions at upstream pressure of 25 MPa and temperature of 313 K PLGA allowed appreciable formation of PLGA particles, according to observations by scanning electron microscopy (SEM) technique, and facilitated maintaining a stable operation of the apparatus. Details of the preliminary RESS experiments will be given and discussed later in **Chapter III**. Thus, the pressure and temperature parameters were fixed and set to these values $\left(P = 25\ MPa, T = 313\ K\right)$ in calculations of the phase equilibrium modeling.

2.3.1 Determination and Optimization of Parameters

Modeling the solubility of a solid in SCF solvent with the Sanchez-Lacombe EOS requires several characteristic parameters of the pure components. Binary interaction parameters are necessary to represent the behavior of the multicomponent system. For CO_2 (1) + PLGA (2) + ethanol (3) ternary system, the values of the pure component parameters were taken from the literature as basic input. These values are presented in **Table 2.1** and **Table 2.2**.

The binary interaction parameters are independent of pressure, but a function of

temperature (Matsuyama and Mishima, 2006). Arce and Aznar (2006) have studied phase equilibrium of PLGA + SC-CO_2 systems for different compositions of PLA and PGA. They reported useful correlations between the binary interaction parameter and temperature for Sanchez-Lacombe EOS in the form of $k_{ij} = C_1 + \frac{C_2}{T}$. For the PLGA used in this study, the PLA:PGA copolymer ratio is 85:15. The dependence of binary interaction parameter (k_{12}) on temperature $(T(K))$ in the range of 312.15 – 364.85 K can be expressed by:

$$k_{12} = -0.2228 + \frac{83.1521}{T} \qquad (2.19)$$

To determine the binary interaction parameter between CO_2 and ethanol, k_{13}, the Sanchez-Lacombe EOS have been used to correlate the vapor-liquid equilibria of ethanol/CO_2 systems at elevated pressures by Joung et al. (2001). A linear dependence of k_{13} on temperature $T(K)$ was found in the range of 313.4-344.75 K, which can be expressed by:

$$k_{13} = 2.41\times10^{-4}T - 4.84\times10^{-2} \qquad (2.20)$$

In the determination of the binary interaction parameter between PLGA and ethanol, k_{23}, due to the scarceness of experimental data under high pressure in the literature, this study makes use the experimental data reported by Eser and Tihminlioglu (2006) for this binary system at low pressures, given in **Table 2.3**. This

treatment is reasonably effective under the assumption that, as mentioned earlier, the binary interaction parameter is independent or a weak function of pressure in the range of certain temperatures. To apply the experimental data in the determination of k_{23}, the temperature dependence of k_{23} was treated by a linear approximation in the range of 353 – 373 K, which can be expressed by:

$$k_{23} = -1.10\times10^{-4}T + 5.9197\times10^{-2} \quad (2.21)$$

Table 2.1 Molecular weights (M_w) and structures of pure components

Component	M_w (g mol^{-1})	Molecular structure
CO_2 (1)	44.01	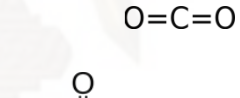
PLGA (2)	62,500[a]	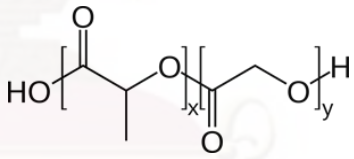
Ethanol (3)	46.07	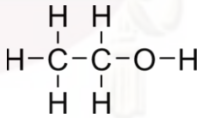

[a] average value

Table 2.2 Characteristic parameters of pure components for Sanchez-Lacombe EOS

Component	P^* (MPa)	T^* (K)	ρ^* (kg/m^3)	Reference
CO_2 (1)	720.3	278.5	1580	Sanchez and Lacombe, 1976; Spyriouni and Economou, 2005
PLGA (2)	620.3	631.0	1362.8	Aionicesei et al., 2009
Ethanol (3)	1069	413.0	963.0	Sanchez and Lacombe, 1976

The straight line in **Figure 2.1** represents the above equation fit to the experimental data. Clearly, It is reasonable to use **Equation (2.21)** for extrapolation of the experimental data to neighboring values of temperature, if necessary.

Table 2.3 Experimental data of binary interaction parameters for PLGA-ethanol system at various temperatures (Eser and Tihminlioglu, 2006)

Interaction parameter of PLGA (2)-ethanol (3) system (k_{23})			
353 K	363 K	373 K	393 K
0.0204	0.0192	0.0182	0.0218

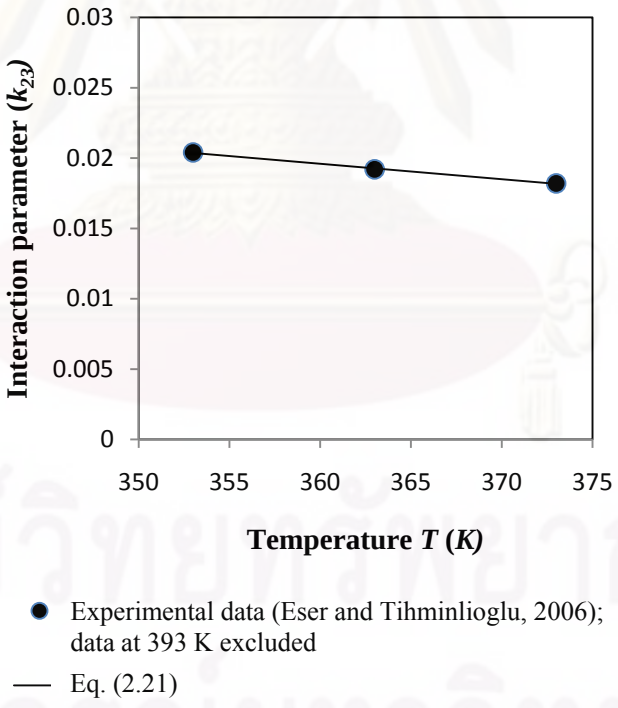

Figure 2.1 Temperature dependence of interaction parameter between PLGA and ethanol (k_{23})

The interaction parameters between CO_2 and PLGA (k_{12}), CO_2 and ethanol (k_{13}), and PLGA and ethanol (k_{23}) were determined at the operating conditions by setting $T = 313\,K$ in **Equation (2.19) – Equation (2.21)**. The values are tabulated in **Table 2.4**.

Table 2.4 Interaction parameters for CO_2 (1) + PLGA (2) + ethanol system at 313 K

k_{12}	k_{13}	k_{23}
0.04286	0.02703	0.02477

For a binary system consisting of a solute and a solvent, the binary interaction parameter (k_{ij}) is a measure of the strength of interaction between the solute and the solvent, and therefore as a guide in the prediction of solute-solvent compatibility. In general, the rather small value of k_{ij} indicates strong interaction between the solute and the solvent molecules (Derawi et al., 2003). The values of k_{ij} can range from minus in a highly miscible system to positive in an immiscible system (- 0.10105 in water-ethanol system and 0.276 in water-benzene system (Ashour and Aly, 1994), for examples). According to this criterion, it can be expressed as neither CO_2 nor ethanol were good solvents for PLGA. But, ethanol can be considered as a better solvent for PLGA than CO_2. In addition, a comparison among the calculated values of k_{ij} suggested that the interactions in the ternary system can be represented in the order of favorable interaction by:

$$CO_2 - PLGA \;<\; CO_2 - ethanol \;<\; PLGA - ethanol$$

The chemical structure plays an important role in the interactions between CO_2 – PLGA, CO_2 – ethanol, and PLGA – ethanol. Due to the symmetry of molecular structure, CO_2 has no dipole moment and a very low polarity. The van der Waals forces in CO_2 are generally responsible for their interactions with other molecules. Since ethanol is polar and capable of being both donor and acceptor of hydrogen bonds, it has a fairly high polarity and forms self-associates by hydrogen bonding of its hydroxyl group. The CO_2 – ethanol interaction in the binary mixture is mainly contributed by the ethanol self-association through hydrogen bonding with the CO_2 molecule. Furthermore, at the pressure and temperature conditions of this study, CO_2 and ethanol form a completely miscible phase, according to vapor-liquid equilibrium data in the literature (Suzuki and Sue, 1990; Jennings et al., 1991; Yoon et al., 1993). In the case of CO_2 – PLGA and PLGA – ethanol binary mixtures, the polarity and van der Waals forces of CO_2 are too weak for PLGA, while ethanol has too high polarity and forms self-associates with PLGA between their polar end groups. However, the polarity matching to PLGA is improved and the degree of ethanol self-association with PLGA is reduced in the ternary mixture. On the other hand, it may be considered that PLGA and ethanol form a microemulsion in the SC-CO_2 single phase. In this case, ethanol is considered as a cosolvent. Consequently, it is reasonable to conclude that the CO_2 + PLGA + ethanol mixture forms a single-phase supercritical solution at the operating conditions of this study.

The interaction parameters χ_{ij} corresponding to the calculated values of k_{ij} were determined by using **Equation (2.16)** with the numerical values presented in **Table 2.2** and **Table 2.4**, yielding:

$$\chi_{12} = 23453.6 \quad mol \cdot m^{-3}$$
$$\chi_{13} = 31410.4 \quad mol \cdot m^{-3}$$
$$\chi_{23} = 38817.8 \quad mol \cdot m^{-3}$$

The next step requires introduction of phase composition parameters to the calculations as variable parameters. Let (W_1, W_2, W_3) be the equilibrium phase composition (on the basis of mass fractions) of the ternary mixture, governed by the equality constraints of the sum of the mass fractions equal to unity:

$$W_1 + W_2 + W_3 = 1 \qquad (2.22)$$

the closed pack volume fractions of the components can be expressed as functions of the mass fractions by expanding **Equation (2.13)**:

$$\phi_1 = \frac{\frac{W_1}{\rho_1^*}}{\frac{W_1}{\rho_1^*} + \frac{W_2}{\rho_2^*} + \frac{W_3}{\rho_3^*}} \qquad \phi_2 = \frac{\frac{W_2}{\rho_2^*}}{\frac{W_1}{\rho_1^*} + \frac{W_2}{\rho_2^*} + \frac{W_3}{\rho_3^*}} \qquad \phi_3 = \frac{\frac{W_3}{\rho_3^*}}{\frac{W_1}{\rho_1^*} + \frac{W_2}{\rho_2^*} + \frac{W_3}{\rho_3^*}}$$

Substitutions numerical values for the characteristic densities, listed in **Table 2.2**, yielded expressions for ϕ_1, ϕ_2 and ϕ_3 as functions of the mass fractions, in the following equations:

$$\phi_1 = \frac{W_1}{W_1 + 1.15938W_2 + 1.64071W_3} \quad (2.23)$$

$$\phi_2 = \frac{W_2}{0.86253W_1 + W_2 + 1.41516W_3} \quad (2.24)$$

$$\phi_3 = \frac{W_3}{0.60949W_1 + 0.70663W_2 + W_3} \quad (2.25)$$

The corresponding expressions for the characteristic parameters of the mixture were derived through **Equation (2.10)** – **Equation (2.25)** by use of some pre-determined numerical values. A series of steps was taken in the following order:

I. The characteristic pressure P^* was obtained by substitutions of **Equation (2.23)** – **Equation (2.25)** and the values of R, T, P_1^*, P_2^*, P_3^*, χ_{12}, χ_{13} and χ_{23} into the expanded form of **Equation (2.15)**:

$$P^* = \phi_1 P_1^* + \phi_2 P_2^* + \phi_3 P_3^* - RT\left[\phi_1\phi_2\chi_{12} + \phi_1\phi_3\chi_{13} + \phi_2\phi_3\chi_{23}\right] \quad (2.26)$$

II. To determine the characteristic temperature T^*, an expression for v_0 was first obtained by using the expanded form of **Equation (2.18)**:

$$\frac{1}{v_0} = \frac{\phi_1 P_1^*}{RT_1^*} + \frac{\phi_2 P_2^*}{RT_2^*} + \frac{\phi_3 P_3^*}{RT_3^*} \quad (2.27)$$

and followed by substitutions into **Equation (2.17)**.

III. The characteristic volume v^* was determined through the expansion of **Equation (2.12)**:

$$\frac{1}{v^*} = \frac{\phi_1}{v_1^*} + \frac{\phi_2}{v_2^*} + \frac{\phi_3}{v_3^*} \quad (2.28)$$

where v_1^*, v_2^* and v_3^* were first determined using **Equation (2.10)**.

IV. The size parameter r was determined by substitutions into **Equation (2.11)**.

V. The effective molecular weight of the mixture M_w was determined by substitutions of **Equation (2.23) – Equation (2.25)** and the numerical values of molecular weights into the expanded form of **Equation (2.14)**:

$$\frac{1}{M_w} = \frac{\phi_1}{M_{w,1}} + \frac{\phi_2}{M_{w,2}} + \frac{\phi_3}{M_{w,3}} \quad (2.29)$$

VI. The characteristic density ρ^* was obtained by **Equation (2.10)**.

By setting $P = 25\,MPa$ and $T = 313\,K$ in **Equation (2.7)** and **Equation (2.8)**, the reduced pressure and temperature, $\tilde{P}$ and $\tilde{T}$, were determined, respectively. The Sanchez-Lacombe EOS in **Equation (2.6)** and the equality constraint in

Equation (2.22) were then used to perform the ternary phase equilibrium calculations. Since the mass fractions W_1, W_2 and W_3 were introduced as variable parameters into the above derivations, a system of two equations and four variables was formed and can be expressed by:

$$\begin{aligned} F(W_1, W_2, W_3, \rho) &= \tilde{P} + \tilde{\rho}^2 + \tilde{T}\left[\ln\left(1-\tilde{\rho}\right) + \left(1-\frac{1}{r}\right)\tilde{\rho}\right] = 0 \\ G(W_1, W_2, W_3) &= W_1 + W_2 + W_3 - 1 = 0 \end{aligned} \qquad (2.30)$$

The system of **Equation (2.30)** has infinite solutions. To solve this equation system for a unique set of solutions, it was necessary to identify the independent and dependent variables.

2.3.2 Obtaining Independent Variable Data

Because PLGA represented a very small amount compared to the whole mixture, therefore a very limited concentration in the CO_2-rich phase, the ternary phase equilibrium calculations were carried out under the assumption that the PLGA-dilute (CO_2-rich) phase did not contain PLGA. Such treatment was not expected to cause significant errors in the calculations, and was found in similar calculations carried out by several researchers (Daneshvar et al., 1990; Kiran et al., 1993; Xiong and Kiran, 1994; Matsuyama and Mishima, 2006). In the absence of PLGA, CO_2 and ethanol forms a stable homogeneous dense phase under high pressure conditions (Suzuki et al., 1990; Jennings et al., 1991; Yoon et al., 1993; Pohler and Kiran, 1997; Zuniga-Moreno and Galicia-Luna, 2002). At the pressure and temperature of this

study ($P = 25\ MPa, T = 313\ K$), Pohler and Kiran (Pohler and Kiran, 1997) and Zuniga-Moreno and Galicia-Luna (Zuniga-Moreno and Galicia-Luna, 2002) have reported on the high-pressure volumetric properties of CO_2 + ethanol system (Pohler and Kiran, 1997). Mass fraction-density data were reported for the mixtures at various mass fractions of CO_2 and ethanol, as presented in **Table 2.5**. These experimental data can be treated as a set of values for the independent variables in the ternary phase equilibrium calculations.

Table 2.5 Phase equilibrium data of CO_2 (1) + ethanol (3) system at 25 MPa and 313 K (w = mass fraction, ρ = density)

w_1	w_3	$\rho\left(kg/m^3\right)$
0.0000	1.0000	795.70[a]
0.1000	0.9000	804.90[a]
0.2237	0.7763	835.82[b]
0.3022	0.6978	852.86[b]
0.3966	0.6034	866.57[b]
0.5456	0.4544	882.26[b]
0.7621	0.2379	884.00[b]
0.9000	0.1000	849.10[a]
1.0000	0.0000	851.10[a]

[a] Pohler and Kiran, 1997; [b] Zuniga-Moreno and Galicia-Luna, 2002

2.3.3 Ternary Phase Equilibrium Calculations

Before applying the data in **Table 2.5** to the calculations, the values of the mass fractions were adjusted to their corresponding values in the ternary system by using the following equations:

$$
\begin{aligned}
W_1 &= \frac{m_1}{m_1 + m_2 + m_3} \\
W_2 &= \frac{m_2}{m_1 + m_2 + m_3} \\
W_3 &= \frac{m_3}{m_1 + m_2 + m_3} \\
m_1 &= w_1 \rho V \\
m_3 &= w_3 \rho V = (1 - w_1) \rho V
\end{aligned}
\qquad (2.31)
$$

where m_1, m_2, and m_3 are the amount (mass) of CO_2, PLGA and ethanol in the mixture, respectively; w_1, w_3 and ρ are the experimental data of mass fractions for CO_2 and ethanol, and density of the mixture, respectively; V is the mixture volume. For this study, the mixture volume was set equal to the volume of the extraction chamber, $V = 1500\, ml = 1.5 \times 10^{-3}\, m^3$. The two equation system in **Equation (2.30)** was then reduced to one equation, which can be expressed as:

$$
F(w_1, \rho : W_2) = \tilde{P} + \tilde{\rho}^2 + \tilde{T}\left[\ln(1 - \tilde{\rho}) + \left(1 - \frac{1}{r}\right)\tilde{\rho} \right] = 0 \qquad (2.32)
$$

In this equation, w_1 and ρ were the independent variables and W_2 was the dependent variable. The phase equilibrium calculations were carried out for the mass fractions of CO_2, ethanol and PLGA through **Equation (2.32)** by trial and error in a spreadsheet, adjusting the values of W_2 until $F(w_1, \rho : W_2) = 0$. **Table 2.6** shows the calculations necessary for the determination of the mass fractions. The results of the calculations are tabulated in **Table 2.7** for the values of mass fractions at different ternary equilibrium phase compositions.

Table 2.6 The Sanchez-Lacombe EOS phase equilibrium calculations for CO_2 (1) + PLGA (2) + Ethanol (3) system at 25 Mpa and 313 K. The system volume is 1500 mL.

w_1	w_3	ρ (kg/m^3)	W_1	W_2	W_3	P*	T*	r	ρ*	Pr	Tr	ρr	$F(w_1, \rho: W_2)$
0	1	795.7	0	0	1	1.07E+09	4.13E+02	1.49E+01	9.62E+02	2.34E-02	7.58E-01	8.27E-01	-3.84E-02
0	1	795.7	0	0.33855191	0.66144809	9.30E+08	4.30E+02	1.69E+01	9.62E+02	2.69E-02	7.28E-01	8.27E-01	1.96E-05
0	**1**	**795.7**	**0**	**0.338442**	**0.661558**	**9.30E+08**	**4.30E+02**	**1.69E+01**	**9.62E+02**	**2.69E-02**	**7.28E-01**	**8.27E-01**	**1.81E-06**
0	1	795.7	0	0.33836858	0.66163142	9.30E+08	4.30E+02	1.69E+01	9.62E+02	2.69E-02	7.28E-01	8.27E-01	-1.01E-05
0	1	795.7	0	0.45588202	0.54411798	8.79E+08	4.41E+02	1.82E+01	9.62E+02	2.85E-02	7.09E-01	8.27E-01	2.18E-02
0.1	0.9	804.9	0.05469681	0.45303192	0.49227128	8.61E+08	4.36E+02	1.75E+01	1.00E+03	2.90E-02	7.18E-01	8.03E-01	5.15E-02
0.1	0.9	804.9	0.07071485	0.2928515	0.63643365	9.29E+08	4.21E+02	1.58E+01	1.00E+03	2.69E-02	7.44E-01	8.03E-01	2.35E-02
0.1	0.9	804.9	0.08578889	0.14211106	0.77210005	9.91E+08	4.12E+02	1.49E+01	1.00E+03	2.52E-02	7.60E-01	8.03E-01	4.78E-03
0.1	**0.9**	**804.9**	**0.090577**	**0.094227**	**0.815196**	**1.01E+09**	**4.10E+02**	**1.46E+01**	**1.00E+03**	**2.48E-02**	**7.64E-01**	**8.03E-01**	**5.85E-07**
0.1	0.9	804.9	0.09058409	0.09415913	0.81525678	1.01E+09	4.10E+02	1.46E+01	1.00E+03	2.48E-02	7.64E-01	8.03E-01	-5.85E-06
0.2237	0.7763	835.82	0.12444232	0.44370887	0.4318488	840171031	428.277798	1.65E+01	1.06E+03	2.98E-02	7.31E-01	7.90E-01	5.54E-02
0.2237	0.7763	835.82	0.15992165	0.2851066	0.55497175	903999036	412.285979	1.49E+01	1.06E+03	2.77E-02	7.59E-01	7.90E-01	2.62E-02
0.2237	**0.7763**	**835.82**	**0.206367**	**0.077482**	**0.716151**	**9.87E+08**	**399.491**	**1.37E+01**	**1.06E+03**	**2.53E-02**	**7.83E-01**	**7.90E-01**	**5.76E-07**
0.2237	0.7763	835.82	0.20638252	0.07741385	0.71620363	986567696	399.487851	1.37E+01	1.06E+03	2.53E-02	7.84E-01	7.90E-01	-6.25E-06
0.2237	0.7763	835.82	0.2237	0	0.7763	1016906824	396.275811	1.33E+01	1.06E+03	2.46E-02	7.90E-01	7.90E-01	-7.18E-03
0.3022	0.6978	852.86	0.16961485	0.43873311	0.39165203	8.25E+08	4.23E+02	1.59E+01	1.10E+03	3.03E-02	7.40E-01	7.78E-01	6.09E-02
0.3022	0.6978	852.86	0.27530029	0.08901295	0.63568676	9.62E+08	3.94E+02	1.32E+01	1.10E+03	2.60E-02	7.95E-01	7.79E-01	5.42E-03
0.3022	**0.6978**	**852.86**	**0.291205**	**0.036382**	**0.672413**	**9.82E+08**	**3.91E+02**	**1.29E+01**	**1.10E+03**	**2.55E-02**	**8.00E-01**	**7.79E-01**	**3.17E-06**
0.3022	0.6978	852.86	0.29122738	0.03630912	0.67246349	9.82E+08	3.91E+02	1.29E+01	1.10E+03	2.55E-02	8.00E-01	7.79E-01	-3.89E-06
0.3022	0.6978	852.86	0.3022	0	0.6978	9.96E+08	3.90E+02	1.28E+01	1.10E+03	2.51E-02	8.04E-01	7.79E-01	-3.41E-03
0.3966	0.6034	866.57	0.3966	0	0.6034	9.69E+08	3.81E+02	1.22E+01	1.14E+03	2.58E-02	8.22E-01	7.57E-01	6.57E-03
0.3966	0.6034	866.57	0.33262627	0.16130541	0.50606831	9.07E+08	3.90E+02	1.29E+01	1.14E+03	2.76E-02	8.03E-01	7.57E-01	2.47E-02
0.3966	0.6034	866.57	0.28642446	0.27780016	0.43577539	8.64E+08	3.99E+02	1.37E+01	1.14E+03	2.90E-02	7.85E-01	7.57E-01	4.20E-02
0.3966	0.6034	866.57	0.25149218	0.36587954	0.38262829	8.31E+08	4.08E+02	1.44E+01	1.14E+03	3.01E-02	7.67E-01	7.57E-01	5.78E-02
0.3966	0.6034	866.57	0.22415435	0.43481002	0.34103563	8.06E+08	4.17E+02	1.52E+01	1.14E+03	3.10E-02	7.51E-01	7.57E-01	7.22E-02
0.5456	0.4544	882.26	0.5456	0	0.4544	9.22E+08	3.65E+02	1.12E+01	1.23E+03	2.71E-02	8.58E-01	7.17E-01	1.80E-02
0.5456	0.4544	882.26	0.45890821	0.15889258	0.38219921	8.63E+08	3.75E+02	1.19E+01	1.23E+03	2.90E-02	8.35E-01	7.17E-01	3.72E-02
0.5456	0.4544	882.26	0.39598856	0.27421451	0.32979693	8.23E+08	3.85E+02	1.26E+01	1.23E+03	3.04E-02	8.12E-01	7.17E-01	5.52E-02
0.5456	0.4544	882.26	0.34824205	0.36172645	0.2900315	7.93E+08	3.96E+02	1.34E+01	1.23E+03	3.15E-02	7.91E-01	7.17E-01	7.15E-02
0.5456	0.4544	882.26	0.31077072	0.43040557	0.25882371	7.71E+08	4.05E+02	1.41E+01	1.23E+03	3.24E-02	7.72E-01	7.17E-01	8.61E-02
0.7621	0.2379	884	0.7621	0	0.2379	8.38E+08	3.37E+02	9.72E+00	1.38E+03	2.98E-02	9.30E-01	6.42E-01	2.24E-02
0.7621	0.2379	884	0.6412085	0.15862944	0.20016206	7.86E+08	3.50E+02	1.04E+01	1.38E+03	3.18E-02	8.95E-01	6.42E-01	4.39E-02
0.7621	0.2379	884	0.55341982	0.27382256	0.17275761	7.53E+08	3.63E+02	1.12E+01	1.38E+03	3.32E-02	8.63E-01	6.42E-01	6.33E-02
0.7621	0.2379	884	0.48677486	0.36127168	0.15195347	7.30E+08	3.75E+02	1.19E+01	1.38E+03	3.43E-02	8.34E-01	6.42E-01	8.02E-02
0.7621	0.2379	884	0.43445598	0.42992261	0.13562141	7.13E+08	3.87E+02	1.26E+01	1.38E+03	3.51E-02	8.08E-01	6.42E-01	9.49E-02
0.9	0.1	849.1	0.9	0	0.1	7.74E+08	3.14E+02	8.82E+00	1.49E+03	3.23E-02	9.96E-01	5.71E-01	1.99E-02
0.9	0.1	849.1	0.75232829	0.16407968	0.08359203	7.27E+08	3.30E+02	9.57E+00	1.49E+03	3.44E-02	9.48E-01	5.71E-01	4.30E-02
0.9	0.1	849.1	0.64628591	0.28190455	0.07180955	6.99E+08	3.46E+02	1.03E+01	1.49E+03	3.57E-02	9.04E-01	5.71E-01	6.31E-02
0.9	0.1	849.1	0.5664443	0.37061745	0.06293826	6.82E+08	3.62E+02	1.11E+01	1.49E+03	3.67E-02	8.65E-01	5.71E-01	7.99E-02
0.9	0.1	849.1	0.50416071	0.43982143	0.05601786	6.69E+08	3.76E+02	1.18E+01	1.49E+03	3.74E-02	8.33E-01	5.71E-01	9.40E-02
1	0	851.1	1	0	0	7.20E+08	2.95E+02	8.17E+00	1.58E+03	3.47E-02	1.06E+00	5.39E-01	5.90E-03
1	0	851.1	0.83624275	0.16375725	0	6.80E+08	3.13E+02	8.92E+00	1.58E+03	3.68E-02	9.99E-01	5.39E-01	3.20E-02
1	0	851.1	0.71857147	0.28142853	0	6.58E+08	3.32E+02	9.67E+00	1.58E+03	3.80E-02	9.44E-01	5.39E-01	5.38E-02
1	0	851.1	0.62993117	0.37006883	0	6.45E+08	3.49E+02	1.04E+01	1.58E+03	3.87E-02	8.97E-01	5.39E-01	7.17E-02
1	0	851.1	0.56075813	0.43924187	0	6.37E+08	3.65E+02	1.12E+01	1.58E+03	3.92E-02	8.58E-01	5.39E-01	8.64E-02

Table 2.7 Calculated mass fractions of CO_2 (1) + PLGA (2) + ethanol (3) system at 25 MPa and 313 K

W_1	W_2	W_3
0.0000	0.3384	0.6616
0.0906	0.0942	0.8152
0.2064	0.0775	0.7161
0.2912	0.0364	0.6724
0.3966	0.0000	0.6034
0.5456	0.0000	0.4544
0.7621	0.0000	0.2379
0.9000	0.0000	0.1000
1.0000	0.0000	0.0000

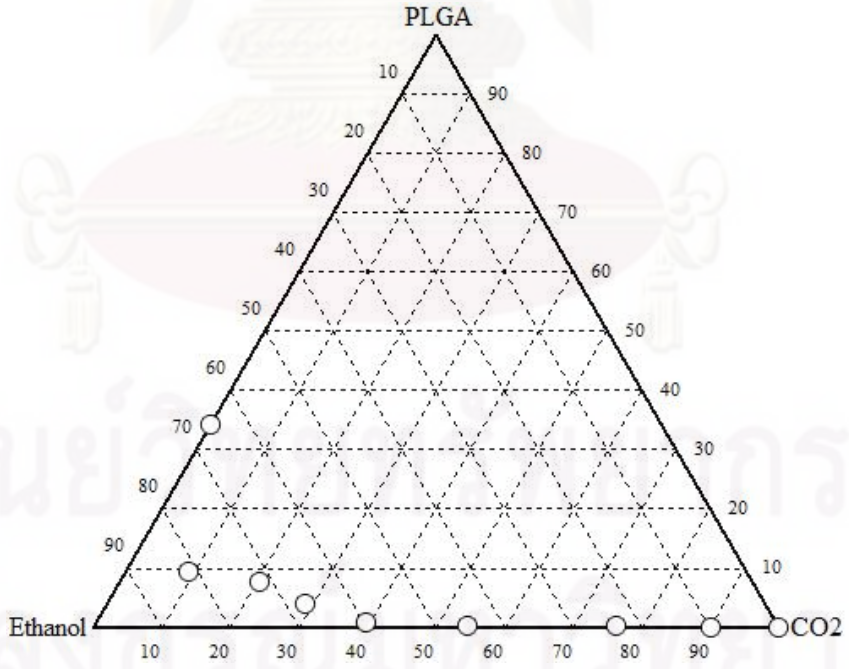

Figure 2.2 Predicted solubilities of PLGA in a mixture of CO_2 and ethanol at 25 MPa and 313 K

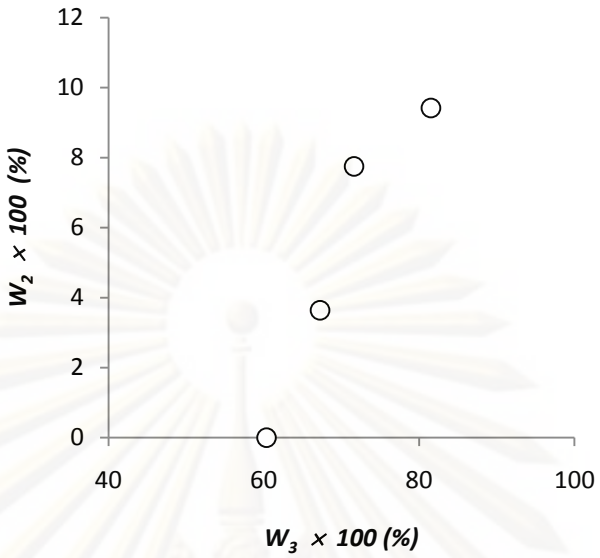

Figure 2.3 Effect of ethanol concentration on PLGA solubility in CO_2 (1) + PLGA (2) + ethanol (3) system at 25 MPa and 313 K

The solubilities of PLGA in a mixture of SC-CO_2 and ethanol at $25\ MPa$ and $313\ K$ are presented in a ternary phase equilibrium diagram, as shown in **Figure 2.2**. The solubility behavior of PLGA in this system may be described as follows. Without PLGA, the mixture of CO_2 and ethanol forms a single supercritical fluid phase as mentioned earlier. It was clearly seen that PLGA does not dissolve in pure SC-CO_2. The solubility of PLGA is strongly dependent on the concentration of ethanol. The effect of ethanol on the enhancement of PLGA solubility is also observed in **Figure 2.3**. Inspite of the fact that ethanol, in pure form, is not a good solvent for PLGA, it should be noted that ethanol is capable of being a fairly good cosolvent for this system. Similar results were reported for other ternary systems of polymer in the mixture of SC-CO_2 and ethanol (Mishima et al., 1999; Matsuyama et al., 2000;

Matsuyama and Mishima, 2006). As a result of the phase equilibrium calculations, a PLGA solubility of about 33 wt.% in pure ethanol was predicted at this pressure and temperature, suggesting a possible application of high pressured or even supercritical ethanol in the pharmaceutical production of PLGA particles. In the mixture of SC-CO_2 and ethanol, the maximum value of 9.42 wt.% is achieved for the PLGA solubility at 81.52 wt.% ethanol. While the PLGA solubility in SC-CO_2 increases with the concentration of ethanol, it may be unchanged or very slightly changed within the concentration range below 50 wt.% ethanol. According to these results, it may be possible to apply the RESS process for the production of PLGA particles with ethanol as a cosolvent.

2.4 Conclusions

The solubility data of PLGA in the mixture of SC-CO_2 and ethanol at 25 MPa and 313 K were predicted by a ternary phase equilibrium modeling using the Sanchez-Lacombe EOS together with mixing rules. The calculations were performed under the assumption that the PLGA concentration in the polymer-dilute phase was zero. As the calculation results show, PLGA is not soluble in pure SC-CO_2 or even in the SC-CO_2 mixed with ethanol up to 50 wt.% . The cosolvent effect of ethanol on the solubility enhancement of PLGA was observed in the range of ethanol concentrations above 50 wt.%. that the PLGA solubility increases with the ethanol concentration. The Sanchez-Lacombe EOS with the mixing rules provides an appreciable tool for the investigation of phase equilibrium behavior and the solubility modeling of PLGA in the ternary mixture of this study.

CHAPTER III

FORMATION OF POLY($_{D,L}$-LACTIC-CO-GLYCOLIC ACID) PARTICLES BY RAPID EXPANSION OF SUPERCRITICAL SOLUTION WITH ETHANOL AS COSOLVENT

3.1 Introduction

Over the two last decades, a number of different techniques using supercritical fluids (SCF) as solvents or anti-solvents have been developed for the preparation of fine particles of polymers and polymer composites. Due to their favorable solvent properties, i.e. gas-like mass transfer and liquid-like density properties, SCFs could replace the conventional organic liquid solvents. It is possible to produce nano- or micron-size particles for both low and high molecular weight materials. For pharmaceutical applications, carbon dioxide (CO_2) has already been used as a common SCF as it is non-toxic and offers a solvent-free final product inert in nature.

When a supercritical solution of a solute in CO_2 expands across an orifice or a capillary, the solvent density decreases dramatically and the polymer is rejected from the solution. This process was first named for short as the Rapid Expansion of Supercritical Solution or RESS by Petersen et al. (Petersen et al., 1986). This process is very rapid because the expansion occurs at the speed of sound, and the reduction across the expansion device leads to both uniform conditions and very high supersaturation ratios in the post-expansion jet. These features make the RESS process favorable for formation of fine particles of polymer with narrow particle size distributions (Debenedetti, 1990).

3.2 Literature Review

The basic concept of RESS was first described 120 years ago by Hannay and Hogarth (1879). They found that a solid could become crystalline or could be brought down as a „snow" in a gas, or on a glass as a „frost", when the solid was precipitated by suddenly reducing the gas pressure. However, the concept of RESS was really understood and developed after the studies of Krukonis et al. (1984) and Matson and Petersen (1987) on RESS of hydrocarbon-based polymers. They reported on particle formation from polypropylene, polystyrene, polyphenyl sulfone and PMMA using propylene, pentane, and propane as SCFs. However, a concern with these studies was the use of the flammable solvents.

Smith et al. (1986) studied performance of capillary restrictors in Supercritical Fluid Chromatography (SFC) and found that expansion of a SCF solvent from too low a temperature could result in formation of a condensed solvent phase. The expansion process was directly observed and solvent droplet size was found to be strongly dependent on the SCF temperature, with average droplet size decreasing to under 0.2 μm above the critical temperature and being negligible for reduced temperature > 1.3. Kinetic considerations of the SCF expansion process were very detailed. In addition, the expansion of the SCF solvent dissolved with nonvolatile compounds was investigated for formation of ultrafine powder and the results with polycarbosilane were presented as an example.

In the early 1990"s, the focus on particle formation by RESS moved to biopolymers that dissolved in non-flammable SCFs such as CO_2. Due to the low solubility of the biopolymers in SC-CO_2, cosolvents were often used to enhance the biopolymer solubilities. Tom and Debenedetti (1991; 1994) reported on particle

formation from $_{L}$-PLA and $_{D,L}$-PLA using SC-CO_2. In their work, the polymers were dissolved in SC-CO_2 with $CHClF_2$ as a cosolvent and precipitated by RESS. It was found that different morphologies of the precipitate, e.g. microparticles, microspheres, agglomerates, or dendrites, could be obtained depending on the type of the expansion device (orifices or capillaries), pre-expansion temperature, and solvent composition. Precipitating using orifices resulted in various morphologies, while using capillaries resulted in microparticle formation. In addition to $_{L}$-PLA and $_{D,L}$-PLA, Lele and Shine (Lele and Shine, 1992) also reported on particle formation from poly(caprolactone) (PCL) using supercritical chlorodifluoromethane (CDFM).

In more recent years, various publications have shown that RESS enable the particle formation of polymers and thermally sensitive materials with particle sizes less than 500 nm (Turk, 1999; Helfgen et al., 2000; Hils et al., 2000). Reviews have become more general, discussing RESS as one of several alternatives for particle formation using SCFs (Subramaniam et al., 1997; Subra and Jestin, 1999; Kikic and Sist, 2000). Such a development is not surprising as many of the other SCF techniques have been developed to overcome the major disadvantages of RESS, the limited solubility of many polymers in SC-CO_2. To overcome the difficulties associated with SCF-insoluble polymer compounds, Mishima et al. (1996) have developed a modified RESS technique called Rapid Expansion of Supercritical Solution with a Non-solvent (RESS-N), wherein a polymer dissolved in SC-CO_2 mixed with a non-solvent for the polymer as cosolvent is sprayed through a nozzle to atmospheric pressure. The solubility of the polymer in SC-CO_2 was found to be increased significantly by the cosolvent, but in pure form the polymer itself was insoluble in the cosolvent (Mishima et al., 1997; Mishima et al., 2000).

In order to obtain sub-micron size particles of water-insoluble polymer compounds, Henriksen et al. (1997) applied the method invented by Frederiksen et al. (1997), called Rapid Expansion of Supercritical Solution into Aqueous Solution (RESAS), by submerging the nozzle in an aqueous solution containing one or more surfactants. In addition, Young et al. (2000) reported on the application of the RESAS technique to precipitate cyclosporine by spraying into a solution of Tween-80 polymer. The mean particle size of the precipitated cyclosporine was found in between 400 and 700 nm and the solubility of cyclosporine increased significantly. Pace et al. (1999) have improved the RESAS technique by dissolving a surface modifier together with a polymer in a SCF solvent and expanding it in an aqueous solution containing surface modifiers and additives. These techniques were later named as Rapid Expansion of Liquefied Gas Solution (RELGS) and Rapid Expansion of Liquefied Gas Solution and Homogenization (RELGS-H)

3.3 Description of RESS Process

With CO_2 as SCF, the principle of RESS is very simple that it utilizes the high solvent power of SC-CO_2. After loading SC-CO_2 with a solute, the rapid phase change from supercritical to gas-like phase occurs during the expansion in a supersonic free jet, leading to a very high supersaturation, and subsequently particle formation.

As shown in **Figure 3.1**, the RESS process can be considered to consist of four steps: (a) preparation of the supercritical solution, (b) setting of the pre-expansion conditions (c) rapid expansion of the supercritical solution to ambient conditions

through an expansion device, and (d) recovery of the product in the expansion chamber. A schematic diagram of a typical RESS process is shown in **Figure 3.2**.

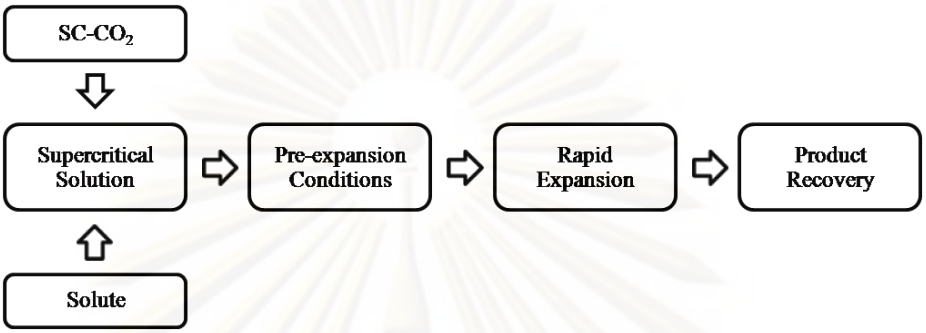

Figure 3.1 Simplified diagram of RESS process

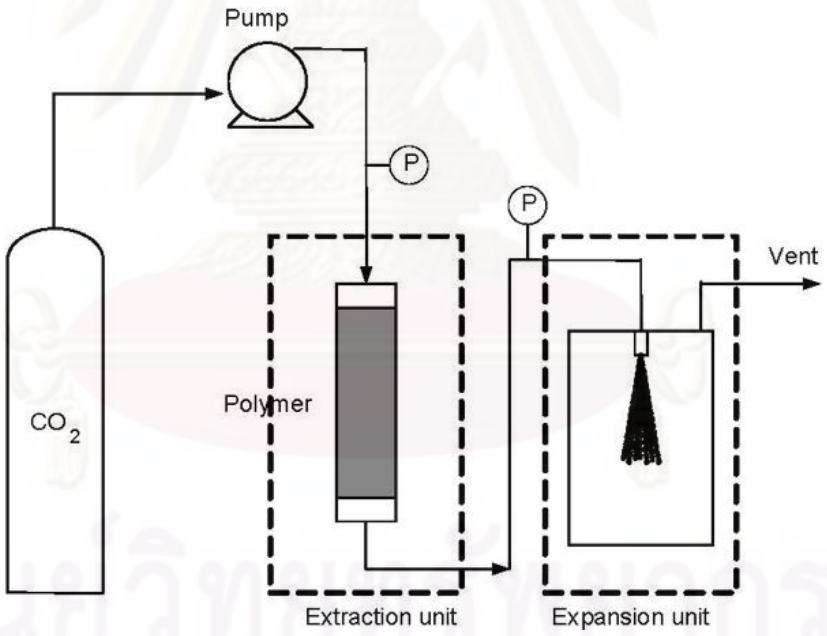

Figure 3.2 A schematic illustration of rapid expansion of supercritical solution (RESS) process

a) *Preparation of supercritical solution.* The supercritical solution is prepared by delivering liquefied CO_2 from a cylinder through an

extraction chamber (autoclave or high-pressure chamber) loaded with the solid solute of interest at a defined supercritical extraction pressure and temperature condition. If the mean residence time of the SC-CO_2 in the extraction chamber is sufficient, the solute attains its equilibrium value at the chamber outlet.

By recalling that the degree of supersaturation (S) is defined as

$$S = \frac{y}{y_{eq}} \qquad (3.1)$$

where y and y_{eq} are, respectively, the mole fraction and equilibrium mole fraction of solute at the defined temperature and pressure at the same location in the process. Referring to **Figure 3.2**, the solution is prepared at any value of the solubility up to the value corresponding to the equilibrium solute concentration, i.e. $S \leq 1$, and leaves the extraction chamber at saturated conditions, i.e. $S = 1$.

b) *Setting of pre-expansion conditions.* After a supercritical solution of the desired solubility has been prepared, the pre-expansion conditions, the conditions just upstream of the expansion device, are established. The pre-expansion pressure is determined by the CO_2 pump and is held constant. The pre-expansion temperature is then established by heating the expansion device, usually a capillary nozzle. This temperature must be set high enough to prevent formation of dry ice which frequently leads to clogging of the nozzle. Heating the nozzle can increases the

solubility of the solute in SC-CO_2 $(S<1)$ and helps ensure that no precipitation of the solute occurs before the actual rapid expansion process. However, for polymer-CO_2 systems which exhibit retrograde behavior, heating the nozzle may decrease the solute solubility and causes a saturated solution to precipitate prior to the expansion $(S>1)$ (Lele and Shine, 1994; Mawson et al., 1995). In addition, for thermally sensitive polymers, an upper limit of pre-expansion temperature must be determine in order to prevent the thermal effects on the polymer properties. (Larson and King, 1986; Reverchon et al., 1995).

c) *Rapid expansion of supercritical solution to ambient conditions through an expansion device.* After the pre-expansion conditions are established, the supercritical solution is rapidly expanded across a nozzle. During expansion, the density of the SC-CO_2 decreases dramatically to gas-like values, resulting in very high supersaturations and precipitation of the solute from solution. The nucleation process, which subsequently leads to the solute precipitation, is initiated by pressure reduction. The depressurization travels at the speed of sound which favors uniform conditions during the expansion.

A typical nozzle used for the expansion is made of a capillary tube with an inner diameter ranging from 50 to 300 μm and a length-to-diameter ratio (*L/D*) from 150 to 6000.

d) *Recovery of product.* Scanning. The expansion chamber should be completely contained so that CO_2 can be vented. Electron Microscopy (SEM) stages covered with sticky carbon tape are used for recovery of

the product in the expansion chamber. (Alessi et al., 1996; Blasig et al., 2002). For particle size characterization, SEM is commonly used. An online particle size measurement method has been developed based on a three-wavelength extinction technique (Turk, 1999).

3.4 Poly($_{D,L}$-lactic-co-glycolic acid), PLGA

Poly($_{D,L}$-lactic-co-glycolic acid) or PLGA is a copolymer of hydrophobic poly lactic acid (PLA) and hydrophilic poly glycolic acid (PGA). It is known to be superior in biocompatibility and biodegradability, and is a useful material as base material for sustained-release formulation in drug delivery applications.

PLGA has a molecular structure as shown in **Figure 3.3**. It can be synthesized by means of random ring-opening co-polymerization of two different monomers, the cyclic dimers (1,4-dioxane-2,5-diones) of glycolic acid and lactic acid. During polymerization, successive monomeric units (of glycolic or lactic acid) are linked together in PLGA by ester linkages, yielding a linear aliphatic polyester as a product (Astete and Sabliov, 2006). Different forms of PLGA can be obtained depending on the ratio of lactide to glycolide used for the polymerization. These are usually identified in regard to the monomers' ratio used. For example, PLGA 75:25 identifies a copolymer whose composition is 75% lactic acid and 25% glycolic acid.

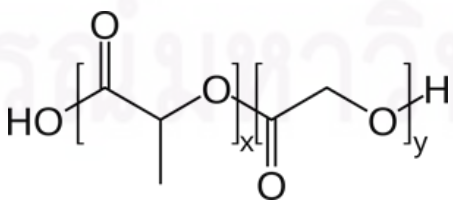

Figure 3.3 Molecular structure of PLGA

PLGA is amorphous polymer that has a glass transition temperature in the range of 40 to 60°C. It can be dissolved by common solvents, such as chlorinated solvents, tetrahydrofuran (THF), acetone or ethyl acetate. In the presence of water, PLGA degrades by hydrolysis of its ester linkages. The time required for degradation of PLGA is related to the ratio of PLA to PGA used in polymerization. Ratios higher in PLA show longer degradation times. For example, PLGA with a 75:25 ratio has a degradation time of 4 to 5 months, while 50:50 PLGA show a degradation time of 1 to 2 months (Saltzman, 2001). Beside its sustained-release property, PLGA can be fabricated into solid scaffold for use in cartilage regeneration (Astete and Sabliov, 2006).

3.5 Experimental

In this study, particle formation of PLGA by RESS process with ethanol as cosolvent has been studied in detail. A series of batch RESS experiments were carried out using the apparatus setup shown in **Figure 3.4** at pre-expansion pressure and temperature of 25 MPa and 313 K, and atmospheric post-expansion conditions. The expansion process was performed through capillary nozzles into ambient air. By using the solubility data from the solubility modeling work discussed in **Chapter II**, cosolvent concentrations up to 23.8 wt.% were used . The experimental results have been presented in terms of particle size, morphology and particle size distribution. The influences of change in cosolvent concentration on product characteristics were studied and discussed.

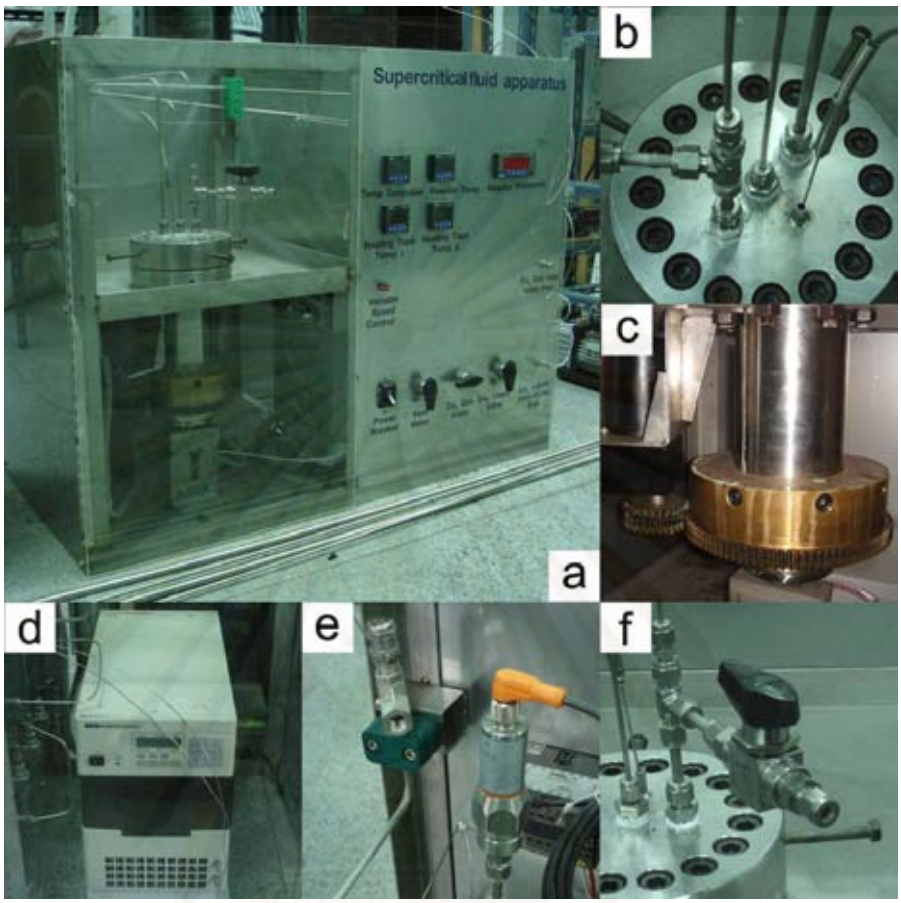

Figure 3.4 RESS experimental apparatus used in this study: (a) Apparatus housing with control panel; (b) Vessel cap with bolts, ports, thermocouple and vent pipe; (c) Magnetic stirrer and heater; (d) HPLC pump; (e) Pressure transducer and vent hole; (f) Spraying device.

3.5.1 Materials

Poly(lactic-co-glycolic acid) (PLGA) having properties shown in **Table 3.1** were purchased from Aldrich Chemicals Ltd. In each experiment, PLGA granules were grounded and classified to a certain size range of 100-200 μm. Liquid CO_2 (critical temperature $T_c = 304K$, critical pressure $P_c = 7.4\,MPa$, Suzuki Shokan Co.

Ltd., Tokyo, Japan) was used as solvent. Due to the limited solubility of PLGA in SC-CO_2, ethanol (special grade; > 99.5%; Kanto Chemical Co., Inc., Tokyo, Japan) was employed as cosolvent. All chemicals and materials were used as received.

Table 3.1 Properties of PLGA (reported by supplier; Aldrich Chemicals Ltd.)

$PLA:PGA$	M_w	$T_g\,(K)$
85:15	50,000-75,000	318-323

3.5.2 Experimental Procedure

Apparatus. **Figure 3.5** depicts schematic diagram of the experimental apparatus, which consists of a high-pressure pump (3), a stirred high-pressure vessel (6), and a spray nozzle (9). The high-pressure pump was equipped with a refrigerator (2) before the suction part to avoid cavitation. The high-pressure vessel had a capacity of 1,500 ml and maximum allowable operating pressure and temperature of 30 MPa and 473 K, respectively. During each experiment, the vessel temperature was kept constant at 313 K by using an automatically controlled electric heater (7). The spray nozzle (11) was simply made from a stainless steel tube with a length of 10 mm and was equipped with a shut-off valve (8). The spray nozzles has an inner diameter of 0.1 mm. In the case that the nozzle is easily clogged, a spray nozzle with an inner diameter of 0.3 mm may be employed. Temperature of the nozzle was kept constant at 423 K by a ribbon heater (10) to prevent the nozzle clogging with dry ice during spraying. A planar target (100mm×100mm×10 mm) (12) covered with aluminum foil was employed to collect samples of particles generated from the spray for characterization.

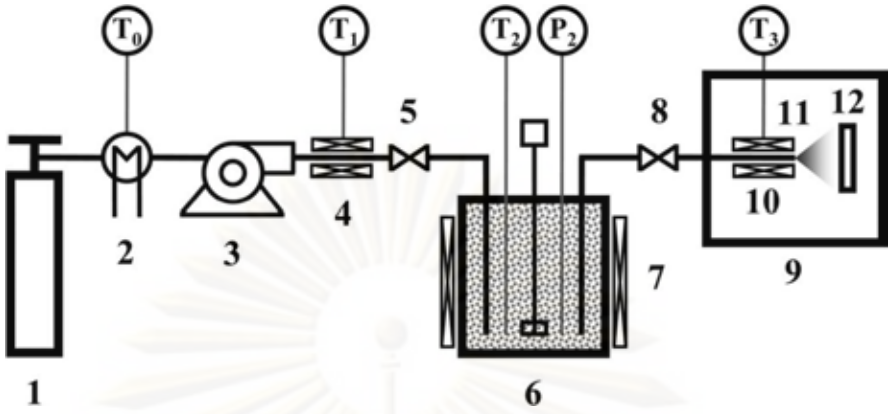

Figure 3.5 Schematic diagram of experimental apparatus: (1) CO_2 cylinder; (2) refrigerator; (3) HPLC pump; (4) heater; (5) regulating valve; (6) high-pressure vessel; (7) vessel heater; (8) shut-off valve; (9) atmospheric chamber; (10) ribbon heater; (11) nozzle; (12) target plate

Procedure. Meanwhile, the PLGA polymer used in this study has a limited solubility in SC-CO_2 because of its very high molecular weight (Tom et al., 1994). In order to increase the PLGA solubility in SC-CO_2 to a beneficial extent, ethanol was used as cosolvent. A 2 g portion of PLGA with different amounts of ethanol was placed in the high-pressure vessel for preparation of SC-CO_2 solution. After being carefully sealed, the vessel was heated and fed with CO_2 via the high-pressure pump until the desired supercritical conditions were achieved. The mixture in the vessel was stirred by a mixing paddle rotating at 300 rpm, and was left for 3 hours to achieve equilibrium. The prepared supercritical solution was then sprayed through the nozzle to allow its rapid expansion. The target plate was placed against the sprayed flow at a distance of 300 mm from the nozzle tip within a chamber under atmospheric conditions. In order to evaluate the particle formation performance, effect of

cosolvent concentration and diameter size of the spray nozzle on the size and size distribution of the particle samples was investigated. The experimental parameters and conditions used in this study are listed in **Table 3.2**. **Figure 3.6** depicts step-by-step conceptual representation of polymer particle formation using RESS.

Table 3.2 Experimental parameters and conditions of RESS process

Material	Solvent	CO_2; P_c = 7.4 MPa; T_c = 304 K; T_0 = 266 K; T_1 = 353 K
	Cosolvent	ethanol; 0-23.8 wt% (polymer-free basis); ρ = 789 kg/m^3
	Polymer	Poly(D,L-lactide-co-glycolide), PLGA; 85:15; M_w = 50,000-75,000; T_g = 318-323 K
Dissolution	Vessel	Cylinder; 1,500 ml
	Agitation	300 rpm; 180 min
	Conditions	P_2 = 25 MPa; T_2 = 313 K
Expansion	Nozzle	stainless steel; d = 0.1, 0.3 mm; L = 10 mm; T_3 = 423 K
	Spraying time	3 s
	Target distance	300 mm

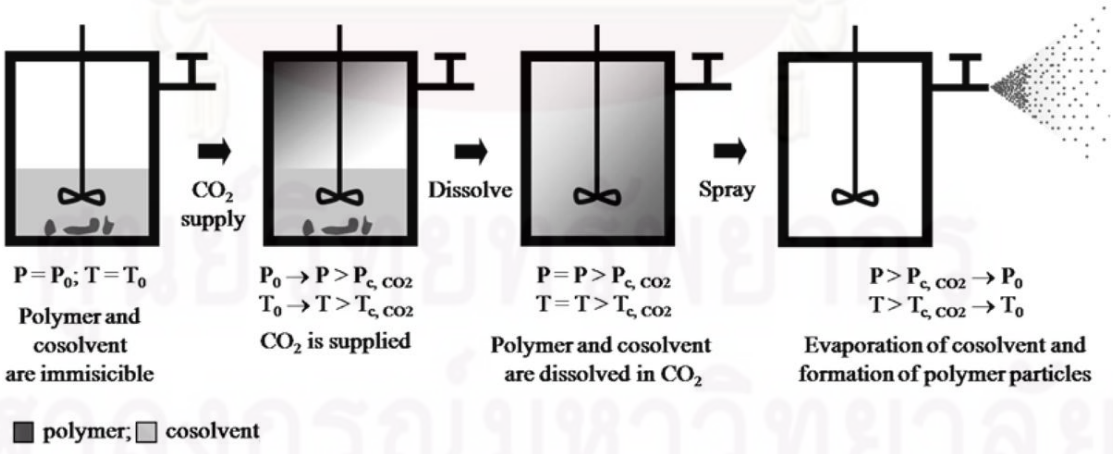

Figure 3.6 Schematic representation of polymer particle formation process by RESS with a cosolvent

Field emission scanning electron microscopy (FE-SEM; Hitachi, S-900) was used to examine the particle samples obtained from each experiment. For SEM sample preparation, the aluminum foil uncovered from the target plate was cut into a small piece, mounted on a specimen stub with conductive paint and coated with platinum by a sputtering device (Hitachi, E-1030) for 20 s. The SEM was operated at an accelerating voltage of 10 kV and a magnification between 1,000 and 200 k. The SEM images were processed for particle size analysis by using image-analyzing software (Image-Pro Plus version 3.0; Media Cybernetics).

3.6 Results and Discussion

3.6.1 Formation of PLGA particles by RESS

It is commonly accepted that ethanol is an environmentally friendly cosolvent used in the RESS of CO_2-insoluble pharmaceutical materials due to its low toxicity. In comparison with other alcohols, ethanol is a more economical commercial solvent of which scalable production is available. Thereby, ethanol has been chosen as the cosolvent in this work. Although results of the solubility modeling presented in Chapter II predicts that PLGA may have very limited or no solubility in pure SC-CO_2, it was reported that the PLGA solubility could be enhanced in mixture of SC-CO_2 and ethanol (Mishima et al., 2000). Since ethanol is capable of being both donor and acceptor of hydrogen bonds, it can self-associate through hydrogen bonding with both CO_2 molecules and hydroxyl groups on the backbone chains of PLGA, which leads to significantly improved PLGA solubility in SC-CO_2. The solubility enhancement of various polymers by ethanol cosolvent has been reported and discussed in several papers (Mishima et al., 1997; Guan et al., 1999; Mishima et al., 1999; Chafer et al.,

2004).

A solution of PLGA in SC-CO_2 plus ethanol was prepared at 25 MPa and 313 K. Under these conditions, several researchers have reported that CO_2 and ethanol become miscible at all compositions and form a single supercritical fluid phase (Jenning et al., 1991, Suzuki et al., 1991; Pohler and Kiran, 1997; Zuniga-Moreno and Galicia-Luna, 2002). A different amount of ethanol was added to the high pressure vessel at 0, 100, 200, 300 and 400 ml, respectively. Because the amount of PLGA dissolved in the CO_2-ethanol mixtures was very small, compared to that of CO_2 and ethanol, the ethanol concentration in the mixtures could be estimated, regardless of PLGA presented in the mixtures, from the vapor-liquid equilibrium data of CO_2 + ethanol system at 25 MPa and 313 K, reported by Pohler and Kiran (Pohler and Kiran, 1997) and Zuniga-Moreno and Galicia-Luna (Zuniga-Moreno and Galicia-Luna, 2002). The vapor-liquid equilibrium data necessary for evaluations of the ethanol concentration are summarized in **Table 3.3**. According to the varied amount of ethanol mentioned above, the calculated values of the polymer-free concentration of ethanol are 0, 6.2, 12.1, 17.8, and 23.8 wt.%, respectively.

In the experiments using pure SC-CO_2 and SC-CO_2 incorporated with 6.2 wt.% ethanol, negligible amounts of polymer particles were detected in the collected samples under SEM observations, thereby indicating negligible particle formation during the RESS process. This implied that both pure SC-CO_2 and SC-CO_2 incorporated with ethanol at 6.2 wt.% were unable to dissolve PLGA to a sufficient extent. As a result, supersaturation was not achieved to trigger particle nucleation in these cases.

Table 3.3 Phase equilibrium data of CO_2 (1) + ethanol (3) system at 25 MPa and 313 K (w = mass fraction, ρ = density)

w_1	w_3	$\rho\left(kg/m^3\right)$
0.0000	1.0000	795.70[a]
0.1000	0.9000	804.90[a]
0.2237	0.7763	835.82[b]
0.3022	0.6978	852.86[b]
0.3966	0.6034	866.57[b]
0.5456	0.4544	882.26[b]
0.7621	0.2379	884.00[b]
0.9000	0.1000	849.10[a]
1.0000	0.0000	851.10[a]

[a] Pohler and Kiran, 1997; [b] Zuniga-Moreno and Galicia-Luna, 2002

Figure 3.7 shows typical SEM images of PLGA particles produced by RESS using SC-CO_2 mixed with ethanol at 12.1**,** 17.8 and 23.8 wt.%. The charged amount of PLGA in SC-CO_2 with 23.8 wt.% ethanol was approximately 0.60 wt.% of the total amount of supercritical solution. Also in **Figure 3.7** it is clearly observable that the generated particles exhibit a nearly spherical shape with submicron size distributed in a narrow range. At the higher ethanol concentrations, the resulting PLGA particles were micrometer in size with an irregular surface. However, the increase in ethanol concentration could result in much smaller particles with smooth surface. This is attributed to higher vaporization of ethanol due to the higher ethanol weight percent and rigorous shear stress due to the rapid expansion of SC-CO_2 flow (Mohamed et al., 1989; Dixon et al., 1993).

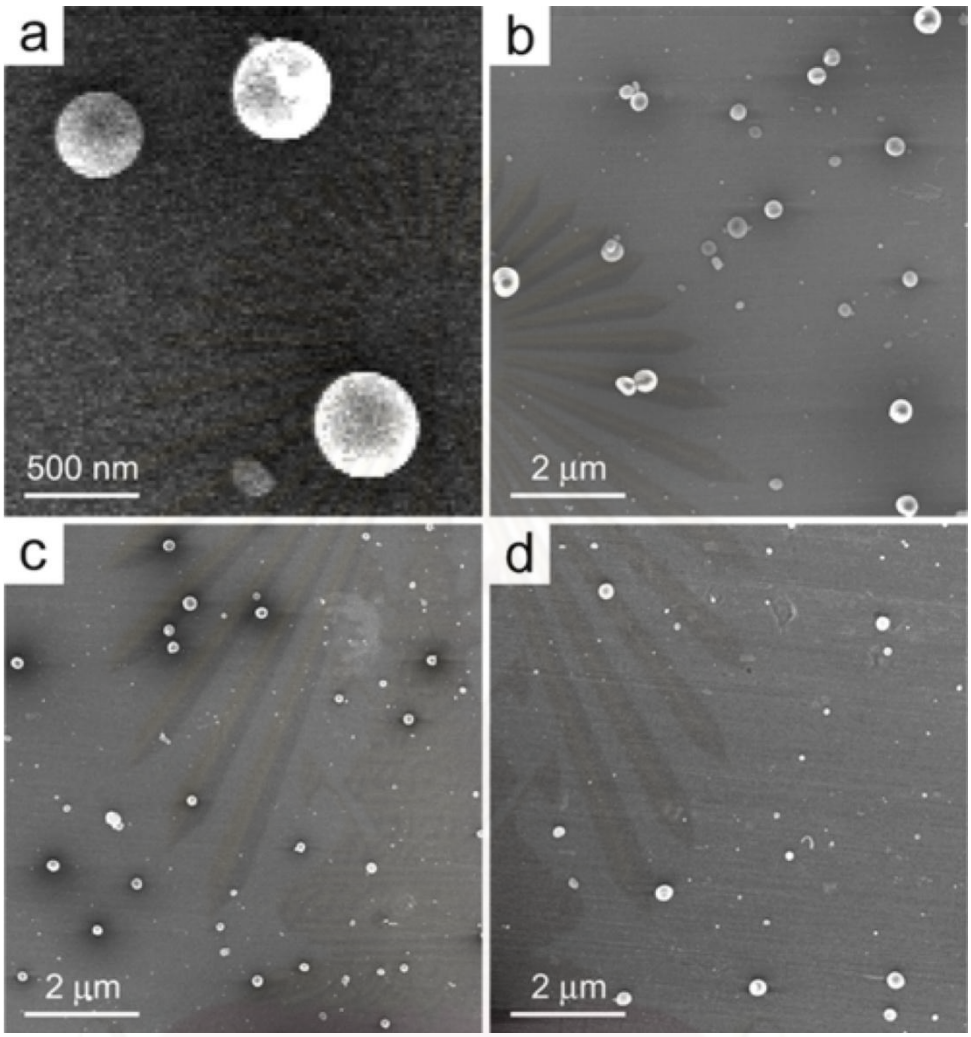

Figure 3.7 SEM images of PLGA particles produced by RESS using ethanol cosolvent at different ethanol concentrations: (a) and (b) 12.1 wt.%; (c) 17.8 wt.%; (d) 23.8 wt.%.

On the basis of these experimental results, the formation of PLGA particles via RESS could be described as follows. Under the equilibrium condition of SC-CO_2, PLGA, CO_2, and ethanol would form a single homogeneous supercritical solution though saturation of PLGA was not yet achieved. During the rapid expansion, phase transition from supercritical to gas-like state of CO_2 taking place in the post-

expansion free jet would result in a drastic increase in the PLGA solubility in the droplets, leading to precipitation of the dissolved polymer. As mentioned previously, since ethanol could not single-handedly dissolve PLGA, it also vaporized out during the expansion and then did not remain in the polymer (Dixon et al., 1993). Therefore, it is reasonable to consider that the precipitated polymer particles were solvent-free and did not undergo an agglomeration process because of its dilute solid content. These results suggested that the generated polymer particles would possibly be employed to coat core particles.

3.6.2 Effect of Cosolvent Concentration

Analyses of typical SEM images of particle samples obtained from the experiments at different cosolvent concentrations were carried out to determine their size distribution. At least 300 particles dispersed in different regions of the SEM images were taken into account in the determination of their size distribution.

Figure 3.8 reveals that the PLGA particles produced by RESS at different ethanol concentrations all exhibit log-normal size distribution behavior. The obtained geometric mean and standard deviation of the distribution were plotted as function of the ethanol concentration, as shown in **Figure 3.9**. It is clearly seen that the particle size distribution of the prepared PLGA particles was strongly dependent on the ethanol concentration. As the ethanol concentration was increased from 12.1 to 23.8 wt.%, the particle geometric mean decreased to a minimum of 55 nm while the geometric standard deviation increased to a maximum of 1.67. The decreased average size of precipitated PLGA particles would be ascribed to the increase in the PLGA solubility, thereby increasing the supersaturation of PLGA in the sprayed mixture

after its rapid expansion. According to the classical nucleation theory (Mohamed et al., 1989; Debenedetti, 1996), higher nucleation rate and smaller critical nucleus size could be expected if the dissolved polymer concentration becomes increased. Meanwhile, a higher supersaturation ratio would also result in the occurrence of "nucleation bursts" which could generate several families of random size particles in the early stage of nucleation (Giulietti et al., 2001). It is also noteworthy that an increase in the particle number concentration could provide higher coagulation frequency. These opposing phenomena were responsible for a smaller mean size but wider distribution of the resulting PLGA particles when a higher concentration of ethanol was used.

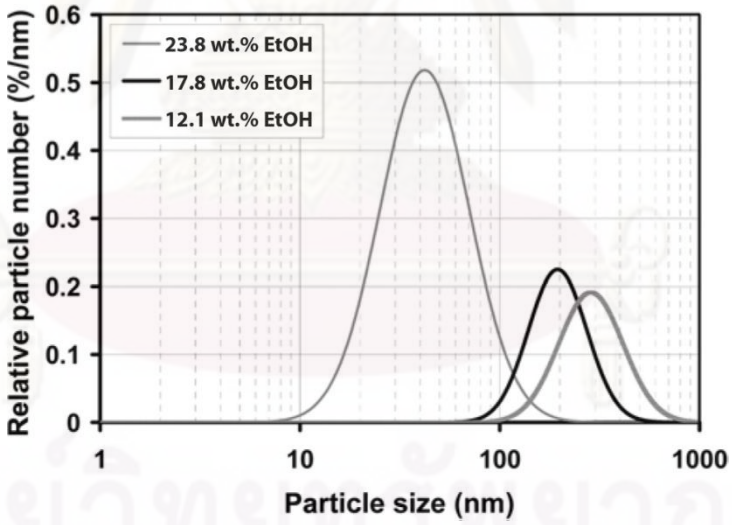

Figure 3.8 Dependence of particle size distribution of PLGA particles on ethanol concentration: log-normal particle size distributions

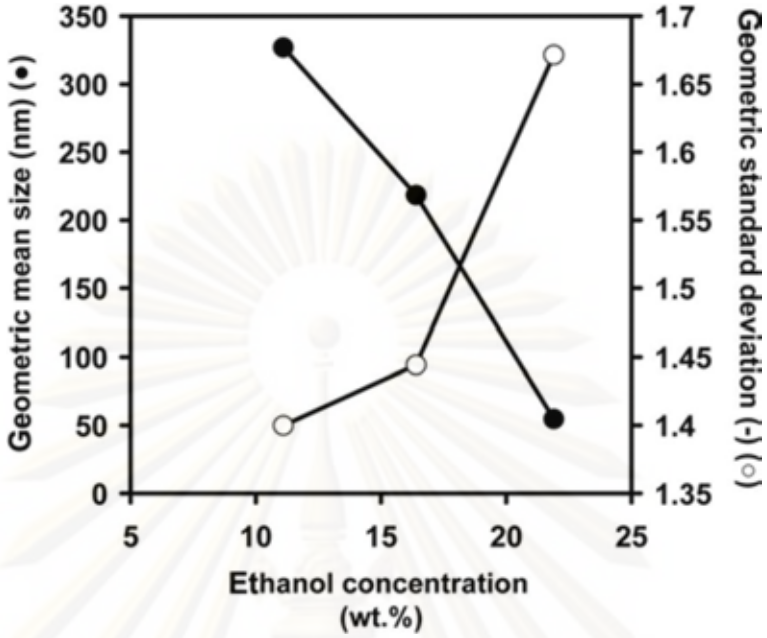

Figure 3.9 Dependence of particle size distribution of PLGA particles on ethanol concentration: mean particle size and standard deviation of particle size distribution as function of ethanol concentration

3.7 Conclusions

The rapid expansion of supercritical solution (RESS) process using ethanol as cosolvent was successfully carried out to produce non-agglomerated submicron particles of PLGA at 25 MPa and 313 K. Ethanol concentrations up to 23.8 wt.% were used. Notably, in contrast to the modeling results presented in **Chapter II**, the experimental results revealed that, with the assistance of ethanol cosolvent below 50 wt.%, it was possible to dissolve PLGA in SC-CO_2 to an extent sufficient for reliably achieving precipitation of PLGA by RESS. The inconsistency between the modeling and experimental results may be due to the wrong choice of Mixing rules, the inaccuracy of the binary interaction values taken from the literature, and the use of

oversimplified assumption of negligible amount of PLGA applied to the ternary mixture calculations. However, the experimental results supported the modeling"s prediction that the cosolvent concentration played a key role in the solubility behavior of PLGA in SC-CO_2, and correspondingly in the control of PLGA particle size and size distribution; the higher the cosolvent concentration, the higher the PLGA solubility, the smaller the average particle size and wider particle size distribution of the generated particles. According to the experimental results, a minimum average size of 55 nm was achieved for the generated PLGA particles obtained at 23.8 wt.% ethanol concentration. The influence of cosolvent concentration on the particle size and size distribution can be well described by the classical nucleation theory. The experimental results also suggested that coating of core particles with the precipitated PGLA would be possibly achieved by means of a modification to RESS of PLGA with SC-CO_2 and ethanol as cosolvent.

CHAPTER IV

COATING OF MICROSIZE SILICA AND NANOSIZE TITANIUM DIOXIDE POWDERS WITH POLY($_{D,L}$-LACTIC-CO-GLYCOLIC ACID) BY RAPID EXPANSION OF SUPERCRITICAL SUSPENSIONS

4.1 Introduction

Coating of powders has found its application in various industries, including pharmaceuticals, foods, agriculture and energetic materials. Normally, coating is considered as a shell-like barrier that protects powders from exposure to the environment or allows modification of powder surface functionality (Jono et al., 2000). In the pharmaceutical industry, the general purposes of coating are to provide protection from rapid degradation, control of release rate and prevention of side effect of therapeutic agents. While the conventional process used for coating powders is generally based on fluidization technique, there is a limitation for powders smaller than 70 μm in diameter because of poor fluidization behavior (Geldart, 1973). Emulsion-based techniques, such as water-in-oil-in-water (w/o/w) double emulsions or solid-in-oil-in-water (s/o/w) emulsions, may be used for coating ultra fine powders. However, due to the common use of organic solvents and harsh processing conditions, these emulsion-based techniques involve some drawbacks including alteration of structure of therapeutic agent, presence of residual organic solvent in the coated

powders and emission of volatile organic compounds to the environment (Fu et al., 1999; Wang et al., 2004).

In the last few decades, numerous attempts have been made on the application of supercritical fluids (SCFs) to overcome the problems of organic solvent in the conventional coating processes (Jung and Perrut, 2001). SCFs exhibit both liquid-like and gas-like properties with densities and solvent characteristics similar to those of the liquid and mass transfer similar to the gas. For pharmaceutical applications, carbon dioxide (CO_2) is the most commonly used SCF, due to its inert properties, non-toxicity, non-polluting nature and mild critical conditions.

Several studies have been reported on coating of microscale and nanoscale particles with polymers by using supercritical carbon dioxide (SC-CO_2) via different approaches (Mishima et al., 2000; Ribeiro Dos Santos et al., 2002; Tsutsumi et al., 2003; Wang et al., 2004). Process variables, such as feed composition of polymer and size of the host particles, were experimentally found to be the key parameters affecting the coating performance in these processes.

As mentioned earlier in **Chapter II**, it is well-known that the simplest SCF technique for formation of pharmaceutical particles and composite materials is the rapid expansion of supercritical solution (RESS) (Tom et al., 1994). With the RESS technique, a solute is dissolved in SC-CO_2 and the solution is then instantaneously depressurized by spraying it through a capillary nozzle, causing precipitation of the solute as SC-CO_2 vaporizes. Submicron- and nano-sized dry particles with a narrow particle size distribution could be prepared from various pharmaceutical compounds and polymers (Jung and Perrut, 2001). Meanwhile, there are also other similar processes recognized as supercritical antisolvent (SAS) or gas antisolvent (GAS) (Yeo

et al., 1993) and solution enhanced dispersion by supercritical fluids (SEDS) (Hanna and York, 1994). All of those processes have been discussed in **Chapter III** for both advantages and disadvantages, depending on conditions of their applications.

In the previous chapters (**Chapter II** and **Chapter III**), an initial investigation on the application of RESS process with ethanol as cosolvent for formation of PLGA (Poly($_{D,L}$-lactide-co-glycolide)) particles has been carried out. As suggested by the results of the investigation, the RESS process with ethanol as cosolvent is modified for coating of ultra fine powders with PLGA in this study. Microsize silica (SiO_2) and nanosize titanium dioxide (TiO_2) particles were chosen as preformed drug ultra fine powders, while PLGA was used as the coating material. Basically, PLGA-coated ultra fine powders can be used to investigate simple-diffusion controlled release of the drugs in subcutaneous and intravenous applications (Jono et al., 2000). Effects of the process parameters, which were the particle size of ultra fine core powder, spray nozzle diameter as well as powder to-polymer weight ratio, and mechanism of the coating process are presented and discussed based on the characterization results of coated powders regarding morphology and internal structure of coated particles.

4.2 Literature Review

Due to the limited solubility of several polymers in SC-CO_2 leading to low productivity of the RESS process for producing particles, the interest in application of RESS has shifted to particle coatings or producing composite particles as these applications did not require mass production of particles. In most cases, the RESS processes were carried out in a modified way in which a SC-CO_2 solution of polymer containing a suspension of microparticles of drugs was rapidly expanded. This

modified process was sometimes known as Rapid Expansion of Supercritical Suspension (Tsutsumi et al., 2000) or RESS coprecipitation. The earliest studies on the RESS coprecipitation were conducted by Debenedetti et al. (1993) on $_{D,L}$-PLA/lovastatin system and by Kim et al. (1996) on $_{L}$-PLA/naproxen system. In these studies, the polymer and drug were dissolved together in SC-CO_2 and expanded to atmospheric pressure. It was found that spherical polymer particles with embedded drug were produced along with some pure polymer and drug particles. Analysis of the produced particles showed that it was very difficult to control the concentration of the drug in polymer phase since proper manipulation of sequence of supersaturation of the two compounds was not achieved. For this reason, the research focus of RESS coprecipitation in later years moved to particle coating which was the more active area.

Many authors demonstrated that the RESS coprecipitation technique was useful for particle coating when the core particles were absolutely insoluble in SC-CO_2. Mishima et al. (2000) successfully coated protein microparticles with biopolymers using RESS process. In their work, microparticles of SC-CO_2-insoluble proteins (lysozyme and lipase) were suspended in a SC-CO_2 solution of polymer (polyethyleneglycols (PEG), PMMA, $_{L}$-PLA, $_{D,L}$-PLGA) containing a cosolvent (alcohols) which was a non-solvent for the polymer. The suspension was then sprayed to atmospheric pressure, resulting in polymer-coated protein microparticles. The coating process took advantage of the solubility difference of polymer (soluble) and protein (insoluble) in supercritical mixtures of CO_2 and cosolvent. The study showed that the thickness of polymer coating layer was controlled by varying the compositions of polymer and protein in the feed.

In 2003, Matsuyama et al. (2003) successfully produced microcapsules by encapsulating medicines with polymers using the RESS coprecipitation technique assisted with a cosolvent which was a non-solvent for the polymers. The authors introduced a new term namely Rapid Expansion of Supercritical Solution with a Non-solvent or RESS-N for this process. The particle encapsulation process was carried out by first preparing a suspension of medicine (p-acetamidophenol, acetylsalicylic acid, 1,3-dimethylxanthine, flavones and 3-hydroxyflavone) in SC-CO_2 containing a cosolvent (alcohols) and dissolved polymer (PEGs, PMMA, ethyl cellulose and PEG-PPG-PEG triblock copolymer) and then spraying the resulting suspension through a nozzle to atmospheric pressure. They found that the solubilities of the polymer and the medicine were very low in pure CO_2 and in pure cosolvent; however, the polymer solubility became significantly increased in the mixture of the two. During RESS-N, microcapsules consisting of the medicine as core and the polymer as coating were formed according to the precipitation of the polymer onto the medicine particles. The thickness of polymer coating was controlled with changes in the feed composition of the polymer. The authors also noted advantages of this process associated with the use of the non-solvent in (1) raising the polymer solubility in SC-CO_2, (2) producing solvent-free product and (3) preventing agglomeration of the produced microcapsules.

Turk et al. (2003) conducted and described the coprecipitation process of β-sitosterol and Eudragit (an ethyl acrylate-methyl methacrylate copolymer) by RESS. This process led to formation of finely-divided β-sitosterol/ Eudragit particles with less than 500 nm in diameter.

Tsutsumi et al. (2003) also applied the RESS coprecipitation technique to coat 1-μm and 20-nm SC-CO_2-insoluble core particles with paraffin in an impinging-

stream reactor. Paraffin was a low-molecular weight polymer which had reasonably high solubility in SC-CO_2. In their work, supercritical suspensions were formed by dispersing the core particles in supercritical solutions of paraffin. By means of rapid expansion of the supercritical suspensions from two capillary nozzles located at each side of the impinging-stream reactor, a uniform paraffin coating was achieved in the single 1-μm particle and in the agglomerate of 20-nm particle. They also observed the influence of impinging distance on the coating rate of the core particles.

Besides the RESS coprecipitation methods, it was reported that drug/polymer composite particles could also be generated by impregnating drug materials into polymer matrix using RESS impregnation technique. Cristini et al. (2003) reported the application of this technique to producing microsize composite particles of ibuprofen (drug) within α-lactose and β-cyclodextrin (polymer). In this study, a SC-CO_2 containing dissolved ibuprofen was sprayed into a stirred vessel previously introduced with particles of the polymers. The impregnation of drug into the polymer was allowed by the precipitation of ibuprofen by RESS in the presence of the polymer particles under the vigorous agitation. The study showed an improvement on the dissolution rate of impregnated ibuprofen in the composite particles compared to plain drug particles.

4.3 Description of Rapid Expansion of Supercritical Suspension Process

With CO_2 as SCF, the principle of rapid expansion of supercritical suspension or RESS Coprecipitation process is similar to that of the RESS process for particle formation, which has been described in **Chapter III**. The RESS coprecipitation process for particle coating takes advantage of the difference in solubilities of core

particles and polymer in the mixture of SC-CO_2 and a cosolvent. The insoluble core particles are suspended whereas the polymer is soluble, forming a suspension of the core particles in the supercritical solution of the polymer in SC-CO_2 plus ethanol. During rapid expansion, the polymer will precipitate, cumulatively deposit on the core particle surface and form a polymer shell surrounding the core particles. **Figure 4.1** represents a simplified diagram of the RESS coprecipitation process.

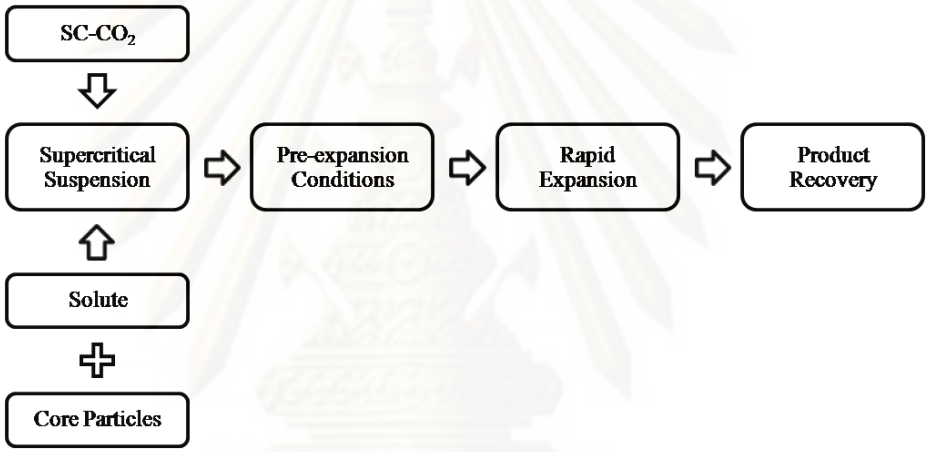

Figure 4.1 Simplified diagram of rapid expansion of supercritical suspension (RESS coprecipitation) process

4.4 Experimental

4.4.1 Materials

Silica (SiO_2) powder with a nominal diameter of 1.4 μm (Kojundo Chemical Lab, Japan) and titanium dioxide (TiO_2) powder with a nominal diameter of 70 nm (Ishihara Sangyo Kaisha, Japan) were employed in this study. Poly($_{D,L}$-lactic-co-glycolic acid) (PLGA) having properties shown in **Table 3.1** were purchased from

Aldrich Chemicals Ltd. In each experiment, PLGA granules were grounded and classified to a certain size range of 100-200 μm. Liquid CO_2 (critical temperature $T_c = 304K$, critical pressure $P_c = 7.4\,MPa$, Suzuki Shokan Co. Ltd., Tokyo, Japan) was used as and solvent. Due to the limited solubility of PLGA in SC-CO_2, ethanol (special grade; > 99.5%; Kanto Chemical Co., Inc., Tokyo, Japan) was employed as cosolvent. All chemicals and materials were used as received.

4.4.2 Apparatus and Procedure

Apparatus. **Figure 4.2** depicts schematic diagram of the experimental apparatus, which consists of a high-pressure pump (3), a stirred high-pressure vessel (6), and a spray nozzle (9). The high-pressure pump was equipped with a refrigerator (2) before the suction part to avoid cavitation. The high-pressure vessel had a capacity of 1,500 ml and maximum allowable operating pressure and temperature of 30 MPa and 473 K, respectively. During each experiment, the vessel temperature was kept constant at 313 K by using an automatically controlled electric heater (7). The spray nozzle (11) was simply made from a stainless steel tube with a length of 10 mm and was equipped with a shut-off valve (8). Two spray nozzles with different inner diameters of 0.1 mm and 0.3 mm were employed for investigating the effect of nozzle diameter size on the morphology, size and size distribution of the product samples. Temperature of the nozzle was kept constant at 423 K by a ribbon heater (10) to prevent the nozzle clogging with dry ice during spraying. A planar target (100mm×100mm×10 mm) (12) covered with aluminum foil and a carbon-coated copper microgrid was employed to collect samples of particles generated from the spray for characterization.

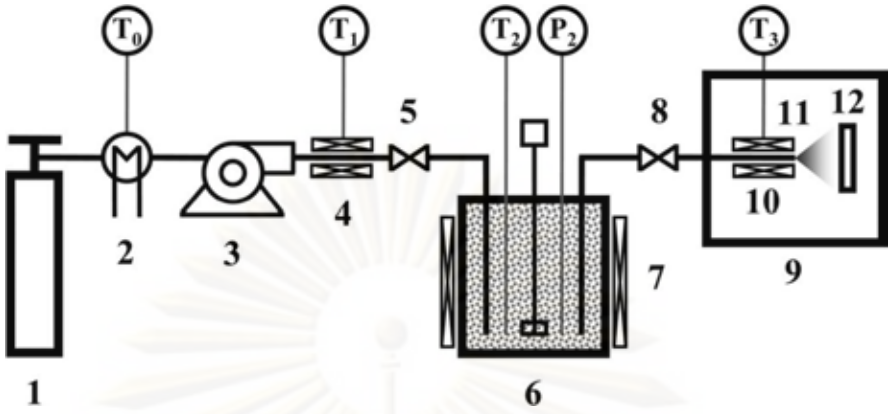

Figure 4.2 Schematic diagram of experimental apparatus: (1) CO_2 cylinder; (2) refrigerator; (3) HPLC pump; (4) heater; (5) regulating valve; (6) high-pressure vessel; (7) vessel heater; (8) shut-off valve; (9) atmospheric chamber; (10) ribbon heater; (11) nozzle; (12) target plate.

Procedure. It should be noted that the ultra fine powder, PLGA and ethanol, in pure form, are not soluble in each other. Thus, they form an immiscible ternary mixture under atmospheric conditions. Experimental procedures similar to those described in **Section 3.5.2** were carried out so as to dissolve PLGA in SC-CO_2 with the aid of ethanol in the presence of microsize SiO_2 or nanosize TiO_2 core particles. It should be noted that in this study nanosized TiO_2 powder was selected because of its low agglomeration and monodispersity compared with those of the more expensive nanosized SiO_2. Under these conditions, the core particles were not dissolved but suspended in a single homogenous supercritical phase of CO_2, ethanol and the dissolved PLGA. The supercritical suspensions were then allowed to expand through the nozzle for a few seconds. It could be observed from each experiment that in the case of PLGA expansion without core particles, there is nothing remaining in the

autoclave. However, when core particles and PLGA were taken into account, after expansion there would be some residues left in the vessel. After expansion, all coated particles were collected for characterization by using the target plate as already mentioned above. In order to evaluate the coating performance, effect of three process parameters, i.e., diameter of the spray nozzle, particle size of the core powder and powder-to-polymer weight ratio, on the coating characteristics was investigated. The experimental parameters and conditions used in this study are listed in **Table 4.1**. **Figure 4.3** depicts step-by-step conceptual representation of polymer coating of powder by RESS coprecipitation process.

Table 4.1 Experimental parameters and conditions of RESS coprecipitation process

Material	Solvent	CO_2; P_c = 7.4 MPa; T_c = 304 K; T_0 = 266 K; T_1 = 353 K
	Cosolvent	ethanol; 0-23.8 wt% (polymer-free basis); ρ = 789 kg/m^3 (reported by supplier)
	Polymer	Poly(D,L-lactide-co-glycolide), PLGA; 85:15; M_w = 50,000-75,000; T_g = 318-323 K; 2 g
	Powder	SiO_2; mean particle size 1.4 μm TiO_2; mean diameter 70 nm
	Core-to-polymer	1:1, 2:1, 3:1, 4:1 (weight ratio)
Dissolution	Vessel	Cylinder; 1,500 ml
	Agitation	300 rpm; 180 min
	Conditions	P_2 = 25 MPa; T_2 = 313 K
Expansion	Nozzle	stainless steel; d = 0.1, 0.3 mm; L = 10 mm; T_3 = 423 K
	Spraying time	3 s
	Target distance	300 mm

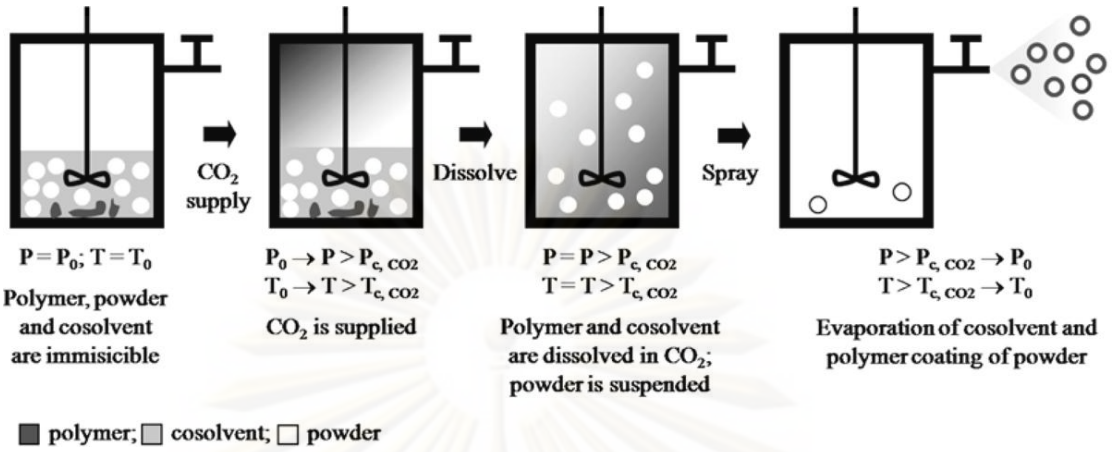

Figure 4.3 Schematic representation of coating of powder with polymer by RESS coprecipitation with a cosolvent

Field emission scanning electron microscopy (FE-SEM; Hitachi, S-900) was used to examine the particle samples obtained from each experiment. For SEM sample preparation, the aluminum foil uncovered from the target plate was cut into a small piece, mounted on a specimen stub with conductive paint and coated with platinum by a sputtering device (Hitachi, E-1030) for 20 s. The SEM was operated at an accelerating voltage of 10 kV and a magnification between 1,000 and 200 k. For verification of polymer coating of the ultra fine powder, the particle samples on the microgrid were further analyzed by a transmission electron microscope (TEM; JEOL 2000-EX) operated at 200 kV in the bright-field mode. To analyze the structures and morphology of the coated powders, the mass-thickness contrast between the coating polymer and the core powder was taken into account.

4.5 Results and Discussion

4.5.1 Effect of RESS on the Deagglomeration of Microsize SiO_2 and Nanosize TiO_2 Powders

Ultra fine particles have a strong tendency to agglomerate due to their van der Waals interactions. In general, spontaneous agglomeration of ultra fine powders could take place and result in particle size enlargement and unstable processing conditions in the conventional coating processes (Mohamed et al., 1989). In the RESS process, in which the expansion flow is considered as a supersonic or at least free jet, tempestuous turbulence is expected to be developed in the rapid expansion flow (Sun et al., 2002; Helfgen et al., 2003). This turbulence could provide an advantageous contribution to the disintegration of agglomerates of ultra fine powders to facilitate the formation of a coating layer on the primary particles.

Figure 4.4 shows typical SEM images of silica and titanium dioxide ultra fine particles before and after performing the rapid expansion of their suspensions in mixtures of SC-CO_2 and ethanol. The suspensions were prepared with 23.8wt.% ethanol in SC-CO_2 under conditions of 25 MPa and 313K. Before rapid expansion, it could be observed that the ultra fine powders could agglomerate to form large particles as revealed in **Figure 4.4(a)** and **Figure 4.4(b)**. The agglomerate sizes are approximately 2-5 μm for the fine silica powder and 3-20 μm for the ultra fine titanium dioxide powder. **Figure 4.4(c)**, **Figure 4.4(d)** and **Figure 4.4(e)**, **Figure 4.4(f)** illustrate the change in the morphology of the ultra fine powders prepared by rapid expansion through nozzles with different diameters of 0.1 and 0.3 mm, respectively. Deagglomeration of the ultra fine powders was observed and consistently indicated by a decrease in the agglomerate size and an increase in the

number concentration of primary particles. It could be implied that the dispersion and deagglomeration of the ultra fine powders were achieved as a combined result of boundary friction due to flow along the nozzle wall, turbulence in the high-velocity fluid and collisions between the ultra fine powder particles along the rapid expansion path. The boundary friction and the turbulence were responsible for fragmentation of large powder agglomerates into smaller ones, whereas the particle collisions could result in either particle coagulation or particle dispersion depending on relative velocities and collision angles of the particles.

Comparison between the SEM images of particle samples produced by these two nozzles suggests that a better dispersion and deagglomeration effect was achieved with the bigger 0.3-mm diameter nozzle, and the effect was stronger for the larger silica fine powder. This reveals the influences of nozzle diameter and particle size of the ultra fine powder on the performance of dispersion and deagglomeration of the ultra fine powder in the rapid expansion process. As pointed out by Smith et al. (Smith et al., 1986), at the same pre- and post-expansion conditions, an increase of the nozzle diameter results in a higher Reynolds number, more turbulence, a higher total flow rate and a larger friction loss. In addition, with shorter residence time the probability of particle coagulation becomes lower. These lead to an improvement of the dispersion and deagglomeration of the ultra fine powders. Accordingly, the cohesive forces are smaller, the number concentration lower and the probability of particle coagulation lower for large particles compared with the small ones. The reasoning supports our experimental results that the dispersion and deagglomeration of the 1.4-μm silica powder were better than that of the 70-nm titanium dioxide powder. It should be noted that in case of the ideal condition, individual core particles

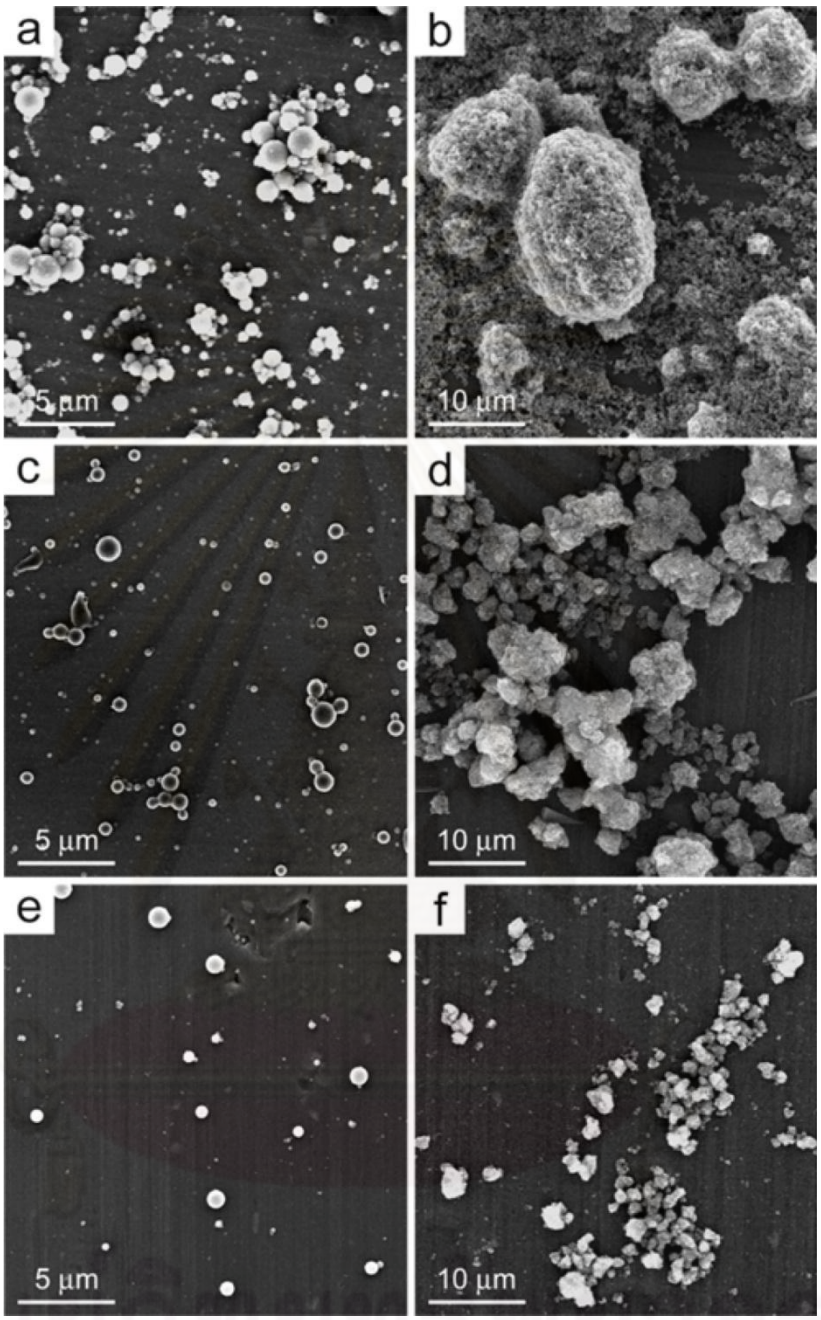

Figure 4.4 Effect of diameter of spray nozzle on the deagglomeration of ultra fine powders. *1.4-µm silica:* (a) before expansion; (c) after expansion (nozzle diameter 0.1 mm); (e) after expansion (nozzle diameter 0.3 mm). *70-nm titanium dioxide:* (b) before expansion; (d) after expansion (nozzle diameter 0.1mm); (f) after expansion (nozzle diameter 0.3mm)

should be obtained if agglomeration can be completely suppressed by the rapid expansion. Therefore, a smaller nozzle would reasonably be expected to provide the well dispersed core particles after the expansion. However, it was coincidentally found that the smaller nozzle was easily clogged. To avoid this difficulty as well as to obtain a favorable coating process with low agglomeration tendency, the 0.3-mm diameter nozzle was selected for the coating of the ultra fine powders, which will be discussed in the next section.

4.5.2 Coating of Microsize SiO_2 and Nanosize TiO_2 Powders with PLGA by Rapid Expansion of Supercritical Suspensions

A series of experiments was carried out on coating 1.4-μm silica particles and 70-nm titanium dioxide particles with PLGA by rapid expansion of supercritical suspensions to investigate the effect of experimental parameters on coating performance. In a real situation, preformed drug particles, i.e. dexamethasome and insulin, would be employed for the coating process to verify their sustain-release performance (Liu et al., 2006; Zolnik and Burgess, 2007). However, because of the economic constraints as well as the scope of this study which focused on the physical aspects of coating, commercial silica and titania particles with designated size were chosen as model particles for coating experiments. Regarding those physical aspects, i.e. coating film thickness and degree of agglomeration, they are useful data for further examination of the releasing rate of coating drug particles.

In all experiments, the supercritical suspensions were prepared by using the conditions at which the solubility of PLGA in the mixture of SC-CO_2 and ethanol could be determined, i.e., the supercritical pressure and temperature of 25 MPa and

313 K, the ethanol concentration of 23.8 wt.% and the polymer solubility of 0.15 wt.%. The powder-to-polymer weight ratio was varied through an adjustment of the powder concentration in the suspension by changing the amount of powder added to the high-pressure vessel at the beginning of each experiment.

Effect of powder-to-polymer weight ratio. **Figure 4.5** shows some samples of the morphology and internal structure of PLGA-coated silica fine powder produced by the rapid expansion of supercritical suspension process at different powder-to-polymer weight ratios. It appears that the coating of silica fine powder was achieved in the form of both individual dispersed particles and agglomerates. The coated silica particles exhibit a core-shell structure, as shown in the bright-field TEM images (**Figure 4.5(b)** and **Figure 4.5(d)**). Due to the stronger interactions between the electrons and silicon than that between the electrons and carbon (a major component of the polymer) in the TEM, the silica particles appear as a darker contrast area than the PLGA phase in these images. It is clearly seen that the darker contrast area is thoroughly covered by the lighter contrast area, indicating that the silica particles were completely coated with a layer of PLGA. The rapid expansion of a suspension of SC-CO_2-insoluble particles in the supercritical CO_2 solution of a polymer led to deposition of the polymer on the surface of the suspended particles, thereby generating polymer film coating on the particle surfaces (Mishima et al., 2000; Tsutsumi et al., 2003). These experimental results consistently agree with this explanation.

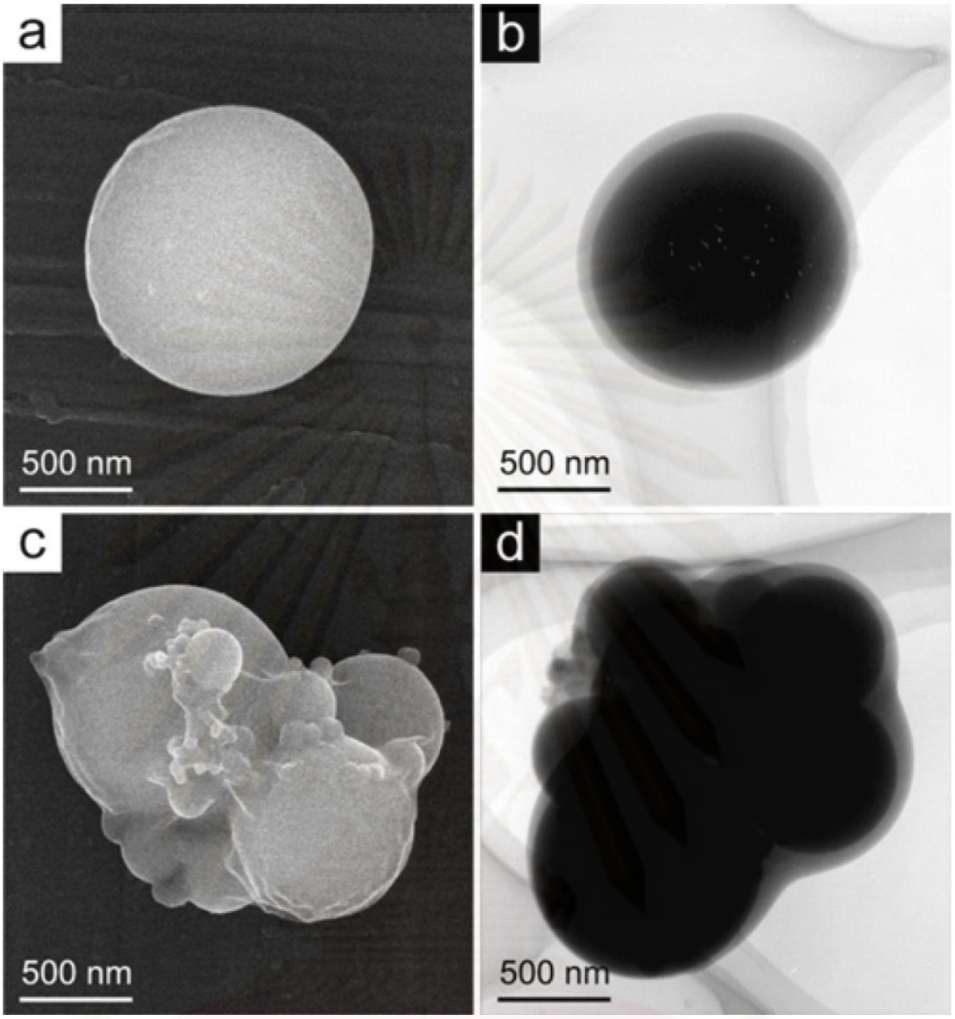

Figure 4.5 SEM and TEM images of PLGA-coated silica fine powder produced by the rapid expansion of supercritical suspension process at powder-to-polymer weight ratios: (a) and (b) 1 : 1; (c) and (d) 3 : 1

When **Figure 4.5** is compared with **Figure 4.4(a)**, it is clear that, as a concurrent result of the rapid expansion of supercritical suspension, the dispersion and segregation of the silica fine powder contributed to the low agglomeration tendency of the coated particles. It was observed that, at the powder-to-polymer weight ratio of 1, there was no significant agglomeration of coated silica particles that took place during

the coating process (**Figure 4.5(a)** and **Figure 4.5(b)**), while the agglomeration process appeared to be enhanced when the powder-to-polymer weight ratio was increased to 3 (**Figure 4.5(c)** and **Figure 4.(d)**). This is mainly attributable to the increased number concentration of silica particles in the rapid expansion flow, resulting in more frequent collisions and higher coagulation probability of the silica particles within the nozzle, and consequently an increase in the degree of particle agglomeration. In addition, it can be observed in the TEM images that the thickness of the coating layer was not uniform and estimated to be around 10-100 nm from the scale bar. It is likely that the PLGA particles, which precipitated and then deposited on the silica particle surface, spread and formed solid bridges between them, thereby resulting in growth of the coating layer. The strong turbulence in the rapid expansion flow dissipated much of the eddy energy (Sun et al., 2002), which can be considered to cause significant disturbances to the just-formed coating layer.

It is interesting to note that, from the experimental results, the coating layer thickness seems not to be sensitive to the change in the powder-to-polymer weight ratio. As a possible assumption, the particle coagulation along the length of the nozzle during the rapid expansion flow plays a significant role in the coating process. Particle coagulation results in a drastic decrease in the particle number and a drastic reduction of the particle surface area, on which coating takes place. The higher the probability of particle coagulation, the more pronounced the reduction of the coating surface area and capability. Since the particle coagulation probability is proportional to the powder-to-polymer weight ratio in the coating process, it might be assumed that the change in powder-to-polymer weight ratio did not provide a significant change in the total coating surface area and it had no influence on the coating layer thickness.

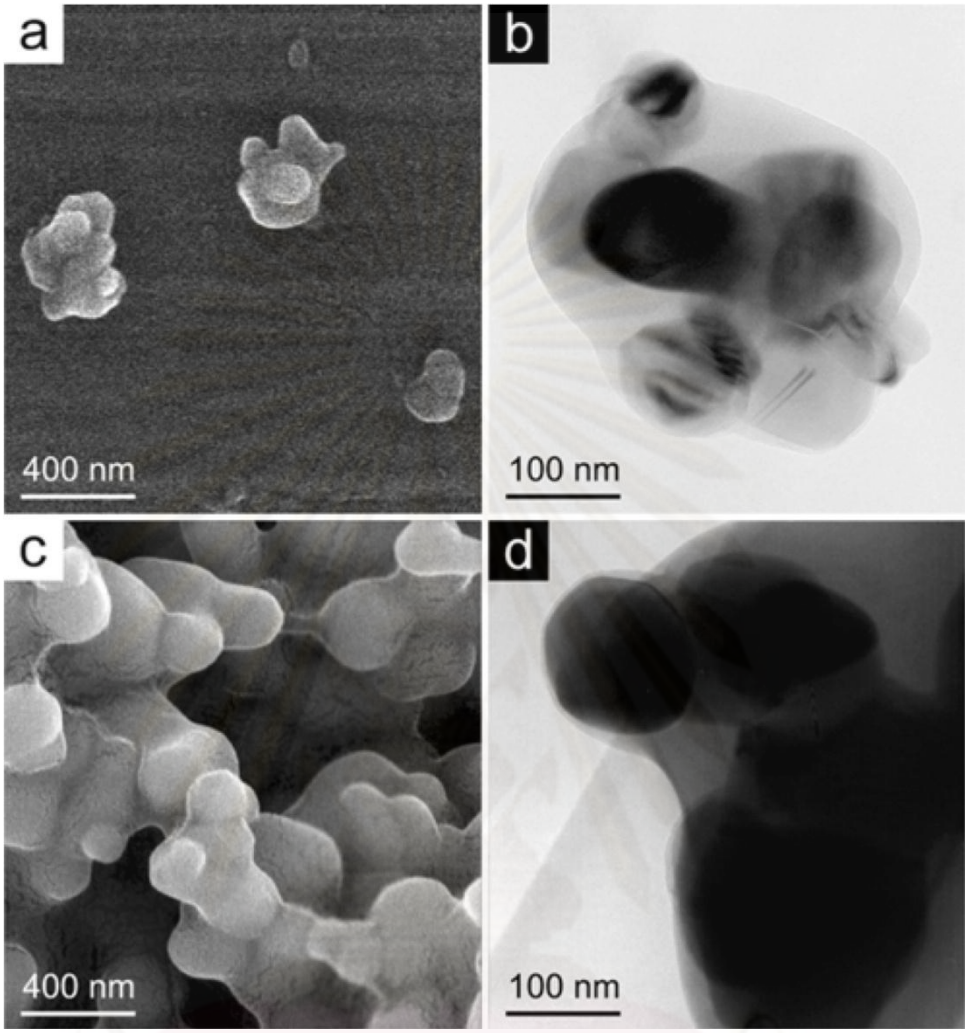

Figure 4.6 SEM and TEM images of PLGA-coated titanium dioxide ultra fine powder produced by the rapid expansion of supercritical suspension process at different/specified powder-to-polymer weight ratios: (a) and (b) 1 : 1; (c) and (d) 3 : 1

Similar results were obtained for the coating of 70-nm titanium dioxide ultra fine powder with PLGA, as shown in **Figure 4.6**. When compared with **Figure 4.5**, the experimental results shown in **Figure 4.6** suggest that the coating of titanium dioxide ultra fine powder with PLGA could also be achieved in the same process as that of silica fine powder. However, SEM and TEM images reveal that the coating of

titanium dioxide ultra fine powder always took place in the form of agglomerates of primary particles. In **Figure 4.6(b)** and **Figure 4.6(d)**, the coated particles are composed of an agglomerate of titanium dioxide particles in the core and a coat of PLGA as shown by the darker and the lighter contrast areas, respectively. It should be noted that no PLGA is observed in the void among the titanium dioxide particles, suggesting that the PLGA coat was formed as a growing layer on the titanium dioxide agglomerate surface, not a coalescence of coated primary particles. The agglomerate sizes are in the range of some hundred nanometers to a few microns, which is consistent with the typical size of agglomerates shown in **Figure 4.4(f)**. Obviously, the flow turbulence and friction loss generated during the rapid expansion of supercritical suspension process was not sufficient to disintegrate agglomerates into primary particles. This is attributable to the extremely strong adhesion forces among the nanosize titanium dioxide particles. The non-uniformity of the coat can also be observed in the TEM images, indicating the deposition of relatively large PLGA particles on the irregular surfaces of the titanium dioxide agglomerates. Anyway, the change of powder-to-polymer weight ratio from 1:1 to 3:1 did not cause a significant change in the coating layer thickness. The thickness is estimated from the scale bar to be around 10-100 nm, which is comparable to that of the fine silica particles.

Table 4.2 summarizes the results on size measurement of coated silica and titanium dioxide powders obtained from experiments using 0.3-mm diameter nozzle at different powder-to-polymer weight ratios. Influence of the powder-to-polymer weight ratio on the average size of the coated powders is depicted virtually in **Figure 4.7**. It could be clearly confirmed that, with the increase in the powder-to-polymer weight ratio, the average sizes of the coated silica and titanium dioxide powders

became larger, indicating the higher agglomeration and possibly the thicker coating layer. However, the silica powders exhibited a much lower degree of agglomeration regarding a lower increasing rate of the average sizes with respect to the increased powder weight ratio in comparison with those of the titanium dioxide powder.

Table 4.2 Average sizes $\left(\overline{d}_p\right)$ of coated 1.7-μm silica and 70-nm titanium dioxide powder obtained by using 0.3-mm diameter nozzle at different powder-to-poymer weight ratios

	Powder-to-polymer weight ratio			
	1:1	2:1	3:1	4:1
$\overline{d}_{p,SiO_2}$ (nm)	1500	1600	2000	2200
$\overline{d}_{p,TiO_2}$ (nm)	80	110	380	700

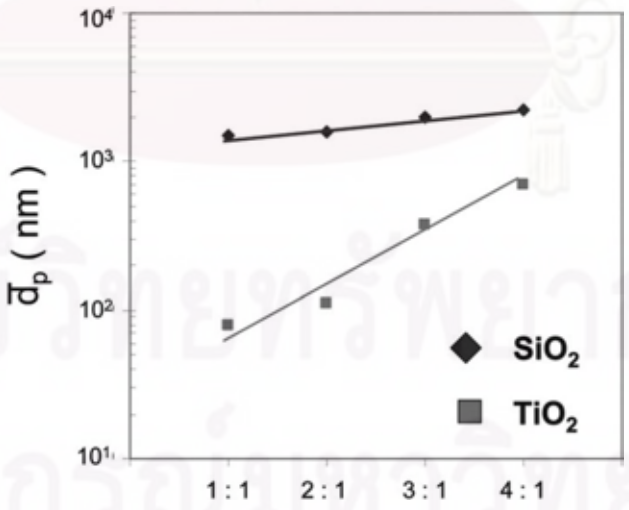

Figure 4.7 Effect of powder-to-polymer weight ratio on the average sizes of coated silica and titanium dioxide powders

Table 4.3 Influence of powder-to-polymer weight ratio and nozzle diameter on coating operatability

Powder-to-polymer weight ratio	Nozzle diameter size	
	0.1 mm	0.3 mm
1 : 1	total ice clogging	uniform spraying $\overline{d}_{p,SiO_2} = 1500\ nm$ $\overline{d}_{p,TiO_2} = 80\ nm$
2 : 1	partial ice clogging $\overline{d}_{p,SiO_2} = 1700\ nm$ $\overline{d}_{p,TiO_2} = 120\ nm$	uniform spraying $\overline{d}_{p,SiO_2} = 2000\ nm$ $\overline{d}_{p,TiO_2} = 380\ nm$
3 : 1	uniform spraying $\overline{d}_{p,SiO_2} = 2000\ nm$ $\overline{d}_{p,TiO_2} = 380\ nm$	uniform spraying $\overline{d}_{p,SiO_2} = 2000\ nm$ $\overline{d}_{p,TiO_2} = 380\ nm$
4 : 1	partial ice clogging $\overline{d}_{p,SiO_2} = 2000\ nm$ $\overline{d}_{p,TiO_2} = 380\ nm$	partial ice clogging $\overline{d}_{p,SiO_2} = 2000\ nm$ $\overline{d}_{p,TiO_2} = 380\ nm$

Effect of nozzle diameter size. **Table 4.3** summarizes the effect of nozzle diameter size on coated product characteristics and the operatability of RESS process investigated in this study. It could be clearly observed that there was only a limited condition of operable RESS when the 0.1-mm diameter nozzle was employed. With a lower powder-to-polymer weight ratio, or in other words “a high fraction of polymer”, rapid expansion could only be conducted at the first short moment, then the nozzle tip would be totally covered by ice due to the isenthalpic Joule-Thompson effect. A higher polymer fraction would lead to a more serious Joule-Thompson effect because of its fluid behavior (Tom et al., 1994). On the other hand, when the powder-to-

polymer weight ratio was increased to 4:1, the clogging of nozzle was caused by the sticking of the agglomeration of coated powders. There was only the condition of powder-to-polymer weight ratio of 3:1 which could provide the coated powders.

On the other hand, with the 0.3-mm nozzle no clogging due to the Joule-Thompson effect could be observed. Coating of powders could be smoothly conducted until the powder-to-polymer weight ratio was increased to 4:1 which partial clogging of the nozzle would take place due to the sticking of agglomerated powders (Mohamed et al., 1989). Similarly, these results would be ascribed that the high powder fraction would bring about the rigorous agglomeration of coated powders as could also be confirmed by the increased average sizes depicted in **Figure 4.7**. For the coated silica particles, the increasing size was relatively low when compared with that of coated titanium dioxide particles which preferred to agglomeration. The agglomeration would be compensated by the shear stress due to the turbulent flow of rapid expansion of the supercritical suspension (Tsutsumi et al., 2003). All the coated powders prepared by the 0.3-mm diameter nozzle possessed the physical characteristics as shown in **Figure 4.5** and **Figure 4.6**. Therefore, it would be worth to mention that the bigger 3-mm diameter nozzle could provide broader range for the RESS of powder coating with PLGA in comparison with the 1-mm diameter nozzle. These results would suggest that there is a possibility to increase the productivity of PLGA-coated powders of either silica or titanium dioxide once a nozzle with an appropriate diameter is selected.

Description of coating mechanism. Based on all the experimental data shown previously, the potential mechanisms that would possibly contribute to the formation

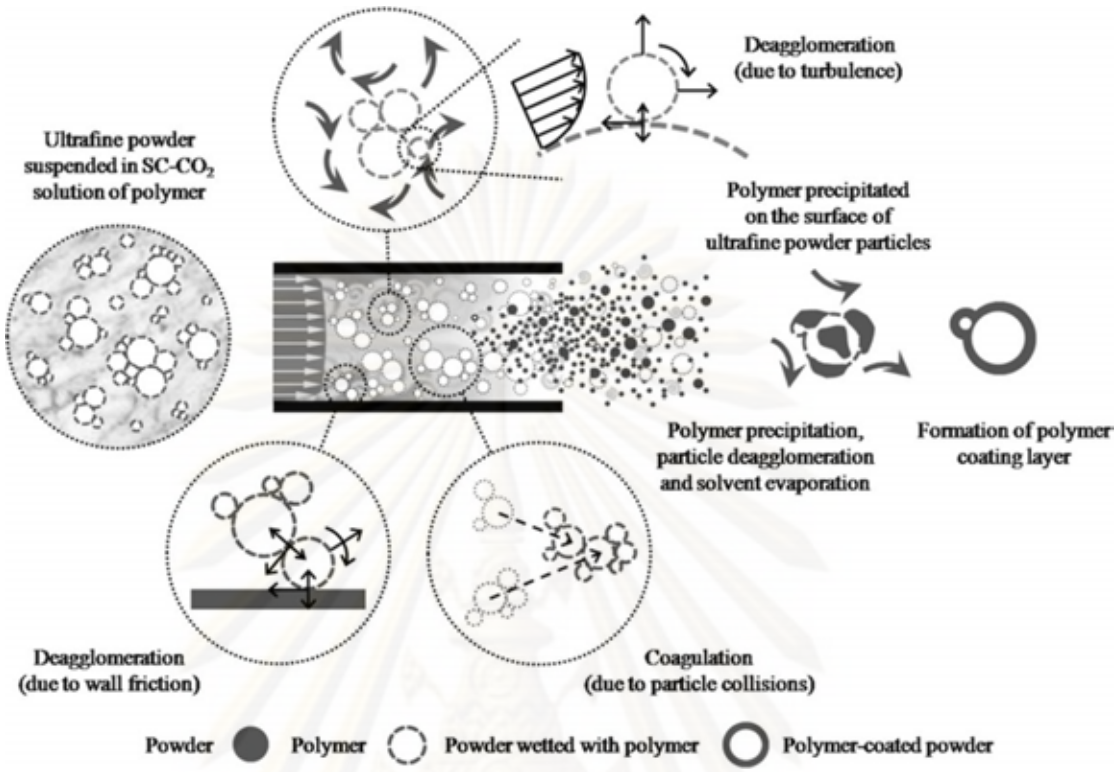

Figure 4.8 Potential mechanism of polymer coating of ultra fine powder by the rapid expansion of supercritical suspension process

of coating on the ultra fine powders are schematically summarized as depicted in **Figure 4.8**. Under the high-pressure condition, PLGA dissolved in SC-CO_2 could be absorbed (wet) onto the surface of the core particles. In the figure, the wet coating layer on the surface of the core particles is represented by the dotted line covering the particle flowing within the nozzle. During the rapid expansion, the vaporization of CO_2 to the ambient leads to the formation of solidified PLGA film on the surface of core particles. Such coating layers would experience impaction among particles and shear forces due to high flow of surrounding gas, resulting in relatively uniform coating layer on the coated particles which would have some remaining agglomera-

tion. The solidified polymer coating layer is represented by a thick solid line covering images of particles after being sprayed out of the nozzle.

4.6 Conclusions

The rapid expansion of supercritical suspension or RESS coprecipitation process was successfully carried out for the preparation of PLGA-coated microsize silica and nanosize titanium dioxide powders. According to competitive influences of phase transition, turbulent flow, boundary friction and particle coagulation along the expansion path, the rapid expansion of supercritical suspension process exhibited two major phenomena, polymer precipitation and deagglomeration of ultra fine powders. These phenomena further resulted in a layer growth of polymer on the surface of deagglomerated ultra fine powders. Coating of the silica fine powder could be achieved in the form of both agglomerates and dispersed particles, depending on the powder-to-polymer weight ratio; whereas, coating in the agglomerate form was inevitable for the titanium dioxide ultra fine powder. In addition, non-uniformity of the coating layer was also observed. Surprisingly, the powder-to-polymer weight ratio appeared to have an insignificant effect on the thickness. To reduce agglomeration tendency, larger spray nozzle diameter, smaller powder particle size and low powder-to-polymer weight ratio are favorable. It is noteworthy that, in pharmaceutical applications, the RESS process with a cosolvent could be a promising environmentally friendly technique for coating CO_2-insoluble ultra fine drug particles with a high molecular-weight polymer with limited solubility in CO_2.

CHAPTER V

CONCLUSIONS AND RECOMMENDATIONS

5.1 Conclusions

5.1.1 Modeling Solubility of Poly($_{D,L}$-lactic-co-glycolic acid) (PLGA) in supercritical carbon dioxide (SC-CO_2) with ethanol as cosolvent

The solubility data of PLGA in the mixture of SC-CO_2 and ethanol at 25 MPa and 313 K were predicted by a ternary phase equilibrium modeling using the Sanchez-Lacombe EOS together with mixing rules. The calculations were performed under the assumption that the PLGA concentration in the polymer-dilute phase was zero. As the calculation results show, PLGA is not soluble in pure SC-CO_2 or even in the SC-CO_2 mixed with ethanol up to 50 wt.% . The cosolvent effect of ethanol on the solubility enhancement of PLGA was observed in the range of ethanol concentrations above 50 wt.%. that the PLGA solubility increases with the ethanol concentration. The Sanchez-Lacombe EOS with the mixing rules provides an appreciable tool for the investigation of phase equilibrium behavior and the solubility modeling of PLGA in the ternary mixture of this study.

5.1.2 Formation of Poly($_{D,L}$-lactic-co-glycolic acid) (PLGA) Particles by Rapid Expansion of Supercritical Solution (RESS) with ethanol as cosolvent

The rapid expansion of supercritical solution (RESS) process using ethanol as

cosolvent was successfully carried out to produce non-agglomerated submicron particles of PLGA at 25 MPa and 313 K. Ethanol concentrations up to 23.8 wt.% were used. Notably, in contrast to the modeling results presented in Chapter II, the experimental results revealed that, with the assistance of ethanol cosolvent below 50 wt.%, it was possible to dissolve PLGA in SC-CO_2 to an extent sufficient for reliably achieving precipitation of PLGA by RESS. The inconsistency between the modeling and experimental results may be due to the wrong choice of Mixing rules, the inaccuracy of the binary interaction values taken from the literature, and the use of oversimplified assumption of negligible amount of PLGA applied to the ternary mixture calculations. However, the experimental results supported the modeling's prediction that the cosolvent concentration played a key role in the solubility behavior of PLGA in SC-CO_2, and correspondingly in the control of PLGA particle size and size distribution; the higher the cosolvent concentration, the higher the PLGA solubility, the smaller the average particle size and wider particle size distribution of the generated particles. According to the experimental results, a minimum average size of 55 nm was achieved for the generated PLGA particles obtained at 23.8 wt.% ethanol concentration. The influence of cosolvent concentration on the particle size and size distribution can be well described by the classical nucleation theory. The experimental results also suggested that coating of core particles with the precipitated PGLA would be possibly achieved by means of a modification to RESS of PLGA with SC-CO_2 and ethanol as cosolvent.

5.1.3 Coating of Microsize Silica (SiO_2) and Nanosize Titanium Dioxide (TiO_2) Powders with Poly($_{D,L}$-lactic-co-glycolic acid) (PLGA) by Rapid Expansion of Supercritical Suspensions

The rapid expansion of supercritical suspension or RESS coprecipitation process was successfully carried out successfully for the preparation of PLGA-coated microsize silica and nanosize titanium dioxide powders. According to competitive influences of phase transition, turbulent flow, boundary friction and particle coagulation along the expansion path, the rapid expansion of supercritical suspension process exhibited two major phenomena, polymer precipitation and deagglomeration of ultra fine powders. These phenomena further resulted in a layer growth of polymer on the surface of deagglomerated ultra fine powders. Coating of the silica fine powder could be achieved in the form of both agglomerates and dispersed particles, depending on the powder-to-polymer weight ratio whereas coating in the agglomerate form was inevitable for the titanium dioxide ultra fine powder. In addition, nonuniformity of the coating layer was also observed. Surprisingly, the powder-to-polymer weight ratio appeared to have an insignificant effect on the thickness. To reduce agglomeration tendency, larger spray nozzle diameter, smaller powder particle size and low powder-to-polymer weight ratio are favorable. It is noteworthy that, in pharmaceutical applications, the RESS process with a cosolvent could be a promising environmentally friendly technique for coating CO_2-insoluble ultra fine drug particles with a high molecular-weight polymer with limited solubility in CO_2.

5.2 Recommendations for Future Work

- The solubility behavior of PLGA in SC-CO_2 with or without ethanol as cosolvent should be investigated by means of spectroscopic techniques.
- For the purpose of improved enhancement of PLGA solubility in SC-CO_2, utilization of DMSO (a solvent for PLGA) or other types of alcohols with an anticipation of better control of coating layer should be investigated.
- Further experiment with pure ethanol at elevated pressures as solvent for PLGA should be investigated.
- For proper particle size distribution characterizations, recovery of particle products should be carried out by means of spraying into water or aqueous solution.
- An improvement for handling particle agglomeration phenomenon is required for a scalable production of coated products.

REFERENCES

Aaltonen, O.; and Rantakyla M. Biocatalysis in supercritical CO_2. Trends Biotechnol. 21 (1991) : 240–248.

Aionicesei, E.; Škerget, M.; and Knez, Z. Mathematical modelling of the solubility of supercritical CO_2 in poly(l-lactide) and poly(d,l-lactide-co-glycolide). J. Supercrit. Fluids. 50 (2009) : 320 – 326.

Alessi, A.; Cortesi, A.; Kikic, I.; Foster, N. R.; Macnaughton, S. J.; and Colombo, I. Particle production of steroid drugs using supercritical fluid processing. Industrial and Engineering Chemistry Research. 35 (1996) : 4718–4726.

Arce, P.; and Aznar, M. Modeling the thermodynamic behavior of poly(lactide-co-glycolide) + supercritical fluid mixtures with equations of state. Fluid Phase Equilibria. 244 (2006) : 16-25.

Areerat, S.; Hayata, Y.; Katsumoto, R.; Kegasawa, T.; Egami, H.; and Ohshima, M. Solubility of carbon dioxide in polyethylene/titanium dioxide composite under high pressure and temperature. J. App. Poly. Sci. 86 (2002) : 282-288.

Ashour, I.; and Aly, G. Representation of vapor-liquid equilibria using selected equations of state. Fluid Phase Equilibria. 98 (1994) : 55 – 69.

Astete, C. E.; and Sabliov, C. M. Synthesis and characterization of PLGA nanoparticles. J. Biomater. Sci. Polym. Ed. 17 (2006) : 247–289.

Bartle, K. D.; Clifford, A. A.; Jafar, S. A.; and Shilstone, G. F. Solubilities of solids and liquids of low volatility in supercritical carbon dioxide. Journal of Physical and Chemical Reference Data. 20 (1991) : 713–756.

Benedetti, L.; Bertucco, A.; and Pallado, P. Production of microparticles of a biocompatible polymer using supercritical carbon dioxide. Biotechnol Bioeng. 53 (1997) : 232–237.

Berends, E. M.; Bruinsma, O. S. L.; and van Rosmalen, G. M. Nucleation and growth of fine crystals from supercritical carbon dioxide. J. Cryst. Growth. 128 (1993) : 50-55.

Berends, E. W.; Bruinsma, O. S. L.; de Graauw, J.; and van Rosmalen, G. M. Crystallization of phenanthrene from toluene with carbon dioxide by the GAS process. AIChE J. 42 (1996) : 431–439.

Bertucco, A.; Pallado, P.; and Benedetti, L. Formation of biocompatible polymer microspheres for controlled drug delivery by a supercritical antisolvent technique. Proceedings of the 3rd Symposium on High Pressure Chemical Engineering. Zurich, Switzerland, 1996 : 217–222.

Blasig, A.; Shi, C.; Enick, R.; and Thies, M. Effect of concentration and degree of saturation on RESS of a CO_2-soluble fluoropolymer. I&ECR. 41 (2002) : 4976 – 4983.

Bleich, J.; and Mueller, B. W. Production of drug loaded microparticles by the use of supercritical gases with the aerosol solvent extraction system (ASES) process. J. Microencapsul. 13 (1996) : 131–139.

Bortner M. J.; and Baird, D. G. Rheology and extrusion of CO_2 plasticized acrylic copolymers. Society of Plastics Engineers. 60 (2002) : 1024-1028.

Brantley, N. H.; Bush. D.; Kazarian, S. G.; and Eckert, C. A. Spectroscopic measurement of solute and cosolvent partitioning between supercritical CO_2 and polymers. J. Phys. Chem. B. 103 (1999) : 10007–10016.

Brennecke, J. F.; and Eckert, C. A. Phaee equilibria for supercritical fluid process design. AIChE J. 35 (1989) : 1409-1427.

Bristow, S.; Shekunov, T.; Shekunov, B. Y.; and York, P. Analysis of the supersaturation and precipitation process with supercritical CO_2. J. Supercrit Fluids. 21 (2001) : 257–271.

Brunner, G. H. Supercritical Fluids as Solvents and Reaction Media. Hamburg : Elsevier Science & Technology Books, 2004.

Bustami, R. T.; Chan, H. K.; Dehghani, F.; Foster, N. R. Generation of microparticles of proteins for aerosol delivery using high pressure modified carbon dioxide. Pharm. Res. 17 (2000) : 1360–1366.

Chafer, A.; Fornari, T.; Berna, A.; and Stateva, R. Solubility of quercitin in supercritical CO2 + ethanol as a modifier: measurements and thermodynamic modeling. Journal of Chemical & Engineering Data. 32 (2004) : 89–96.

Chang, C. J.; and Randolph, A. D. Precipitation of microsize organic particles from supercritical fluids. AIChE J. 35 (1989) : 1876–1882.

Chang, Y.; Lee, D.; and Bae, S. Precipitation of polyethylene-octene elastomer/clay nanocomposite and microcellular foam processed in supercritical carbon dioxide. Polymer International. 55 (2006) : 184 – 189.

Charoenchaitrakool, M.; Dehghani, F.; Foster, N. R.; and Chan, H. K. Micronisation by RESS to enhance the dissolution rates of poorly water-soluble pharmaceuticals. Ind. Eng. Chem. Res. 39 (2000) : 4794–4802.

Chattopadhyay, P.; and Gupta, R. B. Production of griseofulvin nanoparticles using supercritical CO_2 antisolvent with enhanced mass transfer. Int. J. Pharm. 228 (2001) : 19–31.

Chattopadhyay, P.; and Gupta, R. B. Protein nanoparticles formation by supercritical antisolvent with enhanced mass transfer. AIChE J. 48 (2002) : 235–244.

Chen, L.; Qiu, X.; Xie, Z.; Hong, Z.; Sun, J.; Chen, X.; and Jing, X. Poly(L-lactide)/starch blends compatibilized with poly(L-lactide)-g-starch copolymer. Carbohydrate Polymers. 65 (2006) : 75–80.

Chernyak, Y.; Henon, F.; Harris, R. B.; Gould, R. D.; Franklin, R. K.; Edwards, J. R.; DeSimone, J. M.; and Carbonell, R. G. Formation of perfluoropolyether coatings by the rapid expansion of supercritical solutions (RESS) process: Part 1. Experimental results. Ind. Eng. Chem. Res. 40 (2001) : 6118-6123.

Cocero, M. J.; and Ferrero, S. Crystallization of β-carotene by a GAS process in batch: effect of operating conditions. J. Supercrit. Fluids 22 (2002) : 237–245.

Coen, E. M.; Quinn, J. F.; Dehghani, F.; Foster, N. R.; and Davis, T. P. Molecular weight fractionation of poly(methyl methacrylate) using gas anti-solvent techniques. Polymer. 44 (2003) : 3477-3481.

Coimbra, P., Blanco, M. R.; Costa Silva, H. S. R.; Gil, M. H.; and de Sousa, H. C. Experimental determination and correlation of artemisinin's solubility in supercritical carbon dioxide. J. Chem. Eng. Data. 51 (2006) : 1097–1104.

Colussi, S.; Elvassore, N.; and Kikic, I. A comparison between semi-empirical and molecular-based equations of state for describing the thermodynamic of supercritical micronization processes. J. Supercrit. Fluids. 38 (2006) : 18-26.

Daneshvar, M.; Kim, S.; and Gulari, E. High-pressure phase equilibria of poly(ethylene glycol)-carbon dioxide systems. J. Phys. Chem. 94 (1990) : 2124–2128.

Debenedetti, P.G. Homogeneous nucleation in supercritical fluids. AIChE J. 36 (1990) : 1289–1298.

Debenedetti, P. G.; Tom, J. W.; Kwauk, X.; and Yeo, S. D. Rapid expansion of supercritical solutions (RESS): fundamentals and applications. Fluid Phase Equilib. 82 (1993) : 311–321.

Derawi, S. O.; Michelsen, M. L.; Kontogeorgis, G. M.; and Stenby, E. H. Application of the CPA equation of state to glycol/hydrocarbons liquid−liquid equilibria. Fluid Phase Equilib. 209 (2003) : 163 – 184.

DeSimone, J. M.; Guan, Z.; and Elsbernd, C. S. Synthesis of fluoropolymers in supercritical carbon dioxide. Science 257 (1992) : 945–947.

Dixon, D. J.; Johnston, K. P.; and R.A. Bodmeier , Polymeric materials formed by precipitation with a compressed fluid antisolvent. AIChE J. 39 (1993) : 127–139.

Dixon, D. J.; and Johnston, K. P. Supercritical Fluids. New York : John Wiley, 1997.

Dobbs, J. M.; Wong, J. M.; and Johnston, K. P. Nonpolar co-solvents for solubility enhancement in supercritical fluid carbon dioxide. J. Chem. Eng. Data. 31 (1986) : 303-308.

Dobbs, J. M.; Wong, J. M.; Lahiere, R. J.; and Johnston, K. P. Modification of supercritical fluid phase behavior using polar cosolvents. Ind. Eng. Chem. Res. 26 (1987) : 56-65.

Domingo, C.; Berends, E.; and van Rosmalen, G. M. Precipitation of ultrafine organic crystals from the rapid expansion of supercritical solutions over a capillary and a frit nozzle. J. Supercrit. Fluids. 10 (1997) : 39–55.

Domingo, C.; Wubbolts, F. E., Rodríguez-Clemente, R.; and van Rosmalen, G. M. Solid crystallization by rapid expansion of supercritical ternary mixtures, J. Cryst. Growth. 198/199 (1999) : 760–766.

Elvassore, N.; Baggio, M.; Pallado, P.; and Bertucco, A. Production of different morphologies of biocompatible polymeric materials by supercritical CO_2 antisolvent techniques. Biotechnol. Bioeng. 73 (2001) : 449–457.

Eser, H.; and Tihminlioglu, F. Determination of thermodynamic and transport properties of solvents and non-solvents in poly(L-lactide-co-glycolide). J. Appl. Polym. Sci. 102 (2006) : 2426–2432.

Franklin, R. K.; Edwards, J. R.; Chernyak, Y.; Gould, R. D.; Henon, F.; and Carbonell, R. G. Formation of perfluoropolyether coatings by the rapid expansion of supercritical solutions (RESS) process: Part 2. Numerical modeling. Industrial and Engineering Chemistry Research. 40 (2001) : 6127–6139.

Frederiksen, L.; Anton, K.; van Hoogevest, P.; Keller, H. R.; and Leuenberger, H. Preparation of liposomes encapsulating water-soluble compounds using supercritical carbon dioxide. J. Pharm. Sci. 86 (1997) : 921–928.

Fu, K.; Griebenow, K.; Hsieh, L.; Klibanov, A. M.; and Langer, R. FTIR characterization of the secondary structure of proteins encapsulated within PLGA microspheres. J. Control. Release 58 (1999) : 357 – 366.

Fusaro, F.; Muhrer, G.; and Mazzotti, M. Gas antisolvent recrystallization of paracetamol from acetone using compressed carbon dioxide as antisolvent. Cryst. Growth Des. 4 (2004) : 881–889.

Fusaro, F.; Hänchen, M.; Mazzotti, M.; Muhrer, G.; and Subramaniam, B. Dense gas antisolvent precipitation: a comparative investigation of the GAS and PCA techniques. Ind. Eng. Chem. Res. 44 (2005) : 1502–1509.

Geldart, D. Types of gas fluidization. Powder Technology. 7 (1973) : 285–292.

Ghaderi, R.; Artursson, P.; and Carlfors, J. Preparation of biodegradable microparticles using solution-enhanced dispersion by supercritical fluids (SEDS). Pharm. Res. 16 (1999) : 676–681.

Ghaderi, R.; Artursson, P.; Carlfors, J.; A new method for preparing biodegradable microparticles and entrapment of hydrocortisone in DL-PLG microparticles using supercritical fluids. Eur. J. Pharm. Sci. 10 (2000) : 1–9.

Giddings, J. C. Field-flow fractionation of macromolecules. J. Chromatogr. 470 (1989) : 327–335.

Goel, S. K.; and Beckman, E. J. Plasticization of poly(methyl methacrylate) (PMMA) networks by supercritical carbon dioxide. Polymer. 34 (1993) : 1410–1417.

Goodship, V.; and Ogur, E. O. Polymer Processing with Supercritical Fluids. Rapra Review Reports 15. Shropshire : Rapra Technology, 2004.

Giulietti, M.; Seckler, M. M.; Derenzo, S.; Re, M. I.; and Cekinski, E. Industrial crystallization and precipitation from solutions: state of the technique. Braz. J. Chem. Eng. 18 (2001) : 423-427.

Guan, B.; Liu, Z. M.; Han, B. X.; and Yan, H. K. The solubility of behenic acid in supercritical CO_2 with ethanol. J. Supercrit. Fluids. 14 (1999) : 213 – 218.

Guha, S.; and Madras, G. Modeling of ternary solubilities of organics in supercritical carbon dioxide. Fluid Phase Equilibr. 187 (2001) : 255 – 264.

Gupta, R. B.; and Kompella, U. B. Nanoparticle technology for drug delivery. New York : Taylor & Francis Group, 2006.

Gurdial, G. S.; Foster, N. R.; Yun, S. L. J.; and Tilly, K. D. Phase behavior of supercritical fluid-entrainer systems. Kiran, I. E.; and Brennecke, J. F., Supercritical fluid engineering science, fundamentals and applications, 34. Washington : American Chemical Society, 1993.

Gupta, R. B.; and Shim, J. J. Solubility in Supercritical Carbon Dioxide. Boca Raton : CRC Press, 2007.

Hanna, M.; and York, P. Method and apparatus for the formation of particles. World patent WO 95/01221, 1994.

Hanna, M.; and York, P. Method and apparatus for the formation of particles. World patent WO 95/01 221, 1995.

Hanna, M; and York, P. Method and apparatus for the formation of particles. European patent WO 98/36825, 1998.

Hannay, J. B.; and Hogarth, J. On the solubility of solids in gases. Chem News 40 (1879) : 256.

Hartono, R.; Mansoori, G. A.; and Suwono, A. Prediction of solubility of bio-molecules in supercritical solvents. Chemical Engineering Science. 56 (2001) : 6949–6958.

Helfgen, B.; Turk, M.; and Schaber, K. Theoretical and experimental investigations of the micronization of organic solids by rapid expansion of supercritical solutions. Powder Technol. 110 (2000) : 22–28.

Helfgen, B.; Turk, M.; and Schaber, K. Hydrodynamic and aerosol modelling of the rapid expansion of supercritical solutions (RESS-process). J. Supercrit. Fluids 26 (2003) : 225 – 242.

Henon, F. E.; Carbonell, R. G.; and Desimone, J. M. Effect of polymer coatings from CO_2 on water vapor transport in porous media, AIChE J. 48 (2002) : 941-947.

Henriksen, I. B.; Mishra, A. K.; Pace, G. W.; Johnston, K. P.; and Mawson, S. Insoluble drug delivery. Patent WO 97/14407, 1997.

Hils, P.; Helfgen, B.; Turk, M.; Schaber, K.; Martin, H. J.; Schmidt, P. C.; and Wahl, M. A . Nanoscale particles for pharmaceutical purpose by rapid expansion of supercritical solutions (RESS); part I: experiments and modelling, Proceedings of the 7th Meeting on Supercritical Fluids. Antibes, France, 2000.

Hoefling, T. A.; Newman, D. A.; Enick, R. M.; and Beckman, E. J. Effect of structure on the cloud-point curves of silicone-based amphiphiles in supercritical carbon dioxide. J. Supercrit. Fluids. 6 (1993) : 165–171.

Hong, L.; Guo, J.; Gao, Y.; and Yuan, W. Precipitation of microparticulate organic pigment powders by a supercritical antisolvent process. Ind. Eng. Chem. Res. 39 (2000) : 4882–4887.

Howdle, S. M.; Watson, M. S.; Whitaker, M. J.; Popov, V. K., Davies, M. C.; Mandel, F. S.; Wang, J. D.; and Shakesheff, K. M. Supercritical fluid mixing: preparation of thermally sensitive polymer composite containing bioactive materials. J. Chem. Soc. Chem. Commun. (2001) : 109–110.

Hyatt, J. A., Liquid and supercritical carbon dioxide as organic solvents. J. Org. Chem. 49 (1984) : 5097-5101.

Ikushima, Y., Saito, N., Arai, M.; and Arai K. Solvent polarity parameters of supercritical carbon dioxide as measured by infrared spectroscopy. Bull. Chem. Soc. Jpn. 64 (1991) : 2224-2229.

Jarmer, D. J.; Lengsfeld, C. S.; and Randolph, T. W. Manupulation of particle size distribution of poly(L-lactic acid) nanoparticles with a jet-swirl nozzle during precipitation with a compressed antisolvent. J. Supercrit. Fluids. 27 (2003) : 317 – 336.

Jennings, D. W.; Lee, R. J.; and Teja, A. S. Vapor-liquid equilibria in the carbon dioxide + ethanol and carbon dioxide + 1-butanol systems. J. Chem. Eng. Data. 36 (1991) : 303–307.

Jones, D. Pharmaceutical Applications of Polymers for Drug Delivery. Rapra Review Reports 15. Shropshire : Rapra Technology, 2004.

Jono, K.; Ichikawa, H.; Miyamoto, M.; and Y. Fukumori, A review of particulate design for pharmaceutical powders and their production by spouted bed coating. Powder Technol. 113 (2000) : 269–277.

Joung, S. N.; Yoo, C. W.; Shin, H. Y.; Kim, S. Y.; Yoo, K. P.; Lee, C. S.; and Huh, W. S. Measurements and correlation of high-pressure VLE of binary CO_2–alcohol systems (methanol, ethanol, 2-methoxyethanol and 2-ethoxyethanol). Fluid Phase Equilibria. 185 (2001) : 219-230.

Jung, J.; and Perrut, M. Particle design using supercritical fluids: literature and patent survey. J. Supercrit. Fluid 20 (2001) : 179–219.

Kazarian, S. G.; Vincient, M. F.; Bright, F. V.; Liotta, C. L.; and Eckert, C. A. Specific intermolecular interaction of carbon dioxide with polymers, J. Am. Chem. Soc. 118 (1996) : 1729-1736.

Kazarian, S. G.; and Andrew Chan, K. L. Chemical photography of drug release. Macromolecules. 36 (2003) : 9866–9872.

Kerc, J.; Srcic, S.; Knez, Z.; and Sencar-Bozic, P. Micronization of drugs using supercritical carbon dioxide. Int. J. Pharm. 182 (1999) : 33–39.

Kikic, I.; and Sist, P. Applications of supercritical fluids to pharmaceuticals: controlled drug delivery systems. Proceedings of the Second NATO ASI on supercritical fluids. Kiran, E.; Debenedetti, P.G.; and Peters, C.J. (Eds.), Dordrecht, The Netherlands, 2000.

Kim, J.; Paxton, T.; and Tomasko, D. Microencapsulation of Naproxen using rapid expansion of supercritical solutions. Biotechnol. Prog. 12 (1996) : 650–658.

Kiran, E.; Xiong, Y.; and Zhuang, W. Modeling polyethylene solutions in near and supercritical fluids using the Sanchez-Lacombe model. J. Supercrit. Fluids. 6 (1993) : 193–203.

Kitamura, M.; Yamamoto, M.; Yoshinaga, Y.; and Masuoka, H. Crystal size control of sulfathiazole using high pressure carbon dioxide. J. Cryst. Growth. 178 (1997) : 378–386.

Knez, Z. Micronization of pharmaceuticals using supercritical fluids. Proceedings of the 7th Meeting on Supercritical Fluids. Antibes, France, 1 (2000) : 21–26.

Kordikowski, A.; Shekunov, T.; and York, P. Polymorph control of sulfathiazole in supercritical CO_2. Pharm. Res. 18 (2001) : 685–688.

Koushik, K.; and Kompella, U. B. Preparation of large porous deslorelin-PLGA microparticles with reduced residual solvent and cellular uptake using a supercritical carbon dioxide process. Pharm. Res. 21 (2004) : 524–535.

Krukonis, V. J.; McHugh, M. A.; and Seckner, A. J. Xenon as a supercritical solvent. J. Phys. Chem. 88 (1984) : 2687 – 2689.

Lan, H. Y.; Tseng, H. C. Study on the rheological behaviour of PP/supercritical CO_2 mixture. Journal of Polymer Research. 9 (2002) : 157-162.

Laitinen A. Supercritical Fluid Extraction of Organic Compounds from Solids and Aqueous Solutions. PhD Thesis Department of Chemical Technology Helsinki University of Technology, 2000.

Larson, K. A.; and King, M. L. Evaluation of supercritical fluid extraction in pharmaceutical industry. Biotechnology Progress. 2 (1986) : 73–82.

Lee, L. L. Molecular Thermodynamics of Nonideal Fluids. Boston : Butterworth-Heinemann, 1988.

Lele, A. K.; and Shine, A. D. Morphology of polymers precipitated from a supercritical solvent. AIChE J. 38 (1992) : 742 – 752.

Li, G.; Gunkel, F.; Wang, J.; Park, C. B.; and Altstädt, V. Solubility measurements of N_2 and CO_2 in polypropylene and ethene/octene copolymer. J. Appl. Polym. Sci. 103 (2007) : 2945 – 2953.

Liu, Z.; Wang, J.; Song, L; Yang, G; and Han, B. Study on the phase behavior of cholesterol–acetone-CO_2 system and recrystallization of cholesterol by antisolvent CO_2. J Supercrit Fluids. 24 (2002) : 1–6.

Liu, T.; Chen, S.; Lin, Y.; and Liu, D. Synthesis and characterization of amphiphatic carboxymethyl-hexanoyl chitosan hydrogel: water-retention ability and drug encapsulation. Langmuir. 22 (2006) : 9740 – 9745.

Lucien, F. P.; and Foster, N. R. Solubilities of solid mixtures in supercritical carbon dioxide: a review. Journal of Supercritical Fluid. 17 (2000) : 111–134.

Mandel, F. S.; Green, C. D.; and Scheibelhoffer, A. S. Method of preparing coating materials. US patent 5 548 004, 1996.

Mandel, F. S.; Don Wang, J.; and McHugh, M. A. Pharmaceutical material production via supercritical fluids employing the technique of particles from gas saturated solutions (PGSS). Proceedings of the 7th Meeting on Supercritical Fluids. Antibes, France, 1 (2000) : 35–46.

Madras, G.; Kulkarni, C.; and Modak, J. Modeling the solubilities of fatty acids in supercritical carbon dioxide. Fluid Phase Equilibr. 209 (2003) : 207 – 213.

Matson, D. W.; Petersen, R. C.; and Smith, R. D. Rapid expansion of supercritical fluid solutions: solute formation of powders, thin films, and fibers. Ind. Eng. Chem. Res. 26 (1987) : 2298 – 2306.

Matsuyama, H.; Yano, H.; Maki, T.; Teramoto, M.; Mishima, K.; and Matsuyama, K. Formation of porous flat membrane by phase separation with supercritical CO_2, J. Membr. Sci. 194 (2001) : 157–163.

Matsuyama, K.; Mishima, K.; Hayashi, K. I.; Ishikawa, H.; Matsuyama, H.; and Harada, T. Formation of microcapsules of medicines by the rapid expansion of a supercritical solution with a non-solvent, J. Appl. Polym. Sci. 89 (2003) : 742-748.

Matsuyama, K.; and Mishima, K. Phase behavior of CO_2 + polyethylene glycol + ethanol at pressures up to 20 MPa. Fluid Phase Equilibria. 249 (2006) : 173-178.

Mawson, S.; Johnston, K. P.; Combes, J. R.; and DeSimone, J. M. Formation of poly(1,1,2,2-tetrahydroperfluorodecyl acrylate) submicron fibers and

particles from supercritical carbon dioxide solutions. Macromolecules 28 (1995) : 3182 – 3191.

Mchugh, M. A.; and Krukonis, V. J. Supercritical Fluid Extraction. Boston : Butterworth-Heinemann, 1994.

Merrifiel, D.; and Valder, C. Process and apparatus for producing particles using a supercritical fluid. World patent WO 00/37169, 2000.

Mishima, K.; Wada, N.; Uchiyama, H.; and Nagatani, M. Extraction and separation of baicalein and baicalin from scutellaria root using supercritical carbon dioxide. Solv. Extr. Res. Dev. Jpn. 3 (1996) : 231−237.

Mishima, K.; Matsuyama, K.; Uchiyama, H.; and Ide, M. Microcoating of flavone and 3-hydroxyflavone with polymer using supercritical carbon dioxide. Proceedings of the 4th International Symposium on Supercritical Fluids. Sendai, Japan, 1997 : 267–270.

Mishima, K.; Tokuyasu, T.; Matsuyama, K.; Komorita, N.; Enjoji, T.; and Nagatani, M. Solubility of polymer in the mixtures containing supercritical carbon dioxide and antisolvent. Fluid Phase Equilibria. 144 (1998) : 299–305.

Mishima, K.; Matsuyama, K.; and Nagatani, M. Solubilities of poly(ethylene glycol)s in the mixtures of supercritical carbon dioxide and cosolvent. Fluid Phase Equilibria 161 (1999) : 315–324.

Mishima, K.; Matsuyama, K.; Tanabe, D.; Yamauchi, S.; Young, T. J.; and Johnston, K. P. Microencapsulation of proteins by rapid expansion of supercritical solution with a nonsolvent. AIChE J. 46 (2000) : 857–865.

Mohamed, R. S.; Debenedetti, P. G.; and Prudhomme, R. K. Effects of process conditions on crystals obtained from supercritical mixtures. AIChE. 35 (1989) : 325–328.

Moneghini, M.; Kikic, I.; Voinovich, D.; Perissutti, B.; and Filipovic-Grcic, J. Processing of carbamazepine-PEG 4000 solid dispersions with supercritical carbon dioxide: preparation, characterisation, and in vitro dissolution, Int. J. Pharm. 222 (2001) : 129–138.

Montero, P.; Ávalos, A.; and Pérez-Mateos, M. Characterization of polyphenol-oxidase of prawns (Penaeus japonicus). Alternatives to inhibition: additives and high-pressure treatment. Food Chemistry. 75 (2001) : 317–324.

Muller, M.; Meier, U.; Kessler, A.; and Mazzotti, M. Experimental study of the effect of process parameters in the recrystallization of an organic compound using compressed carbon dioxide as antisolvent. Ind. Eng. Chem. Res. 39 (2000) : 2260–2268.

Ngo, T. T.; Bush, D.; Eckert, C. A.; and Liotta, C. L. Spectroscopic measurement of solid solubility in supercritical fluids. AIChE J. 47 (2001) : 2566–2572.

O'Neill, M. L.; Yates, M. Z.; Johnston, K. P.; Smith, C. D.; and Wilkinson, S. P. Dispersion polymerization in supercritical CO_2 with a siloxane-based macromonomer: 1. The particle growth regime. Macromolecules. 31 (1998) : 2838–2847.

Pace, S.; Pace, G.; Parikh, I.; and Mishra, A. Novel injectable formulations of insoluble drugs. Pharm. Technol. 23 (1999) : 116–126.

Pallado, P.; Benedetti, P. L.; and Callegaro, L. Nanospheres comprising a biocompatible polysaccharide. US patent 6 214 384, 2001.

Palakodaty, S.; York, P.; and Pritchard, J. Supercritical fluid processing of materials from aqueous solutions: the application of SEDS to lactose as model substance. Pharm. Res. 15 (1998) : 1835–1843.

Patterson, G. D. On the applicability of raman scattering to the study of reorientational motions in polymers. Macromolecules. 15 (1982) : 204-206.

Pérez de Diego, Y.; Pellikaan, H. C.; Wubbolts, F. E.; Witkamp, G. J.; and Jansens, P. G. Operating regimes and mechanism of particle formation during the precipitation of polymers using the PCA process. J. Supercrit. Fluids. 35 (2005) : 147–156.

Perrut, M. Supercritical fluid applications: industrial developments and economic issues. Industrial and Engineering Chemistry Research. 39 (2000) (12) : 4531–4535.

Pöhler, H.; and Kiran, E. Volumetric properties of carbon dioxide + ethanol at high pressures. J. Chem. Eng. Data. 42 (1997) : 384−388.

Prausnitz, J. M.; Lichtenthaler, R. N.; and Azevedo, E.G. Molecular Thermodynamics of Fluid Phase Equilibria. 2nd ed. New Jersey : Prentice-Hall, 1986.

Randolph, T. W.; Randolph, A. D.; Mebes, M.; and Yeung, S. Sub-micrometer-sized biodegradable particles of poly(l-lactic acid) via the gas antisolvent spray precipitation process. Biotechnol. Prog. 9 (1993) : 429–435.

Rantakyla, M. Particle Production by Supercritical Antisolvent Processing Techniques. PhD Thesis Department of Chemical Technology Helsinki University of Technology, 2004.

Rehman, M.; Shekunov, B. Y.; York, P.; and Colthorpe, P. Solubility and precipitation of nicotinic acid in supercritical carbon dioxide. J. Pharm. Sci. 90 (2001) : 1570–1582.

Reverchon, E.; Donsì, G.; and Sesti Ossèo, L. Modeling of supercritical fluid extraction from herbaceous matrices. Ind. Engng Chem. Res. 32 (1993) : 2721–2726.

Reverchon, E.; Taddeo, R.; and Della Porta, G.. Extraction of sage oil by supercritical CO_2: influence of some process parameters. J. Supercrit. Fluids 8 (1995) : 302–309.

Reverchon, E. Supercritical antisolvent precipitation: its applications to microparticle generation and products fractionation. Proceedings of the 5th Meeting on Supercritical Fluids. Nice, France, 1 (1998) : 221–236.

Reverchon, E. Supercritical antisolvent precipitation of micro- and nanoparticles. J. Supercrit. Fluids. 15 (1999) : 1–21.

Reverchon, E. Particle design using supercritical fluids. Proceedings of the 7th Meeting on Supercritical Fluids. Antibes, France, 1 (2000) : 3–20.

Reverchon, E.; De Marco, I.; Della Porta, G. Rifampicin microparticles production by supercritical antisolvent precipitation. Int. J. Pharm. 243 (2002) : 83–91.

Reverchon, E.; Cardea, S.; and Rappo, E. S. Production of loaded PMMA structures using the supercritical CO_2 phase inversion process. J. Membr. Sci. 273 (2006) : 97–105.

Ribeiro Dos Santos, I.; Richard, J.; Pech, B.; Thies, C.; and Benoit, J. P. Microencapsulation of protein particles within lipids using a novel supercritical fluid process. Int. J. Pharm. 242 (2002) : 69 – 78.

Saltzman, W. M. Drug Delivery: Engineering Principles for Drug Therapy. New York : Oxford University Press, 2001

Sanchez, I. C.; and Lacombe, R. H. An elementary molecular theory of classical fluids. Pure fluids. The Journal of Physical Chemistry. 80 (1976) : 2352–2362.

Sarah, S. L.; Veatch, L.; and Keller, S. L. Separation of liquid phases in giant vesicles of ternary mixtures of phospholipids and cholesterol. Biophys. J. 85 (2003) : 3074–3083

Sencar-Bozic, P.; Srcic, S.; Knez, Z.; and Kerc, J. Improvement of nifedipine dissolution characteristics using supercritical CO_2. Int. J. Pharm. 148 (1997) : 123–130.

Shekunov, B. Y.; Hanna, M.; and York, P. Crystallization process in turbulent supercritical flows. J. Cryst. Growth. 198/199 (1999) : 1345–1351.

Sloan, R.; Hollowood, M. E.; Humphreys, G. O; Ashraf, W.; and York, P. Supercritical fluid processing: preparation of stable protein particles. Proceedings of the 5th Meeting on Supercritical Fluids. Nice, France, 1 (1998) : 301–306.

Smith, R. D.; Fulton, J. L.; Petersen, R. C.; Kopriva, A. J.; and Wright, B. W. Performance of capillary restrictors in supercritical fluid chromatography. Anal. Chem. 58 (1986) : 2057 – 2063.

Smith, R. D.; Kalinoski, H. T.; and Udseth, H. R. Fundamentals and practice of supercritical fluid chromatography-mass spectrometry. Mass Spectrom. Rev. 6 (1987) : 445–496.

Spyriouni,T. ; and Economou, I. G. Evaluation of SAFT and PC-SAFT models for the description of homo- and co-polymer solution phase equilibria. Polymer. 46 (2005) : 10772 - 10781.

Stahl, E.; Schüutz, E.; and Mangold, H. K. Extraction of seed oils with liquid and supercritical carbon dioxide. Journal of Agricultural and Food Chemistry. 28 (1980) : 1153-1159.

Subra, P.; Castellani, S.; Jestin, P.; and Aoufi, A. Extraction of β-carotene with supercritical fluids—Experiments and modeling. Journal of Supercritical Fluids. 12 (1998) : 261–269.

Subra, P.; and Jestin, P. Powders elaboration in supercritical media: comparison with conventional routes. Powder Technol. 103 (1999) : 2 – 9.

Subra, P.; Laudani, C.-G.; Vega-González, A.; and Reverchon, E. Precipitation and phase behavior of theophylline in solvent-supercritical CO_2 mixtures. J. Supercrit. Fluids. 35 (2005) : 95–105.

Subramaniam, B.; Rajewski, R. S.; and Snavely, K. Pharmaceutical processing with supercritical carbon dioxide. J. Pharm. Sci. 86 (1997) : 885–890.

Sun, X.; Wang, T.; Wang, Z.; and Jin, Y. The characteristics of coherent structures in the rapid expansion flow of the supercritical carbon dioxide. J. Supercrit. Fluids 24 (2002) : 231–237.

Sun, Y. P. Supercritical Fluid Technology in Materials Science and Engineering. New York : Marcel Dekker, 2002.

Suzuki, K.; and Sue, H. Isothermal vapor-liquid equilibrium data for binary systems at high pressures: carbon dioxide-methanol, carbon dioxide-ethanol, carbon

dioxide-1-propanol, methane-ethanol, methane-propanol, ethane-ethanol, and ethane-1-propanol systems. J. Chem. Eng. Data. 35 (1990) : 63 – 66.

Tandya, A.; Dehghani, F.; and Foster, N. R. Micronization of cyclosporine using dense gas techniques. J. Supercrit. Fluids. 37 (2006) : 272–278.

Taylor, T. L. Supercritical fluid extraction. New York : John Wiley, 1996.

Thakur, R.; and Gupta, R. B. Rapid expansion of supercritical solution with solid cosolvent (RESS-SC) process: formation of griseofulvin nanoparticles. Ind. Eng. Chem. Res. 44 (2005) : 7380–7387.

Thiering, R.; Charoenchaitrakool, M., Tu, L. S.; Dehghani, F.; Dillow, A. K.; Foster, N. R. Proceedings of the 5th Meeting on Supercritical Fluids. Nice, France, 1998 : 291–296

Thiering, R.; Dehghani, F.; Dillow, A.; and Foster, N. R. Solvent effects on the controlled dense gas precipitation of model proteins. J. Chem. Technol. Biotechnol. 75 (2000) : 42–53.

Thiering, R.; Dehghani, F.; and Foster, N. R. Current issues relating to anti-solvent micronisation techniques and their extension to industrial scales, J. Supercrit. Fluids. 21 (2001) : 159–177.

Thote, A. J.; and Gupta, R. B. Formation of nanoparticles of a hydrophilic drug using supercritical carbon dioxide and microencapsulation for sustained release. Nanomedicine. 1 (2005) : 85-90.

Ting, S. S. T.; Macnaughton, S. J.; Tomasko, D. L.; and Foster, N. R. Solubility of naproxen in supercritical carbon dioxide with and without co-solvents. Ind. Eng. Chem. Res. 32 (1993) : 1471–1481.

Tom, J. W.; and Debenedetti, P. G. Formation of bioerodible polymeric microspheres and microparticles by rapid expansion of supercritical solutions. Biotechnol. Prog. 7 (1991) : 403–411.

Tom, J. W.; Debenedetti, P. G.; and Jerome, R. Precipitation of poly(l-lactic acid) and composite poly(l-lactic acid)–pyrene particles by rapid expansion of supercritical solutions. J. Supercrit. Fluids 7 (1994) : 9–29.

Tomasko, D. L.; Li, H.; Liu, D.; Han, X.; Wingert, M. J.; Lee, J. L.; and Koelling, K. W. A review of CO_2 applications in the processing of polymers. Ind. Eng. Chem. Res. 42 (2003) : 6431–6456.

Tsutsumi, A.; Nakamoto, S.; Mineo, T.; and Yoshida, K. A novel fluidized-bed coating of fine particles by rapid expansion of supercritical fluid solutions. Powder Technol. 85 (1995) : 275–278.

Tsutsumi, A.; Ikeda, M.; Chen, W.; and Iwatsuki, J. A nano-coating process by the rapid expansion of supercritical suspensions in impinging-stream reactors, Powder Technol. 138 (2003) : 211–215.

Turk, M. Formation of small organic particles by RESS: experimental and theoretical investigations. J. Supercrit. Fluids 15 (1999) : 79–89.

Turk, M.; Hils, P.; Helfgen, B.; Schaber, K.; Martin, H. J.; and Wahl, M. A. Micronization of pharmaceutical substances by rapid expansion of supercritical solutions (RESS): a promising method to improve bio-availability of poorly soluble pharmaceutical agents. J. Supercrit. Fluids. 22 (2002) : 75–84.

Vasukumar, K.; and Bansal, K. A. Supercritical fluid technology in pharmaceutical research, Crips. 4 (2003) : 8–12.

Velaga, S. P.; Ghaderi, R.; and Carlfors, J. Preparation and characterization of hydrocortisone particles using a supercritical fluids extraction process. Int. J. Pharm. 231 (2002) : 155–166.

Wang, T. J.; Tsutsumi, A.,; Hasegawa, H.; and Mineo, T. Mechanism of particle coating granulation with RESS process in a fluidized bed. Powder Technol. 118 (2001) : 229–235.

Wang, J.; Chua, K. M., and Wang, C. H. Stabilization and encapsulation of human immunoglobulin G into biodegradable microspheres. J. Colloid Interface Sci. 271 (2004) : 92-101.

Warwick, B.; Dehghani, F.; Foster, N. R.; Biffin, J. R.; Regtop, H. L. Synthesis, purification, and micronization of pharmaceuticals using the GAS antisolvent technique. Ind. Eng. Chem. Res. 39 (2000) : 4571–4579.

Weidner, E.; Steiner, R.; and Knez, Z. Powder generation from poly(ethyleneglycols) with compressible fluids. Proceedings of the 3rd Symposium on High Pressure Chemical Engineering. Zurich, Switzerland, 1996 : 223–228

Weidner, E.; Knez, Z.; and Novak, Z. Process for preparing particles or powders. PCT patent application, European patent 0 744 990, 2000.

Winters, M. A.; Knutson, B. L.; Debenedetti, P. G.; Sparks, H. G.; Przybycien, T. M; Stevenson, C. L.; and Prestrelski, S. J. Precipitation of proteins in supercritical carbon dioxide. J. Pharm. Sci. 85 (1996) : 586–594.

Winters, M. A.; Frankel, D. Z.; and Debenedetti, P. G. Protein purification with vapor-phase carbon dioxide. Biotech. Bioeng. 62 (1999) : 247–258.

Werling, J. O.; and Debenedetti, P. G. Numerical modeling of mass transfer in the supercritical antisolvent process. J. Supercrit. Fluids. 16 (1999) : 167–181.

Wubbolts, F. E.; Bruinsma, O. S. L.; and Van Rosmalen, G. M. Dry-spraying of ascorbic acid or acetaminophen solutions with supercritical carbon dioxide. J. Crys. Growth. 198/199 (1999) : 767–772.

Xiong, Y.; and Kiran, E. High-pressure phase-behavior in polyethylene *n*-butane binary and polyethylene *n*-butane CO_2 ternary-systems. Journal of Applied Polymer Science 53 (1994) : 1179–1190.

Yeo, S.; Lim, G.; Debenedetti, P. G.; and Bernstein, H. Formation of microparticulate protein powders using a supercritical fluid anti-solvent. Biotechnol. Bioeng. 41 (1993) : 341–346.

Yeo, S. D.; Kim, M. S.; and Lee, J. C. Recrystallization of sulfathiazile and chlorpropamide using the supercritical fluid antisolvent process. J. Supercrit. Fluids. 25 (2003) : 143–154.

Yoon, J. H.; Lee, H. S.; and Lee, H. High-pressure vapour-liquid equilibria for carbon dioxide + methanol, carbon dioxide + ethanol, and carbon dioxide + methanol + ethanol. J. Chem. Eng. Data. 38 (1993) : 53–55.

York, P.; Kompella, U. B.; and Shekunov, B. Y. Supercritical Fluid Technology for Drug Product Development. New York : Marcel Dekker, 2004.

Young, T. J.; Mawson, S.; Johnston, K. P.; Henriksen, I. B.; Pace, G. W.; and Mishara, A. K. Rapid expansion from supercritical to aqueous solution to produce submicron suspensions of water-insoluble drugs. Biotechnol. Progr. 16 (2000) : 402–407.

Zolnik, B. S.; and Burgess, D. J. Effect of acidic pH on PLGA microsphere degradation and release. Journal of Controlled Release. 122 (2007) : 338 – 344.

Zúñiga-Moreno, A.; and Galicia-Luna, L. A. Compressed liquid densities of carbon dioxide + ethanol mixtures at four compositions via a vibrating tube densimeter up to 363 K and 25 MPa. J. Chem. Eng. Data. 47 (2002) : 149 – 154.

APPENDICES

APPENDIX A

Publications Authored by B. Kongsombut

International Research Paper

1. **Kongsombut, B.**; Chen, W.; Tsutsumi, A.; Tanthapanichakoon, W.; and Charinpanitkul, T. Formation of deagglomerated PLGA particles and PLGA-coated ultra fine powders by rapid expansion of supercritical solution with ethanol cosolvent. Korean J. Chem. Eng. 25 (2008) : 838 – 845.
2. **Kongsombut, B.**; Tsutsumi, A.; Suankaew, N.; Charinpanitkul, T. Encapsulation of SiO_2 and TiO_2 fine powders with poly($_{D,L}$-lactic-co-glycolic acid) by rapid expansion of supercritical CO_2 incorporated with ethanol cosolvent. Ind. Eng. Chem. Res., 48 (2009) : 11230–11235.

International Conference Proceedings

1. **Kongsombut, B.**; Chen, W.; Tsutsumi, A.; Tanthapanichakoon, W.; and Charinpanitkul, T. Coating of ultrafine powders with PLGA by rapid expansion of supercritical solutions with ethanol cosolvent. *Proceedings of the 8th International Symposium on Supercritical Fluids (ISSF 2006)*, November 5 – 8, 2006, Kyoto, Japan.

Korean J. Chem. Eng., **25**(4), 838-845 (2008)

Formation of deagglomerated PLGA particles and PLGA-coated ultra fine powders by rapid expansion of supercritical solution with ethanol cosolvent

Benjapol Kongsombut*, Wei Chen, Atsushi Tsutsumi**, Wiwut Tanthapanichakoon***, and Tawatchai Charinpanitkul*†**

*Department of Chemical Engineering, Chulalongkorn University, Patumwan, Bangkok 10330, Thailand
**Department of Chemical System Engineering, University of Tokyo, Bunkyo-ku, Tokyo 113-8656, Japan
***National Nanotechnology Center, Thailand Science Park, Klong Luang, Pathumthani 12120, Thailand
(*Received 18 September 2006 • accepted 19 November 2007*)

Abstract−Rapid expansion of supercritical solution (RESS) was used for preparing polymer particles and polymer coating of ultra fine powders. The polymer of pharmaceutical interest was Poly(lactic-co-glycolic acid) (PLGA with PLA : PGA ratio of 85 : 15 and MW of 50,000-75,000) and the simulated core particles were 1.4-μm SiO_2 and 70-nm TiO_2 particles. The supercritical solution was prepared by dissolving PLGA in supercritical carbon dioxide with ethanol as a cosolvent. Supercritical solution of CO_2-PLGA was sprayed through capillary nozzles to ambient conditions, resulting in formation of submicron PLGA particles. Similarly, rapid expansion of supercritical solution of CO_2-PLGA suspended with the core particles could provide solvent evaporation and deposition of submicron PLGA particles on the surface of the core particles, resulting in the formation of coating films on dispersed particles of SiO_2 and agglomerates of TiO_2. The influences of the core particle size, spray nozzle diameter as well as powder-to-polymer weight ratio were also investigated and discussed with respect to the coating performance.

Key words: RESS, Powder Coating, Poly(lactic-co-glycolic acid), Agglomeration, Cosolvent

INTRODUCTION

Coating of powders has found its application in various industries, including pharmaceuticals, foods, agriculture and energetic materials. Normally, coating is considered as a shell-like barrier that protects powders from exposure to the environment or allows modification of powder surface functionality [1]. In the pharmaceutical industry, the general purposes of coating are to provide protection from rapid degradation, control of release rate and prevention of side effect of therapeutic agents. While the conventional process used for coating powders is generally based on fluidization technique, there is a limitation for powders smaller than 70 μm in diameter because of poor fluidization behavior [2]. Emulsion-based techniques, such as water-in-oil-in-water (w/o/w) double emulsions or solid-in-oil-in-water (s/o/w) emulsions, may be used for coating ultra fine powders. However, due to the common use of organic solvents and harsh processing conditions, these emulsion-based techniques involve some drawbacks including alteration of structure of therapeutic agent, presence of residual organic solvent in the coated powders and emission of volatile organic compounds to the environment [3,4].

In the last few decades, numerous attempts have been made on the application of supercritical fluids (SCFs) to overcome the problems of organic solvent in the conventional coating processes [5]. Supercritical fluids exhibit both liquid-like and gas-like properties with densities and solvating characteristics similar to those of the liquid and mass transfer similar to the gas. For pharmaceutical applications, carbon dioxide (CO_2) is the most commonly used SCF due to its inert properties, non-toxicity, non-polluting nature and mild critical conditions. Several studies have been reported on coating of microscale and nanoscale particles with polymers by using supercritical carbon dioxide (SC-CO_2) via different approaches [6-9]. Process variables, such as feed composition of polymer and size of the host particles, were experimentally found to be the key parameters affecting the coating performance in these processes.

The simplest SCF technique for formation of pharmaceutical particles and composite materials is the rapid expansion of supercritical solution (RESS) [10]. With the RESS technique, a solute is dissolved in SC-CO_2 and the solution is then instantaneously depressurized by spraying it through a capillary nozzle, causing precipitation of the solute as SC-CO_2 vaporizes. Submicron- and nano-sized dry particles with a narrow particle size distribution could be prepared from various pharmaceutical compounds and polymers [5]. Meanwhile, there are also other similar processes recognized as supercritical antisolvent (SAS) or gas antisolvent (GAS) [11], aerosol solvent extraction system (ASES) [12-14] and solution enhanced dispersion by supercritical fluids (SEDS) [15]. All of those processes exert both advantages and disadvantages depending on conditions of their applications.

In this study, the RESS process with a cosolvent is used to produce fine particles of polymer and the process is also modified for polymer coating of ultra fine powders. Microsize silica and nanosize titanium dioxide particles were chosen as preformed drug ultra fine powders, while Poly(lactic-co-glycolic acid) (PLGA) copolymer was used as the coating material. Basically, PLGA-coated ultra fine powders can be used to investigate simple-diffusion controlled release of the drugs in subcutaneous and intravenous applications [1]. Effects of the process parameters, which were the particle size of ultra fine core powder, spray nozzle diameter as well as powder-

†To whom correspondence should be addressed.
E-mail: ctawat@chula.ac.th

to-polymer weight ratio, and mechanism of the coating process are presented and discussed based on the characterization results of coated powders regarding morphology and internal structure of coated particles.

EXPERIMENTAL

1. Material

Microsize silica (SiO_2) particles with a mean size of 1.4 μm (Kojundo Chemical Lab, Japan) and nanosize titanium dioxide (TiO_2) particles with a mean size of 70 nm (Ishihara Sangyo Kaisha, Japan) were employed as core particles. Poly(lactic-co-glycolic acid) (PLGA) (PLA : PGA=85 : 15, molecular weight=62,000 and glass transition temperature=47.5 °C, Aldrich Chemicals Ltd.) and liquid CO_2 (critical temperature T_c=304 K, critical pressure P_c=7.4 MPa, Suzuki Shokan Co. Ltd., Tokyo, Japan) were used as coating agent and solvent. Due to the limited solubility of PLGA in SC-CO_2, ethanol (special grade; >99.5%; Kanto Chemical Co., Inc., Tokyo, Japan) was employed as cosolvent. All chemicals and materials were used as received.

2. Experimental Procedure

The experimental apparatus shown schematically in Fig. 1 consists of a high-pressure pump (3), a stirred high-pressure vessel (6), and a spray nozzle (9). The high-pressure pump was installed with a cooler before the suction part to avoid cavitation. The high-pressure vessel had a capacity of 1,500 ml and maximum allowable operating pressure and temperature of 30 MPa and 473 K, respectively. During each experiment, the vessel temperature was kept constant at 313 K by using an automatically controlled electric heater. The spray nozzle was simply made from a stainless steel tube with a length of 10 mm and was equipped with a shut-off valve. Two spray nozzles with different inner diameters of 0.1 mm and 0.3 mm were employed for investigating the effect of nozzle diameter on the coating process. Temperature of the nozzle was kept constant at 423 K by a ribbon heater to prevent the nozzle clogging with dry ice during spraying. A planar target (100 mm×100 mm×10 mm) covered with aluminum foil and a carbon-coated copper microgrid was employed to collect samples of particles generated from the spray for characterization.

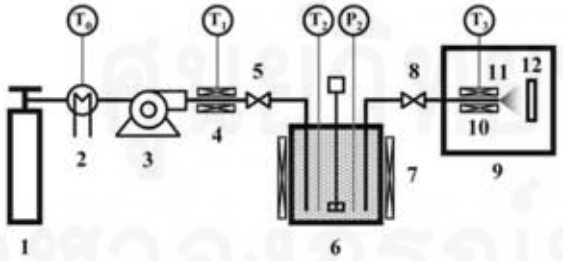

Fig. 1. Schematic diagram of the experimental apparatus.

1. CO_2 cylinder	7. Vessel heater
2. Cooler	8. Shut-off valve
3. HPLC pump	9. Vacuum chamber
4. Ribbon heater	10. Ribbon heater
5. Shut-off valve	11. Nozzle
6. Stirred high-pressure vessel	12. Target plate, or microgrid

The first part of the experimental work was carried out to investigate the applicability of the RESS process for generating polymer particles, which will be used to coat ultra fine powders. For RESS processing of a polymer, the information of its solubility in SC-CO_2 is crucial. To the best of our knowledge, there is no report on the solubility of PLGA in SC-CO_2. PLGA polymer used in our study has a limited solubility in SC-CO_2 because of its very high molecular weight (10). In order to increase the PLGA solubility in SC-CO_2 to a beneficial extent, ethanol was used as cosolvent. 2 g of PLGA with different amounts of ethanol were placed in the high-pressure vessel for preparation of SC-CO_2 solution. After being carefully sealed, the vessel was heated and fed with CO_2 via the high-pressure pump until the desired supercritical conditions were achieved. The mixture in the vessel was stirred by a mixing paddle rotating at 300 rpm, and was left for 3 hours to achieve equilibrium. The prepared supercritical solution was then sprayed through the nozzle to allow its rapid expansion. The target plate was placed against the sprayed flow at a distance of 300 mm from the nozzle tip within a chamber under atmospheric conditions.

In the second part of this work, performance of the RESS process to generate film coating of PLGA on ultra fine powders was investigated with the same apparatus. It is noteworthy that the ultra fine powder, PLGA and ethanol, in pure form, are not soluble in each other. Thus, they form an immiscible ternary mixture under atmospheric conditions. Experimental procedures similar to the first part were carried out so as to dissolve PLGA in SC-CO_2 with the aid of ethanol in the presence of fine SiO_2 or nanosize TiO_2 core particles. Under these conditions, the core particles were not dissolved but suspended in a single homogenous supercritical phase of CO_2, ethanol and the dissolved PLGA. The supercritical suspensions were then allowed to expand through the nozzle for a few seconds. It could be observed from each experiment that in the case of PLGA expansion without core powder, there is nothing remaining in the autoclave. However, when core powder and PLGA were taken into account, after expansion there would be some residues left in the vessel. After expansion, all coated particles were collected for characterization by using the target plate as already mentioned above. In order to evaluate the coating performance, effect of three process parameters, i.e., diameter of the spray nozzle, particle size of the core powder and powder-to-polymer weight ratio, on the coating characteristics was investigated. The experimental parameters and conditions used in this work are listed in Table 1. Fig. 2 depicts step-by-step conceptual representations of polymer particle formation and polymer coating of powder using RESS.

Field emission scanning electron microscopy (FE-SEM; Hitachi, S-900) was used to examine the particle samples obtained from each experiment. For SEM sample preparation, the aluminum foil uncovered from the target plate was cut into a small piece, mounted on a specimen stub with conductive paint and coated with platinum by a sputtering device (Hitachi, E-1030) for 20 s. The SEM was operated at an accelerating voltage of 10 kV and a magnification between 1,000 and 200 k. The SEM images were processed for particle size analysis by using image-analyzing software (Image-Pro Plus version 3.0; Media Cybernetics). For verification of polymer coating of the ultra fine powder, the particle samples on the microgrid were further analyzed by a transmission electron microscope (TEM; JEOL 2000-EX) operated at 200 kV in the bright-

Table 1. Experimental parameters and conditions of RESS processes

Material	Solvent	CO_2; P_c=7.4 MPa; T_c=304 K; T_0=266 K; T_1=353 K
	Cosolvent	ethanol; 0-21.8 wt%*
	Polymer	Poly(D,L-lactide-co-glycolide), PLGA; 85:15; M_w 50,000-75,000; T_g 318-323 K
	Powder	SiO_2; mean particle size 1.4 μm
		TiO_2; mean diameter 70 nm (for coating experiments)
	feed ratio**	1 : 1, 3 : 1 (for coating experiments)
Dissolution	Vessel	Cylinder; 1,500 ml
	Agitation	300 rpm; 180 min
	Conditions	P_2=25 MPa; T_2=313 K
Expansion	Nozzle	stainless steel; d=0.1, 0.3 mm; L=10 mm; T_3=423 K
	spraying time	3 s
	target distance	300 mm

* polymer-free basis; ** powder-to-polymer weight ratio

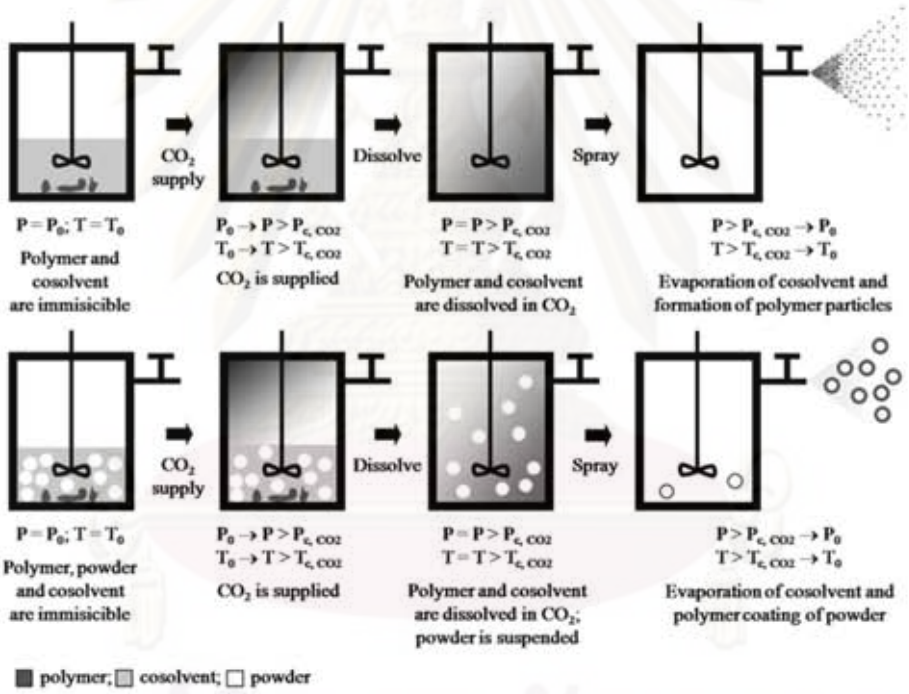

Fig. 2. Schematic representations of polymer particle formation process by RESS with a cosolvent (upper half) and powder coating process by rapid expansion of supercritical suspension with a cosolvent (lower half).

field mode. The mass-thickness contrast between the coating polymer and the core powder was analyzed to reveal the structures and morphology of the coated powders.

RESULTS AND DISCUSSION

1. Formation of PLGA Particles by RESS

Ethanol is a commonly used cosolvent in the RESS of CO_2-insoluble pharmaceutical materials due to its low toxicity. Although PLGA has limited solubility in either SC-CO_2 or ethanol, it was reported that the PLGA solubility becomes higher in the mixture of these two fluids [6]. Since ethanol is capable of being both donor and acceptor of hydrogen bonds, it can self-associate through hydrogen bonding with both CO_2 and PLGA, which leads to significantly improved PLGA solubility in SC-CO_2. The solubility enhancement of various polymers by ethanol cosolvent has been reported and discussed in several papers [16-20].

First, a solution of PLGA in SC-CO_2 plus ethanol was prepared at 25 MPa and 313 K. Under these conditions, CO_2 and ethanol become miscible at all compositions and form a single supercritical fluid phase [21-23]. A different amount of ethanol was added to the pressure vessel at 0, 100, 200, 300 and 400 ml, respectively. Because the amount of PLGA dissolved in the CO_2-ethanol mixtures was very small, compared to that of CO_2 and ethanol, the ethanol

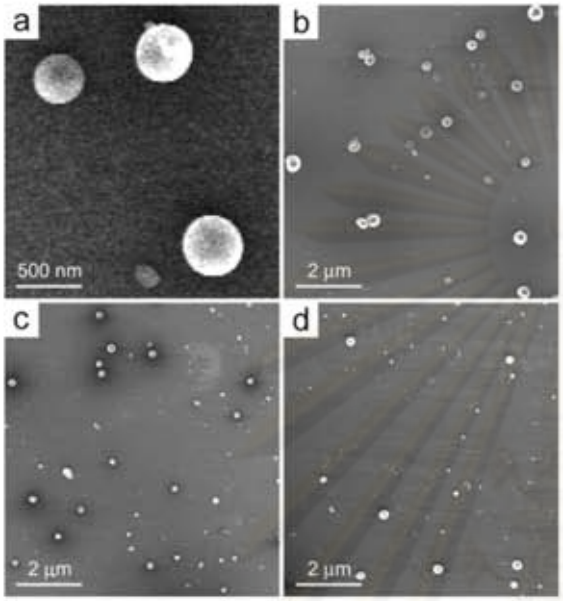

Fig. 3. SEM images of PLGA particles produced by RESS using ethanol cosolvent at different ethanol concentrations: (a) and (b) 11.1 wt%; (c) 16.4 wt%; (d) 21.8 wt%.

concentration in the mixtures could be estimated from the Patel-Teja cubic equation of state extended to binary mixtures [24], regardless of PLGA presence in the mixtures. The CO_2-ethanol interaction parameters used in the calculation were obtained from data reported in the literature [24,25]. According to the varied amount of ethanol mentioned above, the calculated values of polymer-free concentration of ethanol are 0, 5.7, 11.1, 16.4 and 21.8 wt%, respectively.

In experiments using pure CO_2 and CO_2 with 5.7 wt% ethanol, negligible amounts of polymer particles were detected in the collected samples under SEM observations, thereby indicating negligible particle formation during the RESS process. This implied that both the pure CO_2 and the CO_2 mixed with ethanol at 5.7 wt% were unable to dissolve PLGA to a sufficient extent; as a result, supersaturation was not achieved to trigger particle nucleation in these cases. On the other hand, Fig. 3 shows typical SEM images of PLGA particles produced by RESS using CO_2 mixed with ethanol at 11.1, 16.4 and 21.8 wt%. The charged amount of PLGA in SC-CO_2 with 21.8 wt% ethanol was approximately 0.17 wt% of the total amount of supercritical solution. Also in Fig. 3 it is clearly observable that the generated particles exhibit a nearly spherical shape with submicron size distributed in a narrow range.

Based on the experimental results, the formation of PLGA particles via RESS could be described as follows. Under the equilibrium condition of SC-CO_2, PLGA, CO_2 and ethanol would form a single homogeneous supercritical solution though saturation of PLGA was not yet achieved. During the rapid expansion, phase transition of CO_2 taking place in the post-expansion free jet would result in a drastic increase in PLGA concentration in the droplets, leading to precipitation of the dissolved polymer. As mentioned previously, since ethanol could not single-handedly dissolve PLGA, it also vaporized out during the expansion and then did not remain in the polymer [26]. Therefore, it is reasonable to consider that the precipitated polymer particles were solvent-free and did not undergo an agglomeration process because of its dilute solid content. These results suggested that the generated polymer particles could be used to coat some core particles.

Image analyses of typical SEM images of particle samples obtained from the experiments were carried out to determine their size distribution and morphology. At least 300 particles dispersed in different regions of the SEM images were taken into account in the determination of their size distribution. Fig. 4(a) reveals that the PLGA particles produced by RESS at different ethanol concentrations all exhibit log-normal size distribution behavior. The obtained geometric mean and standard deviation of the distribution were plotted as function of the ethanol concentration, as shown in Fig. 4(b). It is clearly seen that the particle size distribution of the prepared PLGA particles was strongly dependent on the ethanol concentration. As the ethanol concentration increased from 11.1 to 21.8 wt%, the particle geometric mean decreased to a minimum of 55 nm, while

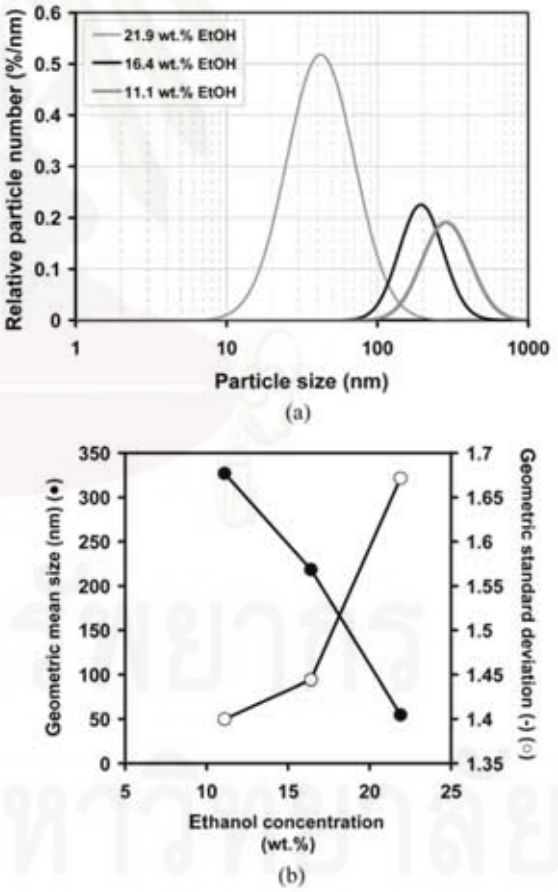

Fig. 4. Dependence of particle size distribution of PLGA particles on ethanol concentration: (a) log-normal particle size distributions; (b) mean particle size and standard deviation of particle size distribution as function of ethanol concentration.

the geometric standard deviation increased to a maximum of 1.67. An increase in the ethanol concentration in the SC-CO_2 mixture resulted in an increase in the PLGA solubility, leading to higher supersaturation of PLGA in the sprayed mixture after its rapid expansion. According to the classical nucleation theory [27,28], higher nucleation rate and smaller critical nucleus size could be expected if the dissolved polymer concentration becomes increased. Meanwhile, a higher supersaturation ratio would also result in the occurrence of "nucleation bursts" which could generate several families of random size particles in the early stage of nucleation [29]. It is also noteworthy that an increase in the particle number concentration could provide higher coagulation frequency. These opposing phenomena were responsible for a smaller mean size but wider distribution of the resulting PLGA particles when a higher concentration of ethanol was used.

2. Effect of RESS on the Deagglomeration of Microsize Silica and Nanosize Titanium Dioxide Powders

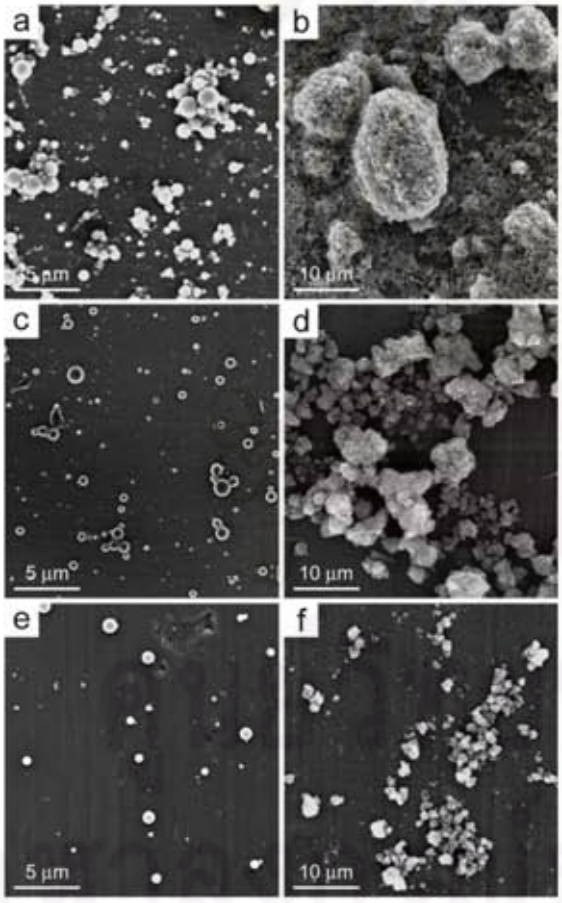

Fig. 5. Effect of diameter of spray nozzle on the deagglomeration of ultra fine powders. 1.4-μm silica: (a) before expansion; (c) after expansion (nozzle diameter 0.1 mm); (e) after expansion (nozzle diameter 0.3 mm). 70-nm titanium dioxide: (b) before expansion; (d) after expansion (nozzle diameter 0.1 mm); (f) after expansion (nozzle diameter 0.3 mm).

Ultra fine particles have a strong tendency to agglomerate due to their van der Waals interactions. In general, spontaneous agglomeration of ultra fine powders could take place and result in particle size enlargement and unstable processing conditions in the conventional coating processes [27]. In the RESS process, in which the expansion flow is considered as a supersonic or at least free jet, tempestuous turbulence is expected to be developed in the rapid expansion flow [30,31]. This turbulence could provide an advantageous contribution to the disintegration of agglomerates of ultra fine powders to facilitate the formation of a coating layer on the primary particles.

Fig. 5 shows typical SEM images of silica and titanium dioxide ultra fine particles before and after performing the rapid expansion of their suspensions in mixtures of SC-CO_2 and ethanol. The suspensions were prepared with 21.8 wt% ethanol in SC-CO_2 under conditions of 25 MPa and 313 K. Before rapid expansion, it could be observed that ultra fine powders could agglomerate to form large particles as revealed in Fig. 5(a) and Fig. 5(b). The agglomerate sizes are approximately 2-5 μm for the fine silica powder and 3-20 μm for the ultra fine titanium dioxide powder. Fig. 5(c), Fig. 5(d) and Fig. 5(e), Fig. 5(f) illustrate the change in the morphology of the ultra fine powders prepared by rapid expansion through nozzles with different diameters of 0.1 and 0.3 mm, respectively. Deagglomeration of the ultra fine powders was observed and consistently indicated by a decrease in the agglomerate size and an increase in the number concentration of primary particles. It could be implied that the dispersion and deagglomeration of the ultra fine powders were achieved as a combined result of boundary friction due to flow along the nozzle wall, turbulence in the high-velocity fluid and collisions between the ultra fine powder particles along the rapid expansion path. The boundary friction and the turbulence were responsible for fragmentation of large powder agglomerates into smaller ones, whereas the particle collisions could result in either particle coagulation or particle dispersion depending on relative velocities and collision angles of the particles. Comparison between the SEM images of particle samples produced by these two nozzles suggests that a better dispersion and deagglomeration effect was achieved with the bigger 0.3-mm diameter nozzle, and the effect was stronger for the larger silica fine powder. This reveals the influences of nozzle diameter and particle size of the ultra fine powder on the performance of dispersion and deagglomeration of the ultra fine powder in the rapid expansion process. As pointed out by Smith et al. [32], at the same pre- and post-expansion conditions, an increase of the nozzle diameter results in a higher Reynolds number, more turbulence, a higher total flow rate and a larger friction loss. In addition, with shorter residence time the probability of particle coagulation becomes lower. These lead to an improvement of the dispersion and deagglomeration of the ultra fine powders. Accordingly, the cohesive forces are smaller, the number concentration lower and the probability of particle coagulation lower for large particles compared with the small ones. The reasoning supports our experimental results that the dispersion and deagglomeration of the 1.4-μm silica powder were better than that of the 70-nm titanium dioxide powder. It should be noted that in case of the ideal condition, individual core particles should be obtained if agglomeration can be completely suppressed by the rapid expansion. Therefore, a smaller nozzle would reasonably be expected to provide the well dispersed

core particles after the expansion. However, it was coincidentally found that the smaller nozzle was easily clogged. To avoid this difficulty as well as to obtain a favorable coating process with low-agglomeration tendency, the 0.3-mm diameter nozzle was selected for the coating of the ultra fine powders, which will be discussed in the next section.

3. Coating of Microsize Silica and Nanosize Titanium Dioxide Powders with PLGA by Rapid Expansion of Supercritical Suspensions

A series of experiments was carried out on coating 1.4-μm silica particles and 70-nm titanium dioxide particles with PLGA by rapid expansion of supercritical suspensions to investigate the effect of experimental parameters on coating performance. In all experiments, the supercritical suspensions were prepared by using the conditions at which the solubility of PLGA in the mixture of SC-CO_2 and ethanol could be determined, i.e., the supercritical pressure and temperature of 25 MPa and 313 K, the ethanol concentration of 21.8 wt% and the polymer solubility of 0.17 wt%. The powder-to-polymer weight ratio was varied through an adjustment of the powder concentration in the suspension by changing the amount of powder added to the high-pressure vessel at the beginning of each experiment.

Fig. 6 shows some samples of the morphology and internal structure of PLGA-coated silica fine powder produced by the rapid expansion of supercritical suspension process at different powder-to-polymer weight ratios. It appears that the coating of silica fine powder was achieved in the form of both individual dispersed particles and agglomerates. The coated silica particles exhibit a core-shell structure, as shown in the bright-field TEM images (Fig. 6(b) and Fig. 6(d)). Due to the stronger interactions between the electrons and silicon than that between the electrons and carbon (a major component of the polymer) in the TEM, the silica particles appear as a darker contrast area than the PLGA phase in these images. It is clearly seen that the darker contrast area is thoroughly covered by the lighter contrast area, indicating that the silica particles were completely coated with a layer of PLGA. The rapid expansion of a suspension of SC-CO_2-insoluble particles in the supercritical CO_2 solution of a polymer led to deposition of the polymer on the surface of the suspended particles, thereby generating polymer film coating on the particle surfaces [6,8]. Our experimental results are consistent with this explanation. When Fig. 6 is compared with Fig. 5(a), it is clear that, as a concurrent result of the rapid expansion of supercritical suspension, the dispersion and deagglomeration of the silica fine powder contributed to the low agglomeration tendency of the coated particles. It was observed that, at the powder-to-polymer weight ratio of 1, there was no significant agglomeration of coated silica particles that took place during the coating process (Fig. 6(a) and Fig. 6(b)), while the agglomeration process appeared to be enhanced when the powder-to-polymer weight ratio was increased to 3 (Fig. 6(c) and Fig. 6(d)). This is mainly attributable to the increased number concentration of silica particles in the rapid expansion flow, resulting in more frequent collisions and higher coagulation probability of the silica particles within the nozzle, and consequently an increase in the degree of agglomeration of the particles. In addition, it can be observed in the TEM images that the thickness of the coating layer was not uniform and estimated to be around 10-100 nm from the scale bar. It is likely that the PLGA particles, which precipitated and then deposited on the silica particle surface, spread and formed solid bridges between them, thereby resulting in growth of the coating layer. The strong turbulence in the rapid expansion flow dissipated much of the eddy energy [30], which can be considered to cause significant disturbances to the just-formed coating layer. It is interesting to note that, from our experimental results, the coating layer thickness seems not to be sensitive to the change in the powder-to-polymer weight ratio. As a possible assumption, the particle coagulation along the length of the nozzle during the rapid expansion flow plays a significant role in the coating process. Particle coagulation results in a drastic decrease in the particle number and a drastic reduction of the particle surface area, on which coating takes place. The higher the probability of particle coagulation, the more pronounced the reduction of the coating surface area and capability. Since the particle coagulation probability is proportional to the powder-to-polymer weight ratio in the coating process, it might be assumed that the change in powder-to-polymer weight ratio did not provide a significant change in the total coating surface area and it had no influence on the coating layer thickness.

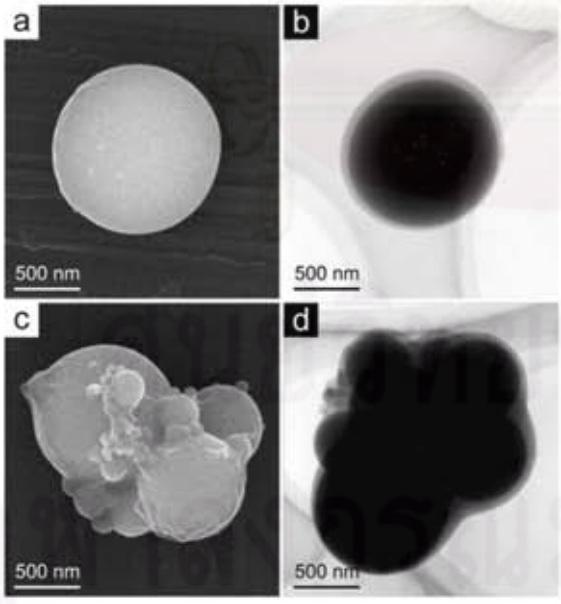

Fig. 6. SEM and TEM images of PLGA-coated silica fine powder produced by the rapid expansion of supercritical suspension process at powder-to-polymer weight ratios: (a) and (b) 1 : 1; (c) and (d) 3 : 1.

Similar results were obtained for the coating of 70-nm titanium dioxide ultra fine powder with PLGA, as shown in Fig. 7. When compared with Fig. 6, the experimental results shown in Fig. 7 suggest that the coating of titanium dioxide ultra fine powder with PLGA could also be achieved in the same process as that of silica fine powder. However, SEM and TEM images reveal that the coating of titanium dioxide ultra fine powder always took place in the form of agglomerates of primary particles. In Fig. 7(b) and Fig. 7(d), the coated particles are composed of an agglomerate of titanium dioxide particles in the core and a coat of PLGA as shown by the darker

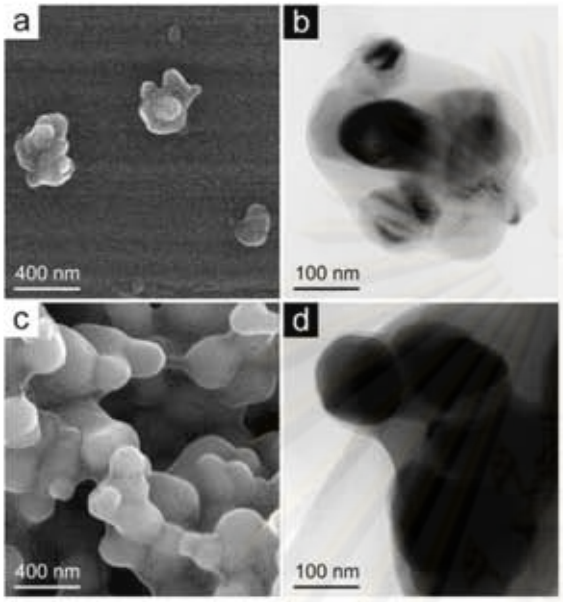

Fig. 7. SEM and TEM images of PLGA-coated titanium dioxide ultra fine powder produced by the rapid expansion of supercritical suspension process at different/specified powder-to-polymer weight ratios: (a) and (b) 1 : 1; (c) and (d) 3 : 1.

and the lighter contrast areas, respectively. It should be noted that no PLGA is observed in the void among the titanium dioxide particles, suggesting that the PLGA coat was formed as a growing layer on the titanium dioxide agglomerate surface, not a coalescence of coated primary particles. The agglomerate sizes are in the range of some hundred nanometers to a few microns, which is consistent with the typical size of agglomerates shown in Fig. 5(f). Obviously, the flow turbulence and friction loss generated during the rapid expansion of supercritical suspension process was not sufficient to disintegrate agglomerates into primary particles. This is attributable to the extremely strong adhesion forces among the nanosize titanium dioxide particles. The nonuniformity of the coat can also be observed in the TEM images, indicating the deposition of relatively large PLGA particles on the irregular surfaces of the titanium dioxide agglomerates. Anyway, the change of powder-to-polymer weight ratio from 1 : 1 to 3 : 1 did not cause a significant change in the coating layer thickness. The thickness is estimated from the scale bar to be around 10-100 nm, which is comparable to that of the fine silica particles. Based on all the experimental data shown previously, the potential mechanisms that would possibly contribute to the formation of coating on the ultra fine powders are schematically summarized as depicted in Fig. 8. Under the high-pressure condition, PLGA dissolved in supercritical CO_2 could be absorbed (wet) onto the surface of the core particles. In the figure, the wet coating layer on the surface of the core particles is represented by the dotted line covering the particle flowing within the nozzle. During the rapid expansion, the vaporization of CO_2 to the ambient leads to the formation of solidified PLGA film on the surface of core particles. Such coating layers would experience impaction among particles and shear forces due to high flow of surrounding gas, resulting in relatively uniform coating layer on the coated particles which would have

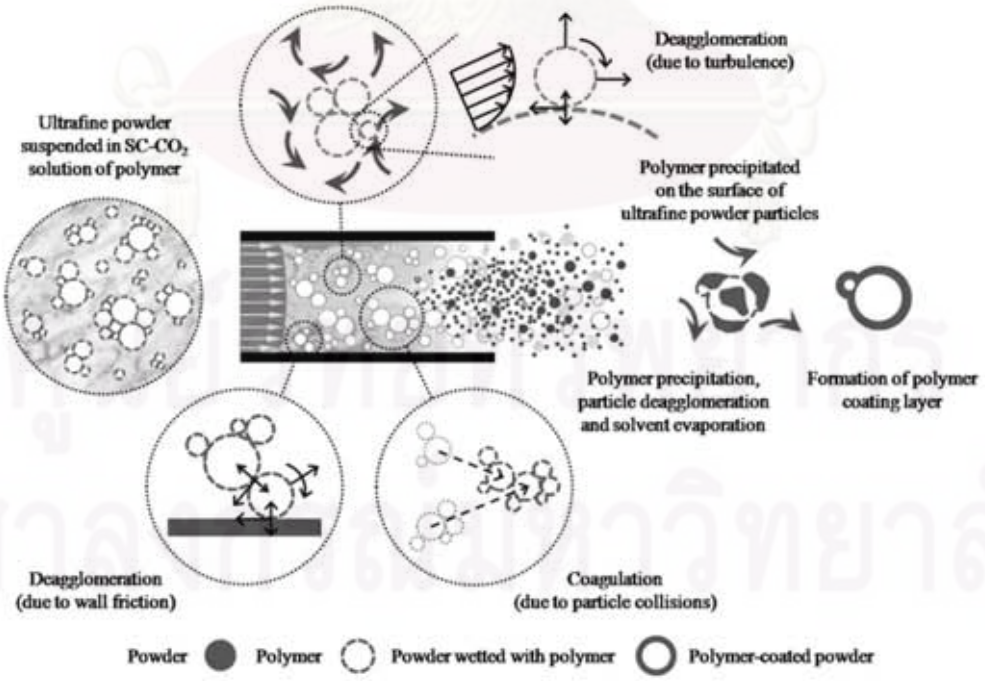

Fig. 8. Potential mechanism of polymer coating of ultra fine powder by the rapid expansion of supercritical suspension process.

some remaining agglomeration. The solidified polymer coating layer is represented by a thick solid line covering images of particles after being sprayed out of the nozzle.

CONCLUSIONS

The rapid expansion of supercritical solution process using ethanol as a cosolvent can produce non-agglomerated submicron particles of PLGA, which could favorably be used for coating ultra fine particles. The cosolvent concentration was found to play a key role in the control of PLGA particle size and size distribution. According to competitive influences of phase transition, turbulent flow, boundary friction and particle coagulation along the expansion path, the rapid expansion of supercritical suspension process exhibited two major phenomena, polymer precipitation and deagglomeration of ultra fine powders. These phenomena further resulted in a layer growth of polymer on the surface of deagglomerated ultra fine powders. Coating of the silica fine powder could be achieved in the form of both agglomerates and dispersed particles, depending on the powder-to-polymer weight ratio; whereas, coating in the agglomerate form was inevitable for the titanium dioxide ultra fine powder. In addition, nonuniformity of the coating layer was also observed. Surprisingly, the powder-to-polymer weight ratio appeared to have an insignificant effect on the thickness. To reduce agglomeration tendency, larger spray nozzle diameter, smaller powder particle size and low powder-to-polymer weight ratio are favorable. It is noteworthy that, in pharmaceutical applications, the RESS process with a cosolvent could be a promising environmentally friendly technique for coating CO_2-insoluble ultra fine drug particles with a high molecular-weight polymer with limited solubility in CO_2.

ACKNOWLEDGMENTS

The authors would like to acknowledge the Thailand Research Fund (TRF) for financial support through the Royal Golden Jubilee (RGJ) Ph.D. program and the Association of International Education, Japan (AIEJ) for partial financial support to B.K. The authors also thank Mr. H. Tsunakawa of the High Voltage Electron Microscope Laboratory, University of Tokyo, for his assistance with TEM observations. Also, partial financial support from University-Industry collaborative project of Chulalongkorn University and New Energy and Industrial Technology Development Organization (NEDO) is acknowledged.

REFERENCES

1. K. Jono, H. Ichikawa, M. Miyamoto and Y. Fukumori, *Powder Technol.*, **113**, 269 (2000).
2. D. Geldart, *Powder Technol.*, **7**, 285 (1973).
3. K. Fu, K. Griebenow, L. Hsieh, A. M. Klibanov and R. Langer, *J. Control. Release*, **58**, 357 (1999).
4. J. Wang, K. M. Chua and C. Wang, *J. Colloid Interf. Sci.*, **271**, 92 (2004).
5. J. Jung and M. Perrut, *J. Supercrit. Fluids*, **20**, 179 (2001).
6. K. Mishima, D. Tanabe and S. Yamauchi, *AIChE J.*, **46**, 857 (2000).
7. I. Ribeiro Dos Santos, J. Richard, B. Pech, C. Thies and J. P. Benoit, *Int. J. Pharm.*, **242**, 69 (2002).
8. A. Tsutsumi, M. Ikeda, W. Chen and J. Iwatsuki, *Powder Technol.*, **138**, 211 (2003).
9. Y. Wang, R. N. Dave and R. Pfeffer, *J. Supercrit. Fluids*, **28**, 85 (2004).
10. J. W. Tom, P. G. Debenedetti and R. Jerome, *J. Supercrit. Fluids*, **7**, 9 (1994).
11. S.-D. Yeo, P. G. Lim, G.-B. Lee and H. Debenedetti, *Biotechnol. Bioeng.*, **41**, 341 (1993).
12. P. G. Debenedetti, G. B. Lim and R. K. Prud'Homme, European Patent EP 0 542 314 (1992).
13. Y.-H. Choi, J.-W. Kim, M.-J. Noh, E.-M. Park and K.-P. Yoo, *Korean J. Chem. Eng.*, **13**, 216 (1996).
14. G-H. Li, J.-H. Chu, E.-S. Song, K.-H. Row, K.-H. Lee and Y. W. Lee, *Korean J. Chem. Eng.*, **23**, 482 (2006).
15. M. Hanna and P. York, Patent WO 95/01221 (1994).
16. M.-J. Noh, T.-G. Kim, I.-K. Hong and K.-P. Yoo, *Korean J. Chem. Eng.*, **12**, 48 (1995).
17. M. Zhong, B. Han and H. Yan, *J. Supercrit. Fluids*, **10**, 113 (1997).
18. B. Guan, Z. Liu, B. Han and H. Yan, *J. Supercrit. Fluids*, **14**, 213 (1999).
19. Q. Li, Z. Zhang, C. Zhong, Y. Liu and Q. Zhou, *Fluid Phase Equili.*, **207**, 183 (2003).
20. A. Chafer, T. Fornari, A. Berna and R. P. Stateva, *J. Supercrit. Fluids*, **32**, 89 (2004).
21. D. W. Jennings, R. J. Lee and A. S. Teja, *J. Chem. Eng. Data*, **36**, 303 (1991).
22. T. Susuki, N. Tsuge and K. Nakahama, *Fluid Phase Equili.*, **67**, 213 (1991).
23. C. Y. Day, C. J. Chang and C. Y. Chen, *J. Chem. Eng. Data*, **41**, 839 (1996).
24. N. C. Patel and A. S. Teja, *Chem. Eng. Sci.*, **37**, 463 (1982).
25. H. P. Gros, S. B. Bottini and E. A. Brignole, *Fluid Phase Equili.*, **139**, 75 (1997).
26. D. J. Dixon, K. P. Johnston and R. A. Bodmeier, *AIChE J.*, **39**, 127 (1993).
27. R. S. Mohamed, D. S. Halverson, P. G. Debenedetti and R. K. Prud'homme, *ACS Symp. Series*, **406**, 355 (1989).
28. P. G. Debenedetti, *Metastable liquids: Concepts and principles*, Princeton University Press, New Jersy (1996).
29. M. Giulietti, M. M. Seckler, S. Derenzo, M. I. Re' and E. Cekinski, *Braz. J. Chem. Eng.*, **18**, 423 (2001).
30. X. Y. Sun, T. J. Wang, Z. W. Wang and Y. Jin, *J. Supercrit. Fluids*, **24**, 231 (2002).
31. B. Helfgen, M. Turk and K. Schaber, *J. Supercrit. Fluids*, **24**, 231 (2003).
32. R. D. Smith, J. L. Fulton, R. C. Petersen, A. J. Kopriva and B. W. Wright, *Anal. Chem.*, **58**, 2057 (1986).

11230 *Ind. Eng. Chem. Res.* **2009,** *48,* 11230–11235

Encapsulation of SiO_2 and TiO_2 Fine Powders with Poly(DL-lactic-co-glycolic acid) by Rapid Expansion of Supercritical CO_2 Incorporated with Ethanol Cosolvent

Benjapol Kongsombut,[†] Atsushi Tsutsumi,[‡] Nara Suankaew,[†] and Tawatchai Charinpanitkul*[,†]

Center of Excellence in Particle Technology, Faculty of Engineering, Chulalongkorn University, Patumwan, Bangkok 10330 Thailand, and Department of Chemical System Engineering, The University of Tokyo, Bunkyo-ku, Tokyo 113-8656 Japan

Rapid expansion of supercritical carbon dioxide solution (RESS) for encapsulating core powders with a polymer shell was experimentally examined. Poly(DL-lactic-co-glycolic acid) polymer (PLGA) and 1.4-μm SiO_2 as well as 70-nm TiO_2 powders were employed as model encapsulating agent and core particles, respectively. A solution of PLGA in supercritical carbon dioxide (SC-CO_2) was prepared incorporated with ethanol cosolvent. The RESS process was then performed by spraying the supercritical mixture through a capillary nozzle, leading to formation of well-dispersed PLGA nanoparticles. The precipitation of PLGA accompanying with its dispersion on core powder surface could be ascribed to the rigorous shear stress acting on the expanding flow of SC-CO_2. The cumulative deposition of the precipitating PLGA could result in the uniform encapsulation of the SiO_2 and TiO_2 powders with 10 to 100 nm-thick PLGA layers in the form of both individual and agglomerating particles. The increased weight ratio of core particle to PLGA could lead to the more promoted encapsulation of core particles due to the higher contact among the core and precipitated PLGA particles after expansion. In comparison with large SiO_2 powders, more rigorous agglomeration of encapsulated TiO_2 powders would be attributed to their higher interparticle collections, which could also interfere with the expansion process.

1. Introduction

Encapsulation of powders could find a variety of applications in various industries related to agricultural, energy conservative, food, and pharmaceutical processes. For instance, the general purposes of pharmaceutical encapsulation are to provide protection from rapid degradation, control of release rate, and prevention of side effect of therapeutic agents. While the conventional process used for encapsulating powders is generally based on fluidization techniques, there is a limitation for powders smaller than 70 μm because of poor fluidization behavior.[1] Emulsion-based techniques, such as water-in-oil-in-water (w/o/w) double emulsions or solid-in-oil-in-water (s/o/w) emulsions, may be used for encapsulating ultrafine powders. However, these emulsion-based techniques involve some drawbacks including alteration of the structure of the therapeutic agent, presence of residual organic solvent in the encapsulated powders, and emission of volatile organic compounds to the environment.[2,3]

In the last few decades, many researchers have paid attention to the application of supercritical fluids (SCFs) to overcome the problems of using organic solvent in the conventional encapsulation processes.[4] Carbon dioxide (CO_2) is the most commonly used SCF in pharmaceutical applications due to its inert properties, nontoxicity, nonpolluting nature, and mild critical conditions. It is well-known that the simplest SCF technique for formation of pharmaceutical particles and composite materials is the rapid expansion of supercritical solution (RESS). With the RESS technique, a solute is dissolved in supercritical carbon dioxide (SC-CO_2) and the solution is then instantaneously depressurized by spraying it through a capillary nozzle, causing precipitation of the solute as SC-CO_2 vaporizes. Submicrometer and nanosized dry particles with a narrow particle size distribution could be obtained for various pharmaceutical compounds and polymers.[4] In this study, the RESS process with a cosolvent is used to produce fine particles of polymer and the process is also modified for polymer coating of ultrafine powders. Micron-sized silica and nanosized titanium dioxide particles were chosen as model particles of preformed drug powders while poly(DL-lactic-co-glycolic acid) (PLGA) copolymer was used as the encapsulating material. Formation of primitive PLGA particles and silica and titania core particles encapsulated by a PLGA shell was experimentally examined and then discussed. The characterization results of encapsulated powders regarding their morphology and internal structure were also reported.

2. Experimental Section

2.1. Materials. As model powders with known sizes, silica (SiO_2) powder with a nominal diameter of 1.4 μm (Kojundo Chemical Lab, Japan) and titanium dioxide (TiO_2) powder with a nominal diameter of 70 nm (Ishihara Sangyo Kaisha, Japan) were employed in this work. Poly(DL-lactic-co-glycolic acid) (PLGA) (molecular weight = 62 000 and glass transition temperature = 47.5 °C (320.5 K), Aldrich Chemicals Ltd.) and liquid CO_2 (critical temperature T_c = 304 K, critical pressure P_c = 7.4 MPa, Suzuki Shokan Co. Ltd., Tokyo, Japan) were used as encapsulating agent and solvent. In each experiment, PLGA granules were grounded and classified to a certain size range of 100−200 μm. Due to the limited solubility of PLGA in SC-CO_2, ethanol (special grade; >99.5%; Kanto Chemical Co., Inc., Tokyo, Japan) was employed as cosolvent. All chemicals and materials were used as received without further purification.

2.2. Experimental Procedure. Figure 1 depicts schematic diagram of the experiment equipment which consists of a high-pressure pump, a stirred high-pressure vessel, and a spray nozzle. The high-pressure pump was equipped with a refrigerator to

* To whom correspondence should be addressed. Tel./Fax: +662-2186480. E-mail: ctawat@chula.ac.th.
[†] Chulalongkorn University.
[‡] The University of Tokyo.

10.1021/ie900690v CCC: $40.75
Published on Web 11/18/2009

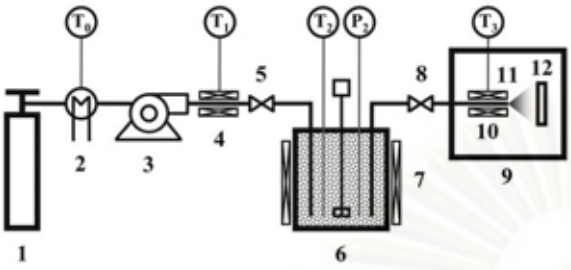

Figure 1. Schematic diagram of experimental apparatus employed in this work: (1) CO_2 cylinder; (2) refrigerator; (3) HPLC pump; (4) heater; (5) regulating valve; (6) high-pressure vessel; (7) vessel heater; (8) shut-off valve; (9) atmospheric chamber; (10) ribbon heater; (11) nozzle; (12) target plate.

avoid cavitation. The high-pressure vessel had a capacity of 1500 mL and maximum allowable operating pressure and temperature of 30 MPa and 473 K, respectively. During each experiment, the vessel temperature was kept constant at 313 K using an automatically controlled electric heater. The spray nozzle was simply made from a stainless steel tube with a length of 10 mm and was equipped with a shut-off valve. A planar target (100 mm × 100 mm × 10 mm) covered with aluminum foil and a carbon-coated copper grid was employed to collect samples of particles generated from the rapidly expanding spray for characterization.

We have focused on experimental investigation using carbon dioxide (CO_2) in the RESS process for generate polymer-encapsulated particles because its critical condition is achievable and easy for handling. Meanwhile, the PLGA polymer used in our study has a limited solubility in SC-CO_2 because of its very high molecular weight.[5] In order to increase the PLGA solubility in SC-CO_2 to a beneficial extent, ethanol was used as cosolvent. A 2 g portion of PLGA with different amounts of ethanol were placed in the high-pressure vessel for preparation of SC-CO_2 solution. After being carefully sealed, the vessel was heated and fed with CO_2 via the high-pressure pump until the desired supercritical conditions were achieved. The mixture in the vessel was stirred by a mixing paddle rotating at 300 rpm and was left for 3 h to achieve equilibrium.[6] The prepared supercritical solution was then sprayed through the nozzle to allow its rapid expansion. The target plate was placed against the sprayed flow at a distance of 300 mm from the nozzle tip within a chamber under the atmospheric condition.

Then, performance of the RESS process to prepare encapsulation of fine powders by PLGA was investigated using the above-mentioned apparatus. It should be noted that the fine powders, PLGA and ethanol, in pure form, are not soluble in each other. Thus they form an immiscible ternary mixture under the atmospheric condition. Experimental procedures similar to the first part were carried out so as to dissolve PLGA in SC-CO_2 with the aid of ethanol in the presence of micrometer-sized SiO_2 or nanosized TiO_2 core particles. It should be noted that in this work nanosized TiO_2 powder was selected because of its low agglomeration and monodispersity compared with those of the more expensive nanosized SiO_2. Under these conditions, the core particles were not dissolved but suspended in a single homogeneous mixture of CO_2, ethanol, and the dissolved PLGA. The supercritical suspensions were then allowed to expand through the nozzle for a few seconds. The same sampling method was employed to obtain coated particles for characterization. In order to evaluate the encapsulating performance, the effect of three process parameters, which were powder-to-polymer weight ratio, diameter of the spray nozzle, and mean diameter of the core powder, on the encapsulating characteristics was investigated. The experimental parameters and conditions used in this work are listed in Table 1.

Table 1. Experimental Parameters and Conditions of RESS Processes

material	solvent	CO_2; P_c = 7.4 MPa; T_c = 304 K T_0 = 266 K; T_1 = 353 K
	cosolvent	ethanol; 0−21.8 wt %
	polymer	poly(D,L-lactic-co-glycolic acid), PLGA; M_w 62 000; T_g 320.5 K
	powder	SiO_2; mean diameter of 1.4 μm TiO_2; mean diameter of 70.0 nm
	powder-to-polymer weight ratio	1:1, 2:1, 3:1, and 4:1
dissolution	vessel	cylinder; 1500 mL
	agitation	300 rpm; 180 min
	conditions	P_2 = 25 MPa; T_2 = 313 K
expansion	nozzle	stainless steel; d = 0.1, 0.3 mm; L = 10 mm; T_3 = 423 K

Field emission scanning electron microscopy (FE-SEM; Hitachi, S-900) was used to examine the particle samples obtained from each experiment. For SEM sample preparation, the aluminum foil uncovered from the target plate was cut into a small piece, mounted on a specimen stub with conductive paint, and coated with platinum by a sputtering device (Hitachi, E-1030) for 20 s. The SEM was operated at an accelerating voltage of 10 kV and a magnification between 1000 and 200 000. The SEM images were processed for particle size analysis by using image-analyzing software (Image-Pro Plus version 3.0; Media Cybernetics). For verification of polymer encapsulation of the core powder, the particle samples on the copper grid were further analyzed by a transmission electron microscope (TEM; JEOL 2000-EX) operated at 200 kV in the bright-field mode. To analyze the structures and morphology of the coated powders, the mass−thickness contrast between the encapsulating polymer and the core powder was taken into account.

3. Results and Discussion

3.1. Formation of PLGA Particles by RESS. PLGA is well-recognized as a biodegradable polymer which is suitable for biomedical applications.[7] Depending upon its molecular weight, PLGA could provide flexible operatability for coating applicationa. PLGA with an average molecular weight of 62 000 and T_g of 320.5 K was chosen regarding to the operating range achievable in this work. Meanwhile, it is commonly accepted that ethanol is an environmentally friendly cosolvent because of its low toxicity. For the cosolvent, in comparison with other alcohols, ethanol is a more economical commercial solvent of which scalable production is available. Thereby, ethanol has been chosen as the cosolvent in this work. Although PLGA has limited solubility in either SC-CO_2 or ethanol, it was reported that the PLGA solubility could be enhanced in mixture of these two fluids.[7] Since ethanol is capable of being both donor and acceptor of hydrogen bonds, it can self-associate through hydrogen bonding with both CO_2 and PLGA, which leads to significantly improved PLGA solubility in SC-CO_2. The solubility enhancement of various polymers by ethanol cosolvent has been reported and discussed in several papers.[8−11]

A solution of PLGA in SC-CO_2 plus ethanol was prepared at 25 MPa and 313 K. Jennings et al.[12] and Suzuki et al.[13] have reported that, under these conditions, CO_2 and ethanol become miscible at all compositions and form a single supercritical fluid phase. A different amount of ethanol was added to the pressure vessel at 0, 100, 200, 300, and 400 mL, respectively. Because the amount of PLGA dissolved in the CO_2−ethanol mixtures

was very small, compared to those of CO_2 and ethanol, the ethanol concentration in the mixtures could be estimated from the Patel−Teja cubic equation of state extended to binary mixtures, regardless of the PLGA presence in the mixtures.[14,15] The CO_2−ethanol interaction parameters used in the calculation were obtained from data reported by Gros et al.[6] According to the varied amount of ethanol mentioned above, the calculated values of the polymer-free concentration of ethanol are 0, 5.7, 11.1, 16.4, and 21.8 wt %, respectively.

In our experiments using pure CO_2 and CO_2 incorporated with 5.7 wt % ethanol, negligible amounts of polymer particles were detected in the collected samples under SEM observations, thereby indicating negligible particle formation during the RESS process. This implied that both pure CO_2 and CO_2 incorporated with ethanol at 5.7 wt % were unable to dissolve PLGA to a sufficient extent. As a result, supersaturation was not achieved to trigger particle nucleation in these cases. Figure 2 shows some typical SEM images of PLGA particles produced by RESS using CO_2 mixed with ethanol at 11.1, 16.4, and 21.8 wt %. The charged amount of PLGA in SC-CO_2 with 21.8 wt % ethanol was approximately 0.17 wt % of the total amount of supercritical solution. Also, it is clearly observable that the generated particles exhibit a nearly spherical shape with size distributed in a narrow range. At the higher ethanol weight percent, the resulting PLGA particles were micrometer in size with an irregular surface. However, the increase in ethanol weight percent could result in much smaller particles with smooth surface. This is attributed to higher vaporization of ethanol due to the higher ethanol weight percent and rigorous shear stress due to the rapid expansion of SC-CO_2 flow.[16,17]

On the basis of these experimental results, the formation of PLGA particles via RESS could be described as follows. Under the equilibrium condition of SC-CO_2, PLGA, CO_2, and ethanol would form a single homogeneous supercritical solution though saturation of PLGA was not yet achieved. During the rapid expansion, phase transition of CO_2 taking place in the postexpansion free jet would result in a drastic increase in the PLGA concentration in the droplets, leading to precipitation of the dissolved polymer. As already mentioned, since ethanol could insignificantly dissolve PLGA with the absence of SC-CO_2, it also vaporized out after the expansion.[6] Therefore, it is reasonable to consider that the precipitated polymer particles were solvent-free and did not undergo an agglomeration process because of its dilute solid content. These results suggested that the generated polymer particles would possibly be employed to encapsulate core particles.

Analyses of typical SEM images of PLGA particles shown in Figure 2 were carried out to determine their size distribution and morphology. At least 300 particles dispersed in different regions of the SEM images were taken into account in the determination of their size distribution. It was also experimentally found that the particle size distribution as well as morphology of the prepared PLGA particles was strongly dependent on the ethanol concentration. As the ethanol concentration was increased from 11.1 to 21.8 wt %, the particle geometric mean decreased to a minimum of 55 nm while the geometric standard deviation increased to a maximum of 1.67. The decreased average size of precipitated PLGA particles would be ascribed to the increase in the PLGA solubility, thereby increasing the supersaturation of PLGA in the sprayed mixture after its rapid expansion. On the basis of the classical nucleation theory,[17] higher nucleation rate and smaller critical nucleus size could be expected if the dissolved polymer concentration becomes increased. Meanwhile, a higher supersaturation ratio would also result in the nucleation of random size particles at its early stage.[18] It is also noteworthy that an increase in the particle number concentration could provide higher coagulation frequency. Therefore, these counterbalancing phenomena were responsible for a smaller mean size but wider distribution of the PLGA particles when a higher concentration of ethanol was introduced to the system. These confirmations suggested that encapsulation of the core powder with the precipitate PGLA would be possibly achieved by RESS of SC-CO_2 with ethanol cosolvent.

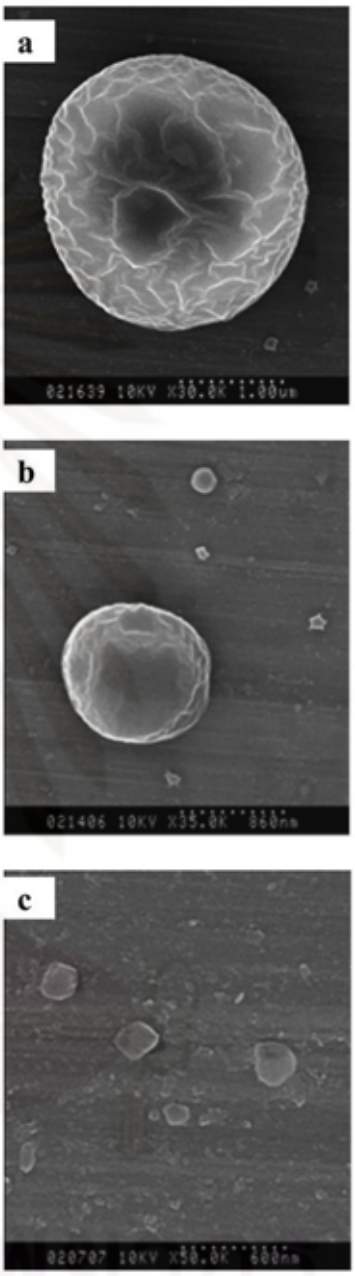

Figure 2. Typical SEM images of PLGA particles produced by RESS using ethanol cosolvent at different ethanol concentrations: (a) 11.1; (b) 16.4; (c) 21.8 wt %.

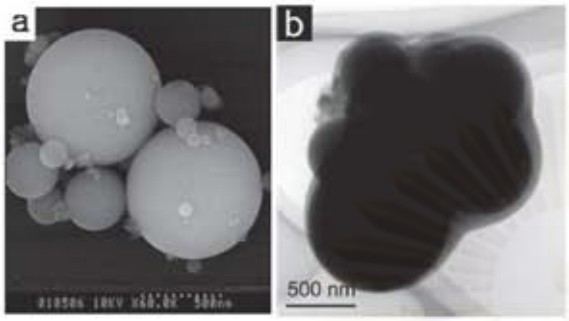

Figure 3. Typical SEM and TEM images of PLGA-enapsulated SiO_2 powder prepared by rapid expansion of supercritical suspension process at a powder-to-polymer weight ratio of 3:1.

3.2. Characteristics of Encapsulated Particles. A series of experiments was carried out on encapsulating 1.4-μm SiO_2 powders and 70-nm TiO_2 powders with PLGA by rapid expansion of SC-CO_2. In a real situation, preformed drug particles, i.e. dexamethasome and insulin, would be employed for the encapsulation to verify their sustain−release perfomance.[8,9] However, because of the economic constraints as well as the scope of this work which focused on the physical aspects of coating, commercial silica and titania particles with designated size were chosen as model particles for coating experiments. Regarding those physical aspects, i.e. coating film thickness and degree of agglomeration, they are useful data for further examination of the releasing rate of coating drug particles.[6−9]

In all experiments, the supercritical suspensions were prepared using the conditions at which the solubility of PLGA in the mixture of SC-CO_2 and ethanol could be designated, i.e. with the supercritical pressure and temperature of 25 MPa and 313 K, the ethanol concentration would be 21.8 wt % and the polymer solubility is 0.17 wt %.[10,18] The powder-to-polymer weight ratio was varied through an adjustment of the powder concentration in the suspension by changing the amount of powder added to the high-pressure vessel at the beginning of each experiment.

Figure 3 shows two typical samples of PLGA-encapsulated silica fine powder produced by the rapid expansion of supercritical suspension process with powder-to-polymer weight ratio of 3:1. It appears that the encapsulating of silica fine powder was achieved in the form of both individual dispersed particles and agglomerates. The encapsulated silica particles exhibit a core−shell structure, as shown in the bright-field TEM image (Figure 3b). It should be noted that due to the stronger interactions between the electrons and silicon than that between the electrons and carbon (a major component of the polymer) in the TEM, the SiO_2 particles appear as a darker contrast area than the PLGA phase in these images. It is clearly seen that the darker contrast area is thoroughly covered by the lighter contrast area, indicating that the SiO_2 particles were completely coated with a layer of PLGA. The rapid expansion of a suspension of SC-CO_2-insoluble particles in the supercritical CO_2 solution of a polymer led to deposition of the polymer on the surface of the suspended particles, thereby generating a polymer encapsulating layer on the particle surfaces.[6,19] It should be noted that these experimental results consistently agree with this explanation. As a concurrent result of the rapid expansion of supercritical suspension, the dispersion and segregation of SiO_2 powder contributed to the low agglomeration tendency of the encapsulated particles.

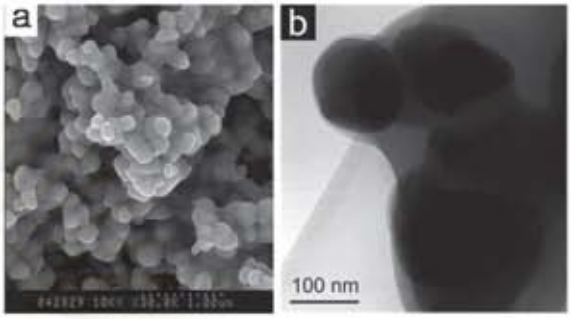

Figure 4. Typical SEM and TEM images of PLGA-encapsulated TiO_2 powder prepared by rapid expansion of supercritical suspension process at a powder-to-polymer weight ratio of 3:1.

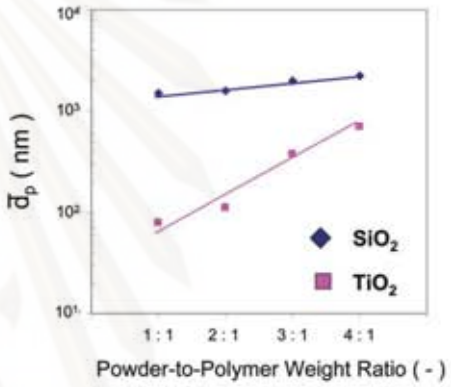

Figure 5. Effect of powder-to-polymer weight ratio on the average diameter of encapsulated powders.

Similar results were obtained for the encapsulation of 70-nm TiO_2 powder with PLGA, as shown in Figure 4. The experimental results suggest that the encapsulation of titanium dioxide powder with PLGA could also be achieved in the same process as that of SiO_2 powder. However, SEM and TEM images reveal that the encapsulation of TiO_2 powder took place in the form of agglomerates of primary particles. In Figure 4, the encapsulated particles are composed of an agglomerate of titanium dioxide particles in the core and a coat of PLGA which could be observed as the darker and the lighter contrast areas, respectively. It should be noted that only few individual PLGA nanoparticles were observed in the void among the TiO_2 particles, suggesting that the PLGA shell was formed as a growing layer on the agglomerated TiO_2 surface.

3.3. Influence of Operating Parameters on the Encapsulated Powder Characteristics. Summarized effect of the powder-to-polymer weight ratio on the average diameter of encapsulated SiO_2 and TiO_2 powders is depicted in Figure 5. It could be clearly confirmed that, with the increase in the powder-to-polymer weight ratio, the average diameters of the encapsulated SiO_2 and TiO_2 powders became larger, indicating the thicker layer of the encapsulating layer as well as the higher agglomeration. However, the SiO_2 powders exhibited a much lower degree of agglomeration regarding a lower increasing rate of the average diameters with respect to the increased powder weight ratio in comparison with those of the TiO_2 powders. As could also be confirmed by the visualized evidence in Figures 3 and 4, the significant agglomeration could be observed when the powder-to-polymer weight ratio was 3:1. This result would mainly be attributable to the fact that, at the high powder-to-

Table 2. Influence of Powder-to-Polymer Weight Ratio and Nozzle Diameter on Encapsulation Operatability

	powder-to-polymer weight ratio			
	1:1	2:1	3:1	4:1
0.1 mm nozzle	total ice clogging	$d_{p,silica}$: 1700 nm $d_{p,titania}$: 120 nm spraying with partial ice clogging	$d_{p,silica}$: 2000 nm $d_{p,titania}$: 380 nm uniform spraying	$d_{p,silica}$: 2100 nm $d_{p,titania}$: 720 nm spraying with partial powder clogging
0.3 mm nozzle	$d_{p,silica}$: 1500 nm $d_{p,titania}$: 80 nm uniform spraying	$d_{p,silica}$: 1600 nm $d_{p,titania}$: 110 nm uniform spraying	$d_{p,silica}$: 2000 nm $d_{p,titania}$: 380 nm uniform spraying	$d_{p,silica}$: 2200 nm $d_{p,titania}$: 700 nm spraying with partial powder clogging

polymer weight ratio, the rapid expansion flow of powder and polymer would result in an increasing collision and coagulation probability of the particles within the nozzle and, consequently, a high degree of agglomeration. In addition, it can be observed in the TEM images (Figure 3b) that the thickness of the encapsulating layer was rather uniform and estimated to be around 30−100 nm. It is likely that the PLGA particles, which precipitated and then deposited on the silica particle surface, spread and formed solid bridges between them, thereby resulting in growth of the coating layer. However, the strong shear stress in the rapid expansion flow could generate the eddy turbulence which could be accounted for significant disturbances to the just-formed polymer coating layer.[20] As a result, particulate SiO_2 powder with rather uniform PLGA layer was obtained.

On the other hand, the agglomerate sizes of encapsulated TiO_2 were in the range of some hundred nanometers. Obviously, the flow turbulence and friction loss generated during the rapid expansion of supercritical suspension process would not be sufficient to disintegrate all of agglomerates into totally separated particles. This would be ascribed to the extremely strong adhesion forces among the TiO_2 powder against the shear stress due to the fluid expansion. The nonuniform PLGA shell could be observed in the TEM images (Figure 4b), indicating the deposition of relatively thick PLGA layer on the surface of the TiO_2 agglomerates. The thickness estimated from the scale bar was ca. 10−90 nm comparable to that of the encapsulated SiO_2 powder.

Table 2 summarizes the effect of nozzle size on the encapsulated product characteristics and the operatability of RESS process investigated in this work. It could be clearly observed that there was only a limited condition of operable RESS when the 0.1-mm nozzle was employed. With a lower powder-to-polymer weight ratio or in other words "a high fraction of polymer", rapid expansion could only be conducted at the first short moment, then the nozzle tip would be totally covered by ice due to the isenthalpic Joule−Thompson effect. A higher polymer fraction would lead to a more serious Joule−Thompson effect because of its fluid behavior.[5] On the other hand, when the powder-to-polymer weight ratio was increased to 4:1, the clogging of nozzle was caused by the sticking of the agglomeration of encapsulated powders. There was only the condition of powder-to-polymer weight ratio of 3:1 which could provide the encapsulated powders.

On the other hand, with the 0.3-mm nozzle no clogging due to the Joule−Thompson effect could be observed. Encapsulation could be smoothly conducted until the powder-to-polymer weight ratio was increased to 4:1 which partial clogging of the nozzle would take place due to the sticking of agglomerated powders.[17] Similarly, these results would be ascribed that the high powder fraction would bring about the rigorous agglomeration of encapsulated powders as could also be confirmed by the increased average diameters depicted in Figure 5. For the encapsulated silica particles, the increasing size was relatively low when compared with that of encapsulated titania which preferred to agglomeration. The agglomeration would be compensated by the share stress due to the turbulent flow of rapid expansion of suspension.[19] All encapsulated powders prepared by the 0.3-mm nozzle possessed the physical characteristics as described in 3.2. Therefore, it would be worth to mention that the bigger 3-mm nozzle could provide broader range for the RESS of powder encapsulation with PLGA in comparison with the 1-mm nozzle. These results would suggest us that there is a possibility to increase the productivity of PLGA-encapsulated powders of either SiO_2 or TiO_2 once a nozzle with an appropriate diameter is selected.

As a summary, all of these experimental results are clear evidence revealing that the process of rapid expansion of SC-CO_2 incorporated with ethanol cosolvent is promising for encapsulation of fine powders with PLGA.[18] While an improvement for handling the agglomeration phenomenon would be required for a scalable production of the encapsulated products, further investigation on the detailed mechanism of polymer layer formation on the encapsulated powder surface would be an issue of interest. In addition, for improving the solubility of PLGA in SC-CO_2, utilization other types of alcohol with an anticipation of better control of encapsulating layer would also be another issue for future investigation.

4. Conclusions

The rapid expansion of supercritical CO_2−PLGA solution with ethanol as a cosolvent could provide small particles of PLGA, which could be precipitated and attached to surface of core particles. It was found that the cosolvent could exert a significant effect on the PLGA particle size and its size distribution. According to competitive influences of phase transition, turbulent flow, boundary friction, and particle coagulation along the expansion path, the rapid expansion of supercritical suspension process exhibited two major phenomena, polymer precipitation, and dispersion of polymer particles. These phenomena further resulted in a layer growth of polymer on the surface of core powders. Encapsulation of the SiO_2 powders could be achieved in the form of both agglomerates and dispersed particles, depending on the powder-to-polymer weight ratio, whereas coating in the agglomerated product was inevitable for the TiO_2 nanoparticles due to the more rigorous agglomeration. It should be noted that a scalable RESS process would be a promising environmentally friendly technique for encapsulation of fine powder using PLGA with designated molecular-weight once the agglomeration of the encapsulated powder could be improved by the deeper understanding of the coating layer formation mechanism.

Acknowledgment

B.K. and T.C would like to acknowledge a financial support of TRF-RGJ from Thailand Research Fund. Also, a partial support from the Centennial Fund of Chulalongkorn University to CEPT is gratefully acknowledged.

Literature Cited

(1) Geldart, D. Types of Gas Fluidization. *Powder Technol.* **1973**, *7*, 285.

(2) Fu, K.; Griebenow, K.; Hsieh, L.; Klibanov, A. M.; Langer, R. FTIR Characterization of the Secondary Structure of Proteins Encapsulated within PLGA Microspheres. *J. Controlled Release* **1999**, *58*, 357.

(3) Wang, J.; Chua, K. M.; Wang, C. Stabilization and Encapsulation of Human Immunoglobulin G into Biodegradable Microspheres. *J. Colloid Interface Sci.* **2003**, *271*, 92.

(4) Jung, J.; Perrut, M. Particle Design Using Supercritical Fluids: Literature and Patent Survey. *J. Sup. Fluids* **2001**, *20*, 179.

(5) Tom, J. W.; Debenedetti, P. G. Precipitation of Poly(L-lactic acid) and Composite Poly(L-lactic acid)-Pyrene Particles by Rapid Expansion of Supercritical Solutions. *J. Sup. Fluids* **1994**, *7*, 9.

(6) Gros, H. P.; Bottini, S. B.; Brignole, E. A. High Pressure Phase Equilibrium Modeling of Mixtures Containing Associating Compounds and Gases. *Fluid Phase Equilib.* **1997**, *139*, 75.

(7) Mishima, K.; Tanabe, D.; Yamauchi, S. Microencapsulation of Proteins by Rapid Expansion of Supercritical Solution with a Nonsolvent. *AIChE J.* **2000**, *46*, 857.

(8) Zolnik, B. S.; Burgess, D. J. Effect of Acidic pH on PLGA Microsphere Degradation and Release. *J. Controlled Release* **2007**, *122*, 338.

(9) Liu, R.; Huang, S. S.; Wan, Y. H.; Ma, G. H.; Su, Z. G. Preparation of Insulin-loaded PLA/PLGA Microcapsules by a Novel Membrane Emulsification Method and its Release in vitro. *Colloids Surf.* **2006**, *51*, 30.

(10) Li, Q.; Zhang, Z.; Zhong, C.; Liu, Y.; Zhou, Q. Solubility of Solid Solutes in Supercritical Carbon Dioxide with and without Cosolvents. *Fluid Phase Equilib.* **2003**, *207*, 183.

(11) Chafer, A.; Fornari, T.; Berna, A.; Stateva, R. P. Solubility of Quercetin in Supercritical CO_2 + Ethanol as a Modifier: Measurements and Thermodynamic Modeling. *J. Sup. Fluids* **2004**, *32*, 89.

(12) Jennings, D. W.; Lee, R. J.; Teja, A. S. Vapor-Liquid Equilibria in the Carbon Dioxide + Ethanol and Carbon Dioxide + 1-Butanol Systems. *J. Chem. Eng. Data* **1991**, *36*, 303.

(13) Susuki, T.; Tsuge, N.; Nakahama, K. Solubilities of Ethanol, 1-Propanol, 2-Propanol and 1-Butanol in Supercritical Carbon Dioxide at 313 and 333 K. *Fluid Phase Equilib.* **1991**, *67*, 213.

(14) Day, C. Y.; Chang, C. J.; Chen, C. Y. Phase Equilibrium of Ethanol + CO2 and Acetone + CO2 at Elevated Pressures. *J. Chem. Eng. Data* **1996**, *41*, 839.

(15) Patel, N. C.; Teja, A. S. A New Cubic Equation of State for Fluids and Fluid Mixtures. *Chem. Eng. Sci.* **1982**, *37*, 463.

(16) Dixon, D. J.; Johnston, K. P.; Bodmeier, R. A. Polymeric Materials Formed by Precipitation with a Compressed Fluid Antisolvent. *AIChE J.* **1993**, *39*, 127.

(17) Mohamed, R. S.; Halverson, D. S.; Debenedetti, P. G.; Prud'homme, R. K. Solids Formation after the Expansion of Supercritical Mixtures. *ACS Symp. Ser.* **1989**, *406*, 355.

(18) Giulietti, M.; Seckler, M. M.; Derenzo, S.; Re, M. I.; Cekinski, E. Industrial Crystallization and Precipitation from Solutions: State of the Technique. *Braz. J. Chem. Eng.* **2001**, *18*, 423.

(19) Tsutsumi, A.; Ikeda, M.; Chen, W.; Iwatsuki, J. A Nano-Coating Process by the Rapid Expansion of Supercritical Suspensions in Impinging-Stream Reactors. *Powder Technol.* **2003**, *138*, 211.

(20) Sun, X. Y.; Wang, T. J.; Wang, Z. W.; Jin, Y. The Characteristics of Coherent Structures in the Rapid Expansion Flow of the Supercritical Carbon Dioxide. *J. Supercrit. Fluids* **2002**, *24*, 231.

Received for review February 27, 2009
Revised manuscript received July 11, 2009
Accepted July 16, 2009

IE900690V

Coating of Ultrafine Powders with PLGA by Rapid Expansion of Supercritical Solutions with Ethanol Cosolvent

Benjapol Kongsombut[1], Wei Chen[2], Atsushi Tsutsumi[2], Wiwut Tanthapanichakoon[3], Tawatchai Charinpanitkul[1]
[1]Center of Excellence in Particle Technology, Faculty of Engineering, Chulalongkorn University, Thailand
[2]Department of Chemical System Engineering, the University of Tokyo, Japan
[3]NANOTEC, National Science and Technology Development Agency, Thailand
Correspondence: ctawat@chula.ac.th, kongsombut@gmail.com

ABSTRACT

For pharmaceutical applications, rapid expansion of supercritical solution (RESS) process has been utilized to generate polymer-coated microscale and nanoscale powders. Poly(DL-lactide-co-glycolide) polymer (PLGA) and core powders, which were 1.4-μm SiO_2 and 70-nm TiO_2 particles, were selected for investigation on coating induced by RESS technique. Supercritical solution was prepared by dissolving PLGA in supercritical carbon dioxide (SC-CO_2) with assistant of ethanol cosolvent. The RESS process was performed by spraying the supercritical solution through a capillary nozzle under ambient conditions. It was found that formation of submicron PLGA particles could take place by the RESS and could be explained by the classical nucleation theory. Meanwhile, precipitation of PLGA accompanying by solvent evaporation and disintegration of agglomeration of the core powders could provide uniformly coated microscale and nanoscale particles. However, under some specific conditions, the cumulative deposition of precipitating PLGA on the coated powders led to the coating of the powders with PLGA in the form of both individual particles and agglomerates. SEM and TEM were employed to examine morphology and internal structure of the PLGA-coated powders.

Keywords: RESS, coating, ultrafine powders, PLGA

1 INTRODUCTION

Coating of powders has provided its application in various industries, including pharmaceuticals, foods, agriculture and energetic materials. The general purposes of pharmaceutical coating are to provide protection from rapid degradation, control of release rate and prevention of side effect of therapeutic agents. While the conventional process used for coating powders is generally based on fluidization technique, there is a limitation for powders smaller than 70 μm because of poor fluidization behavior [1]. Emulsion-based techniques, such as water-in-oil-in-water (w/o/w) double emulsions or solid-in-oil-in-water (s/o/w) emulsions, may be used for coating ultrafine powders. However, these emulsion-based techniques involve some drawbacks including alteration of structure of therapeutic agent, presence of residual organic solvent in the coated powders and emission of volatile organic compounds to the environment [2, 3].

In the last few decades, many researchers have paid their attention on the application of supercritical fluids (SCFs) to overcome the problems of using organic solvent in the conventional coating processes [4]. Carbon dioxide (CO_2) is the most commonly used SCF in pharmaceutical applications due to its inert properties, non-toxicity, non-polluting nature and mild critical conditions. It is well known that the simplest SCF technique for formation of pharmaceutical particles and composite materials is the rapid expansion of supercritical solution (RESS). With the RESS technique, a solute is dissolved in SC-CO_2 and the solution is then instantaneously depressurized by spraying it through a capillary nozzle, causing precipitation of the solute as SC-CO_2 vaporizes. Submicron and nanosize dry particles with a narrow particle size distribution could be obtained for various pharmaceutical compounds and polymers [4]. In this study, the RESS process with a cosolvent is used to produce fine particles of polymer and the process is also modified for polymer coating of ultrafine powders. Microsize silica and nanosize titanium dioxide particles were chosen as pre-formed drug ultrafine powders while poly(lactic-co-glycolic acid) (PLGA) copolymer was used as the coating material. Effects of the process parameters, which were cosolvent concentration and particle size of ultrafine core powder, are presented and discussed based on the characterization results of coated powders regarding their morphology and internal structure.

2 EXPERIMENTAL

2.1 Material

Silica (SiO_2) particles with a mean size of 1.4 μm (Kojundo Chemical Lab, Japan) and titanium dioxide (TiO_2) particles with a mean size of 70 nm (Ishihara Sangyo Kaisha, Japan) were employed as core particles. Poly(DL-lactide-co-glycolic acid) (PLGA) (molecular weight = 62 000 and glass transition temperature = 47.5°C, Aldrich Chemicals Ltd.) and liquid CO_2 (critical temperature T_c = 304 K, critical pressure P_c = 7.4 MPa, Suzuki Shokan Co. Ltd., Tokyo, Japan) were used as coating agent and solvent. Due to the limited solubility of PLGA in SC-CO_2, ethanol (special grade; >99.5%; Kanto Chemical Co., Inc., Tokyo, Japan) was employed as cosolvent. All chemicals and materials were used as received.

2.2 Experimental Procedure

Fig. 1 shows schematic diagram of the experiment equipment which consists of a high-pressure pump, a stirred high-pressure vessel and a spray nozzle. The high-pressure pump was equipped with a cooler to avoid cavitation. The high-pressure vessel had a capacity of 1,500 ml and maximum allowable operating pressure and temperature of 30 MPa and 473 K, respectively. During each experiment, the vessel temperature was kept constant at 313 K using an automatically controlled electric heater. The spray nozzle was simply made from a stainless steel tube with a length of 10 mm and was equipped with a shut-off valve. Two spray nozzles with different inner diameters of 0.1 mm and 0.3 mm were employed for investigating the effect of nozzle diameter on the coating process. Temperature of the nozzle was kept constant at 423 K by a ribbon heater to prevent the nozzle clogging with dry ice during spraying. A planar target (100 mm × 100 mm × 10 mm) covered with aluminum foil and a carbon-coated copper microgrid was employed to collect samples of particles generated from the spray for characterization.

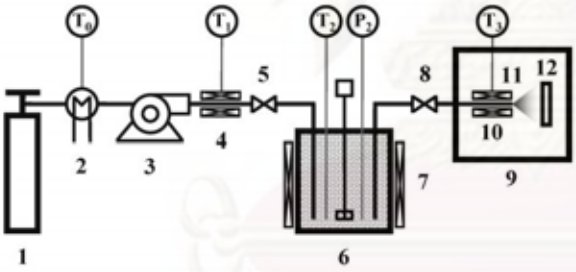

Figure 1. Schematic diagram of the experimental apparatus: 1. CO_2 cylinder; 2. Cooler; 3. HPLC pump; 4. Ribbon heater; 5. Shut-off valve; 6. Stirred high-pressure vessel; 7. Vessel heater; 8. Shut-off valve; 9. Vacuum chamber; 10. Ribbon heater; 11. Nozzle; 12. Target plate, or microgrid.

First, we focused on experimental work for investigating the applicability of the RESS process to generate polymer particles. In general, the information of polymer solubility in SC-CO_2 is crucial for its processing. To the best of our knowledge, there is no report on the solubility of PLGA in SC-CO_2. PLGA polymer used in our study has a limited solubility in SC-CO_2 because of its very high molecular weight [5]. In order to increase the PLGA solubility in SC-CO_2 to a beneficial extent, ethanol was used as cosolvent. 2 g of PLGA with different amounts of ethanol were placed in the high-pressure vessel for preparation of SC-CO_2 solution. After being carefully sealed, the vessel was heated and fed with CO_2 via the high-pressure pump until the desired supercritical conditions were achieved. The mixture in the vessel was stirred by a mixing paddle rotating at 300 rpm, and was left for 3 hours to achieve equilibrium. The prepared supercritical solution was then sprayed through the nozzle to allow its rapid expansion. The target plate was placed against the sprayed flow at a distance of 300 mm from the nozzle tip within a chamber under atmospheric conditions.

Then performance of the RESS process to generate film coating of PLGA on ultrafine powders was investigated using the same apparatus. It should be noted that the ultrafine powder, PLGA and ethanol, in pure form, are not soluble in each others. Thus they form an immiscible ternary mixture under atmospheric conditions. Experimental procedures similar to the first part were carried out so as to dissolve PLGA in SC-CO_2 with the aid of ethanol in the presence of fine SiO_2 or nanosize TiO_2 core particles. Under these conditions, the core particles were not dissolved but suspended in a single homogenous supercritical phase of CO_2, ethanol and the dissolved PLGA. The supercritical suspensions were then allowed to expand through the nozzle for a few seconds. The same sampling method was employed to obtain coated particles for characterization. In order to evaluate the coating performance, effect of three process parameters, i.e. diameter of the spray nozzle, particle size of the core powder and powder-to-polymer weight ratio, on the coating characteristics was investigated. The experimental parameters and conditions used in this work are listed in Table 1.

Table 1. Experimental parameters and conditions of RESS processes

Material	Solvent	CO_2; P_c = 7.4 MPa; T_c = 304 K T_0 = 266 K; T_1 = 353 K
	Cosolvent	ethanol; 0-21.8 wt.%*
	Polymer	Poly(D,L-lactide-co-glycolide), PLGA; 85:15; M_w 50,000–75,000; T_g 318–323K
	Powder	SiO_2; mean particle size 1.4 μm TiO_2; mean diameter 70 nm (for coating experiments)
	feed ratio**	1:1, 3:1 (for coating experiments)
Dissolution	Vessel	Cylinder; 1,500 ml
	Agitation	300 rpm; 180 min
	Conditions	P_2 = 25 MPa; T_2 = 313 K
Expansion	Nozzle	stainless steel; d = 0.1, 0.3 mm; L = 10 mm; T_3 = 423K
	spraying time	3 s
	target distance	300 mm

* polymer-free basis; ** powder-to-polymer weight ratio

.

Field emission scanning electron microscopy (FE-SEM; Hitachi, S-900) was used to examine the particle samples obtained from each experiment. For SEM sample preparation, the aluminium foil uncovered from the target plate was cut into a small piece, mounted on a specimen stub with conductive paint and coated with platinum by a sputtering device (Hitachi, E-1030) for 20 s. The SEM was operated at an accelerating voltage of 10 kV and a magnification between 1000 and 200k. The SEM images were processed for particle size analysis by using image-analyzing software (Image-Pro Plus version 3.0; Media Cybernetics). For verification of polymer coating of the ultrafine powder, the particle samples on the microgrid were further analyzed by a transmission electron microscope (TEM; JEOL 2000-EX) operated at 200 kV in the bright-field mode. To analyze the structures and morphology of the coated powders the mass-thickness contrast between the coating polymer and the core powder was taken into account.

3. RESULTS AND DISCUSION

3.1 Formation of PLGA particles by RESS

It is commonly accepted that ethanol is a suitable cosolvent due to its low toxicity. Although PLGA has limited solubility in either SC-CO_2 or ethanol, it was reported that the PLGA solubility becomes higher in the mixture of these two fluids [6]. Since ethanol is capable of being both donor and acceptor of hydrogen bonds, it can self-associate through hydrogen bonding with both CO_2 and PLGA, which leads to significantly improved PLGA solubility in SC-CO_2. The solubility enhancement of various polymers by ethanol cosolvent has been reported and discussed in several papers [7-10].

First, solution of PLGA in SC-CO_2 plus ethanol was prepared at 25 MPa and 313 K. Jennings et al [11] and Suzuki et al [12] have reported that under these conditions, CO_2 and ethanol become miscible at all compositions and form a single supercritical fluid phase. A different amount of ethanol was added to the pressure vessel at 0, 100, 200, 300 and 400 ml, respectively. Because the amount of PLGA dissolved in the CO_2-ethanol mixtures was very small, compared to those of CO_2 and ethanol, the ethanol concentration in the mixtures could be estimated from the Patel-Teja cubic equation of state extended to binary mixtures [14], regardless of PLGA presence in the mixtures. The CO_2-ethanol interaction parameters used in the calculation were obtained from data available in other literatures [14-15]. According to the varied amount of ethanol mentioned above, the calculated values of polymer-free concentration of ethanol are 0, 5.7, 11.1, 16.4 and 21.8 wt. %, respectively.

In experiments using pure CO_2 and CO_2 with 5.7 wt. % ethanol, negligible amounts of polymer particles were detected in the collected samples under SEM observations, thereby indicating negligible particle formation during the RESS process. This implied that both the pure CO_2 and the CO_2 mixed with ethanol at 5.7 wt. % were unable to dissolve PLGA to a sufficient extent; as a result supersaturation was not achieved to trigger particle nucleation in these cases. On

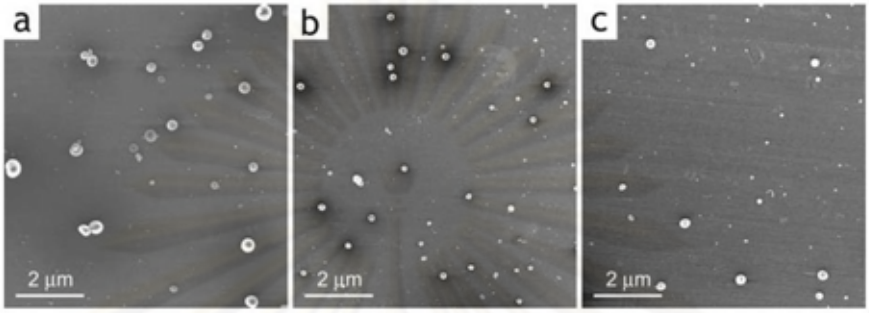

Figure 2. SEM images of PLGA particles produced by RESS using ethanol cosolvent at different ethanol concentrations: (a) 11.1 wt. %; (b) 16.4 wt. %; (c) 21.8 wt. %.

the other hand, Fig. 2 shows typical SEM images of PLGA particles produced by RESS using CO_2 mixed with ethanol at 11.1, 16.4 and 21.8 wt. %. The charged amount of PLGA in SC-CO_2 with 21.8 wt. % ethanol was approximately 0.17 wt. % of the total amount of supercritical solution. Also it is clearly observable that the generated particles exhibit a nearly spherical shape with submicron size distributed in a narrow range.

Based on the experimental results, the formation of PLGA particles via RESS could be described as following. Under the equilibrium condition of SC-CO_2, PLGA, CO_2 and ethanol would form a single homogeneous supercritical solution though saturation of PLGA was not yet achieved. During the rapid expansion, phase transition of CO_2 taking place in the post-expansion free jet would result in a drastic increase in PLGA concentration in the droplets, leading to precipitation of the dissolved polymer. As mentioned previously, since ethanol could not single-handedly dissolve PLGA, it also vaporized out after the expansion [16]. Therefore it is reasonable to consider that the precipitated polymer particles were solvent-free and did not undergo an agglomeration process because of its dilute solid content. These results suggested that the generated polymer particles could be used to coat some core particles.

Analyses of typical SEM images of particle samples obtained from the experiments were carried out to determine their size distribution and morphology. At least 300 particles dispersed in different regions of the SEM images were taken into account in the determination of their size distribution. It was experimentally found that the particle size distribution of the prepared PLGA particles were strongly dependent on the ethanol concentration. As the ethanol concentration increased from 11.1 to 21.8 wt. %, the particle geometric mean decreased to a minimum of 55 nm while the geometric standard deviation increased to a maximum of 1.67. An increase in the ethanol concentration in the SC-CO_2 mixture resulted in an increase in the PLGA solubility, leading to higher supersaturation of PLGA in the sprayed mixture after its rapid expansion. Based on the classical nucleation theory [17-18], higher nucleation rate and smaller critical nucleus size could be expected if the dissolved polymer concentration becomes increased. Meanwhile, a higher supersaturation ratio would also result in the nucleation of random size particles at its early stage [19]. It is also noteworthy that an increase in the particle number concentration could provide higher coagulation frequency. Therefore these opposing phenomena were responsible for a smaller mean size but wider distribution of the PLGA particles when a higher concentration of ethanol was used.

3.2 Coating of core particles with PLGA by rapid expansion of supercritical suspensions

A series of experiments was carried out on coating 1.4-µm silica particles and 70-nm titanium dioxide particles with PLGA by rapid expansion of supercritical suspensions to investigate the effect of experimental parameters on coating performance. In all experiments, the supercritical suspensions were prepared using the conditions at which the solubility of PLGA in the mixture of SC-CO_2 and ethanol could be determined, i.e. the supercritical pressure and temperature of 25 MPa and 313 K, the ethanol concentration of 21.8 wt. % and the polymer solubility of 0.17 wt. %. The powder-to-polymer weight ratio was varied through an adjustment of the powder concentration in the suspension by changing the amount of powder added to the high-pressure vessel at the beginning of each experiment.

Fig. 3 shows two typical samples of PLGA-coated silica fine powder produced by the rapid expansion of supercritical suspension process with powder-to-polymer weight ratio of 3:1. It appears that the coating of silica fine powder was achieved in the form of both individual dispersed particles and agglomerates. The coated silica particles exhibit a core-shell structure, as shown in the bright-field TEM image (Fig. 3(b)). Due to the stronger interactions between the electrons and silicon than that between the electrons and carbon (a major component of the polymer) in the TEM, the silica particles appear as a darker contrast area than the PLGA phase in these images. It is clearly seen that the darker

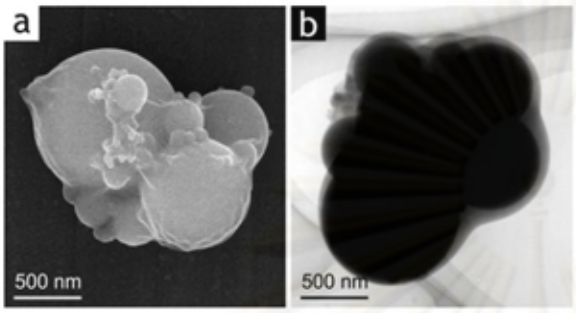

Figure 3 SEM and TEM images of PLGA-coated silica fine powder produced by the rapid expansion of supercritical suspension process at powder-to-polymer weight ratios of 3:1.

contrast area is thoroughly covered by the lighter contrast area, indicating that the silica particles were completely coated with a layer of PLGA. The rapid expansion of a suspension of SC-CO_2-insoluble particles in the supercritical CO_2 solution of a polymer led to deposition of the polymer on the surface of the suspended particles, thereby generating polymer film coating on the particle surfaces [6, 20]. Our experimental results are consistent with this explanation. As a concurrent result of the rapid expansion of supercritical suspension, the dispersion and deagglomeration of the silica fine powder contributed to the low agglomeration tendency of the coated particles. It was observed that the agglomeration process could take place when the powder-to-polymer weight ratio was 3:1 (Fig. 3(a) and Fig. 3(b)). This is mainly attributable to the high number concentration of silica particles in the rapid expansion flow, resulting in frequent collisions and high coagulation probability of the silica particles within the nozzle, and consequently high degree of agglomeration of the particles. In addition, it can be observed in the TEM images that the thickness of the coating layer was not uniform and estimated to be around 10-100 nm from the scale bar. It is likely that the PLGA particles, which precipitated and then deposited on the silica particle surface, spread and formed solid bridges between them, thereby resulting in growth of the coating layer. However, the strong turbulence in the rapid expansion flow dissipated a lot of the eddy energy [21] which can be accounted for significant disturbances to the just-formed coating layer, and hence resulting in non-uniform coating layer.

Similar results were obtained for the coating of 70-nm titanium dioxide ultrafine powder with PLGA, as shown in Fig. 4. The experimental results suggest that the coating of titanium dioxide ultrafine powder with PLGA could also be achieved in the same process as that of silica fine powder. However, SEM and TEM images reveal that the coating of titanium dioxide ultrafine powder always took place in the form of agglomerates of primary particles. In Fig. 4, the coated particles are composed of an agglomerate of titanium dioxide particles in the core and a coat of PLGA which are shown by the darker and the lighter contrast areas, respectively. It should be noted that no PLGA is observed in the void among the titanium dioxide particles, suggesting that the PLGA coat was formed as a growing layer on the titanium dioxide agglomerate surface, not a coalescence of coated primary particles. The agglomerate sizes are in the range of some hundred nanometers to a few microns. Obviously, the flow turbulence and friction loss generated during the rapid expansion of supercritical suspension process was not sufficient to disintegrate agglomerates into primary particles. This is attributable to the extremely strong adhesion forces among the nanosize titanium dioxide particles. The nonuniformity of the coat can also be observed in the TEM images, indicating the deposition of relatively large PLGA particles on the irregular surfaces of the titanium dioxide agglomerates. The thickness is estimated from the scale bar to be around 10-100 nm, which is comparable to that of the fine silica particles.

4. CONCLUSION

The rapid expansion of supercritical solution process with ethanol as a cosolvent can provide non-agglomerated submicron particles of PLGA, which could favorably be used for coating ultrafine particles. It was found that the cosolvent could provide significant effect on the PLGA particle size and size distribution. According to competitive influences of phase transition, turbulent flow, boundary friction and particle coagulation along the expansion path, the rapid expansion of supercritical suspension process exhibited two major phenomena, polymer precipitation and deagglomeration of ultrafine powders. These phenomena further resulted in a layer growth of polymer on the surface of deagglomerated ultrafine powders. Coating of the silica fine powder could be achieved in the form of both agglomerates and dispersed particles, depending on the powder-to-polymer weight ratio, whereas coating in the agglomerate form

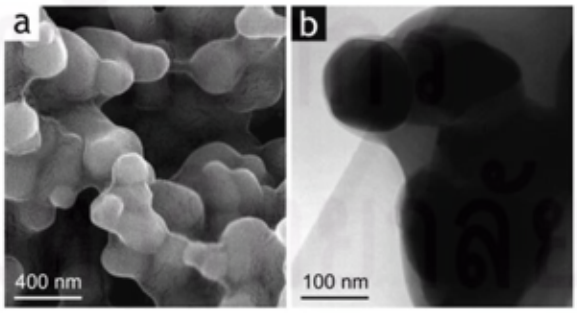

Figure 4. SEM and TEM images of PLGA-coated titanium dioxide ultrafine powder produced by the rapid expansion of supercritical suspension process at powder-to-polymer weight ratios of 3:1.

was inevitable for the titanium dioxide ultrafine powder. In addition, nonuniformity of the coating layer was also observed. It should be remarked that, in pharmaceutical applications, the RESS process with a cosolvent could be a promising environmental-friendly technique for coating ultrafine powder with a high molecular-weight polymer with limited solubility.

REFERENCES

[1] D. Geldart, "Types of Gas Fluidization,", Powder Technol., 7, pp.285-292, 1973.
[2] K. Fu, K. Griebenow, L. Hsieh, A. M. Klibanov and R. Langer, "FTIR Characterization of the Secondary Structure of Proteins Encapsulated within PLGA Microspheres," J. Cont. Rel., 58, pp.357-366, 1999.
[3] J. Wang, K. M. Chua and C. Wang, "Stabilization and Encapsulation of Human Immunoglobulin G into Biodegradable Microspheres," J. Col. Int. Sci., 271, pp.92-101, 2003.
[4] J. Jung and M. Perrut, "Particle Design Using Supercritical Fluids: Literature and Patent Survey," J. Sup. Fluids, 20, pp.179-219, 2001.
[5] J. W. Tom and P. G. Debenedetti, "Precipitation of Poly(L-lactic acid) and Composite Poly(L-lactic acid)-Pyrene Particles by Rapid Expansion of Supercritical Solutions," J. Sup. Fluids, 7, pp.9-29, 1994.
[6] K. Mishima, D. Tanabe and S. Yamauchi, "Microencapsulation of Proteins by Rapid Expansion of Supercritical Solution with a Nonsolvent," AIChE J., 46, pp.857-865, 2000.
[7] M. Zhong, B. Han and H. Yan, "Solubility of Stearic Acid in Supercritical CO_2 with Cosolvents," J. Sup. Fluids, 10, pp.113-118, 1997.
[8] B. Guan, Z. Liu, B. Han and H. Yan, "Solubility of Behenic Acid in Supercritical Carbon Dioxide with Ethanol," J. Sup. Fluids, 14, pp.213-218, 1999.
[9] Q. Li, Z. Zhang, C. Zhong, Y. Liu and Q. Zhou, "Solubility of Solid Solutes in Supercritical Carbon Dioxide with and without Cosolvents," Fluid Phase Eq., 207, pp.183-192, 2003.
[10] A. Chafer, T. Fornari, A. Berna and R.P. Stateva, "Solubility of Quercetin in Supercritical CO_2 + Ethanol as a Modifier: Measurements and Thermodynamic Modeling," J. Sup. Fluids, 32, pp.89-96, 2004.
[11] D. W. Jennings, R. J. Lee and A. S. Teja, "Vapor-Liquid Equilibria in the Carbon Dioxide + Ethanol and Carbon Dioxide + 1-Butanol Systems," J. Chem. Eng. Data, 36, pp.303-307, 1991.
[12] T. Susuki, N. Tsuge and K. Nakahama, "Solubilities of Ethanol, 1-Propanol, 2-Propanol and 1-Butanol in Supercritical Carbon Dioxide at 313 K and 333 K," Fluid Phase Eq., 67, pp.213-226, 1991.
[13] C. Y. Day, C. J. Chang and C. Y. Chen, "Phase Equilibrium of Ethanol + CO_2 and Acetone + CO_2 at Elevated Pressures," J. Chem. Eng. Data, 41, pp.839-843, 1996.
[14] N. C. Patel and A. S. Teja, "A New Cubic Equation of State for Fluids and Fluid Mixtures," Chem. Eng. Sci., 37, pp.463-473, 1982.
[15] H. P. Gros, S. B. Bottini and E. A. Brignole, "High Pressure Phase Equilibrium Modeling of Mixtures Containing Associating Compounds and Gases," Fluid Phase Eq., 139, pp.75-87, 1997.
[16] D. J. Dixon, K. P. Johnston and R. A. Bodmeier, "Polymeric Materials Formed by Precipitation with a Compressed Fluid Antisolvent," AIChE J., 39, pp.127-139, 1993.
[17] R. S. Mohamed, D. S. Halverson, P. G. Debenedetti and R. K. Prud'homme, "Solids Formation after the Expansion of Supercritical Mixtures," ACS Symposium Series, 406, pp.355-378, 1989.
[18] P. G. Debenedetti, "Metastable Liquids: Concepts and Principles," Princeton University Press, 1996.
[19] M. Giulietti, M. M. Seckler, S. Derenzo, M. I. Re' and E. Cekinski, "Industrial Crystallization and Precipitation from Solutions: State of the Technique," Braz. J. Chem. Eng., 18, pp.423-440, 2001.
[20] A. Tsutsumi, M. Ikeda, W. Chen and J. Iwatsuki, "A Nano-Coating Process by the Rapid Expansion of Supercritical Suspensions in Impinging-Stream Reactors," Powder Technol., 138, pp.211-215, 2003.
[21] X. Y. Sun, T. J. Wang, Z. W. Wang and Y. Jin, "The Characteristics of Coherent Structures in the Rapid Expansion Flow of the Supercritical Carbon Dioxide," J. Sup. Fluids, 24, pp.231-237, 2002.

APPENDIX B

Publications Co-Authored by B. Kongsombut

1. Kamraka, J.; **Kongsombut, B.**; Grehan, G.; Saengkaew, S.; Kim, K. S.; and Charinpanitkul, T. Mechanistic study on spraying of blended biodiesel using phase doppler anemometry. Biomass and Bioenergy. 33 (2009) : 1452 – 1457.

BIOMASS AND BIOENERGY 33 (2009) 1452–1457

Available at www.sciencedirect.com

ScienceDirect

http://www.elsevier.com/locate/biombioe

BIOMASS & BIOENERGY

Mechanistic study on spraying of blended biodiesel using phase Doppler anemometry

Juthamas Kamrak[a], *Benjapol Kongsombut*[a], *Gerard Grehan*[b], *Sawitree Saengkaew*[b], *Kyo-Seon Kim*[c], *Tawatchai Charinpanitkul*[a,*]

[a]*Center of Excellence in Particle Technology, Department of Chemical Engineering, Faculty of Engineering, Chulalongkorn University, Payathai Road, Patumwan, Bangkok 10330, Thailand*

[b]*LESP/UMR CNRS6614/INSA et Université de Rouen , BP 12, avenue de l'université , 76801, Saint Etienne du Rouvray, France*

[c]*Department of Chemical Engineering, Faculty of Engineering, Kangwon National University, Chuncheon, Korea*

ARTICLE INFO

Article history:
Received 17 December 2008
Received in revised form
24 May 2009
Accepted 13 June 2009
Published online 9 July 2009

Keywords:
Palm oil
Diesel oil
Atomization
Phase Doppler anemometry
Droplet

ABSTRACT

Droplet size and dynamics of blended palm oil-based fatty acid methyl ester (FAME) and diesel oil spray were mechanistically investigated using a phase Doppler anemometry. A two-fluid atomizer was applied for dispersing viscous blends of blended biodiesel oil with designated flow rates. It was experimentally found that the atomizer could generate a spray with large droplets with Sauter mean diameters of ca. 30 μm at low air injection pressure. Such large droplets traveled with a low velocity along their trajectory after emerging from the nozzle tip. The viscosity of blended biodiesel could significantly affect the atomizing process, resulting in the controlled droplet size distribution. Blended biodiesel with a certain fraction of palm oil-based FAME would be consistently atomized owing to its low viscosity. However, the viscosity could exert only a small effect on the droplet velocity profile with the air injection pressure higher than 0.2 MPa.

1. Introduction

Regarding to a continuous increase in petroleum fuel, biodiesel derived from palm, jatropha and rapeseed as well as used cooking oils has become of increasing interest due to their abundance and renewability [1–3]. To obtain insightful understanding of biodiesel combustion, it is necessary to conduct detailed investigation of its atomization process. In general, required information would include the droplet size and velocity distributions along the plane of injection because they are necessary for effective design of a combustion chamber [4–6]. There are some comprehensive reviews of spray atomization for industrial processes which are dictated by physical properties of atomized liquid [7,8]. However, to improve the combustion performance and particulate emissions, many researchers are still further investigating characteristics of liquid fuel spray with experimental and theoretical approaches. Regarding to various different measuring techniques, such as imaging techniques or hybrid light scattering detection systems combined with a laser Doppler velocimeter (LDV), there are several drawbacks of time consuming, limitation of non-simultaneous measurement, and low reliability [9,10]. Meanwhile, because of less dependence on droplet properties and simplicity, phase Doppler anemometry (PDA) has been considered as a promising alternative method for examining the atomizing behaviors of such mixed fuel. Therefore, this work is focusing on employing PDA for characterizing blended biodiesel

* *Corresponding author.* Tel./fax: +66 2 2186480.
E-mail address: ctawat@chula.ac.th (T. Charinpanitkul).

0961-9534/$ – see front matter © 2009 Elsevier Ltd. All rights reserved.
doi:10.1016/j.biombioe.2009.06.011

prepared from palm oil-based fatty acid methyl ester (FAME) and conventional diesel oil. Droplets sprayed by a typical two-fluid nozzle were experimentally examined and discussed.

2. Experimental

Commercially available palm oil (Morakot Industry Co., Thailand), which mainly contained 43% oleic and 11% linoleic fractions, was employed as a model source for preparing fatty acid methyl ester (FAME) using transesterification method as reported in some previous references [11,12]. Blends of FAME derived from palm oil and petroleum diesel oil with different compositions were prepared using an ultrasonicated homogenizing vessel. The blending compositions, which were remarked as PX:DY whereas P refers to the palm oil-based FAME, D to petroleum diesel, X and Y to per cent by volume of the FAME and diesel oil, respectively, were 0:100, 5:95, 10:90, 20:80, 30:70, 50:50 and 100:0 v/v%. Dynamic viscosities of fuels were measured by a rotating viscometer (RVDV-II, Brookfield). A refractometer (2WAJ, Abbe) was used to measure refractive index of each biodiesel blend. Surface tension was measured by tensiometer (TVT 2-M, Lauda). The physical properties of all blends characterized at 25 °C are summarized in Table 1.

Fig. 1 depicts a schematic diagram of the atomizing set-up consisting of a two-fluid atomizing nozzle (N-23, Pawin Engineering) and a commercial phase Doppler anemometer (PDA) equipped with an argon ion laser (2000 mW at a wavelength of 488 nm) (PDA-15A, Dantec). The blended biodiesel was supplied through the atomizing nozzle under the designated injection pressure controlled by a pneumatic pump. The compressed air was injected through an air inlet port to induce the liquid stream to form a jet of atomized droplets at room temperature.

3. Results and discussion

3.1. Droplet formation and its characteristics

Some previous authors reported that dilution of palm oil with diesel oil would result in only slight difference in atomized spray [1,2]. Meanwhile, other analytical reports also revealed that balancing of blending ratio would affect the blended viscosity and surface tension, leading to different atomizing appearance [5]. In this work, despite of the different blending ratio of palm oil-based FAME to diesel oil, it was difficult to distinguish the difference of spray appearance by visualization. For 100% derived FAME, the spray could be generated only with a sufficiently high air inducing pressure. This is attributed to the lower flow rate hindered by its high viscosity. The higher viscosity and lower volatility of palm oil-based FAME would result in some ignition problems when it is utilized as fuel in diesel engine [3]. Therefore, it is necessary to collect quantitative data for better understanding on its atomization process.

Table 1 – Physical properties of blended biodiesel.

Fuels	Kinematic viscosity $\times 10^{-6}$ ($m^2 s^{-1}$)	Surface tension ($kg s^{-2}$)	Refractive index
Diesel Oil	3.23 ± 0.02	28.00 ± 0.01	1.466
P5:D95	3.49 ± 0.01	28.02 ± 0.05	1.467
P10:D90	4.14 ± 0.07	28.50 ± 0.02	1.467
P20:D80	4.57 ± 0.01	28.05 ± 0.10	1.467
P30:D70	5.26 ± 0.01	28.78 ± 0.15	1.467
P50:D50	8.06 ± 0.01	29.90 ± 0.20	1.468
100% FAME	17.72 ± 0.09	33.23 ± 0.15	1.469

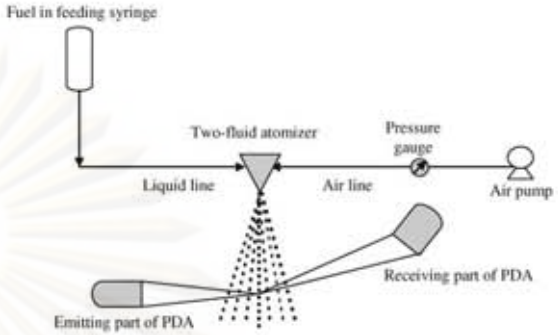

Fig. 1 – Synoptic diagram of spray atomization and measuring system.

Some previous authors have reported that blended mixture of palm oil-based FAME and diesel oil with an optimal ratio of 20:80 or 30:70 could result in a stable spray [4,13]. Based on our data in Table 1, the viscosity and surface tension of blended mixtures of palm oil-based FAME and diesel oil become sharply increased when the volume fraction of palm oil is higher than 20 volume per cent. It was also found that the blended biodiesel oil at a volume ratio of 20:80 could be fed through the two-fluid nozzle after applying the minimal atomizing pressure of 0.05 MPa. Typical snap-shot images of biodiesel spray generated by an external-mixed two-fluid atomizer with different atomizing pressures are depicted in Fig. 2 revealing a perfect full cone of spray with a diverse end at which liquid droplets eventually vaporized into gas vapor. With a further increase in the atomizing pressure from 0.1, 0.2 and 0.3 MPa, liquid droplets leave the nozzle tip more rigorously as could be visually distinguished in Fig. 2(a)–(c), respectively. With the higher injection pressure, the spray angle measured from the visualized images became broader. This is attributed to the higher shear rate due to the turbulent flow of inducing air stream [8,14].

For comparison with experimental results, theoretical analysis of air stream flowing through the two-fluid nozzle for inducing a radial inflow of liquid droplets was conducted. To determine the time-smoothed velocity distribution in the liquid mass flow rate crossing the expanding plane, the following equations of continuity and motion for steady incompressible flow with boundary layer approximation are employed

$$\frac{1}{r}\frac{\partial \overline{u}_r}{\partial r} + \frac{\partial \overline{u}_z}{\partial z} = 0 \quad (1)$$

$$\overline{u}_r \frac{\partial \overline{u}_z}{\partial r} + \overline{u}_z \frac{\partial \overline{u}_z}{\partial z} = \upsilon^{(l)} \frac{1}{r}\frac{\partial}{\partial r}\left(r\frac{\partial \overline{u}_z}{\partial r}\right) \quad (2)$$

with the boundary conditions of

$$r = 0 \rightarrow \overline{u}_r = 0 \quad (3)$$

$$r = 0 \rightarrow \frac{\partial \overline{u}_z}{\partial r} = 0 \quad (4)$$

$$r = \infty \rightarrow \overline{u}_z = 0 \quad (5)$$

$$r = \infty \rightarrow \overline{u}_z = 0 \quad (6)$$

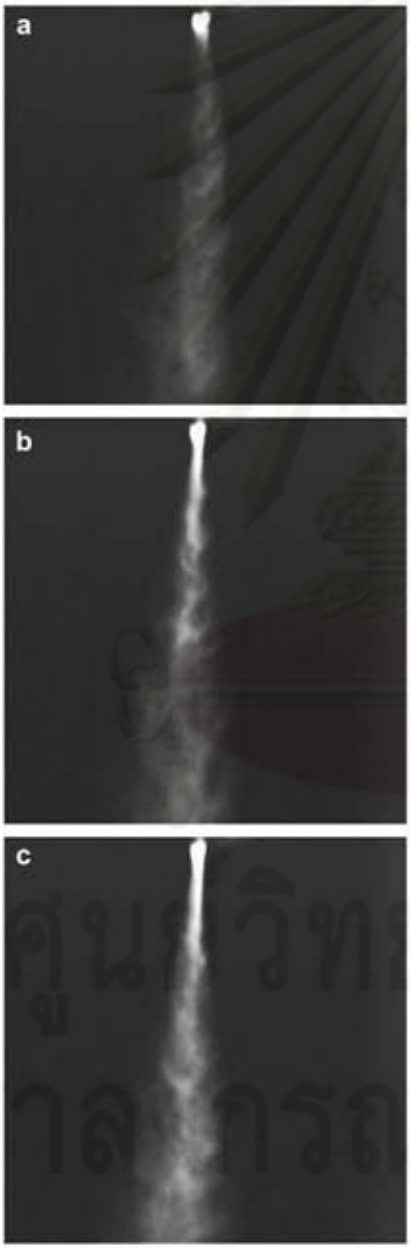

Fig. 2 – Appearance of spray of P20:D80 at different atomizing pressure (a) 0.2, (b) 0.3 and (c) 0.4 MPa.

where $\overline{u}_r$, $\overline{u}_z$, and $\nu^{(t)}$ are radial, axial velocity and turbulent kinematic viscosity, respectively. As seen from Fig. 2, the plume of the spray had comparatively narrow radial distribution therefore only the axial velocity is accounted here for simplification. Based on the Boundary Layer concept, the axial velocity profile $[\overline{u}_z(r,z)]$ can be expressed as:

$$\overline{u}_z = \frac{\frac{3}{8\pi}\frac{J}{\rho\nu^{(t)}z}}{\left[1+\left(\frac{3}{64\pi}\frac{J}{\rho\left(\nu^{(t)}\right)^2}\left(\frac{r}{z}\right)^2\right)\right]^2} \quad (7)$$

where J is the rate of axial momentum flow ($J = 2\pi\rho b^2\overline{u}_{z,max}^2$), ρ and b are the fluid density and the spray radius, respectively [15]. Without the external disturbance, emerging liquid droplets would be entrained by the air flow, leading to a velocity distribution, which would be parabolic function of radial and axial distances.

In general, droplet size distribution is also a crucial parameter for control of blended biodiesel combustion [9,16]. In this work, the PDA was employed for collecting information of droplet size and velocity at each local position within an atomized spray with a statistical sample size of more than 4000 droplets. Fig. 3 reveals that the atomized blended biodiesel oil droplets typically exhibit normal size distribution behavior. With an increase in atomizing air pressure, fraction of droplet smaller than 10 μm would become higher because of the higher shear rate induced by the air flow. Park et al. also reported that compressed air flow could contribute to stretching and thinning of diesel oil droplets, resulting in a decrease in atomized droplet size [7]. For quantitative analysis, Sauter mean diameter (SMD) determined by $SMD = \sum N_i D_i^3 / \sum N_i D_i^2$ was examined with respect to spraying conditions.

The SMD of atomized droplets produced by the two-fluid atomizer is not only injection pressure dependent, but is also affected by density, viscosity and surface tension [7,17,18]. Fig. 4(a) illustrates the SMD distributions of P20:D80 spray along the spray radial distance at the axial position of 50 and 70 mm away from atomizer tip. The larger SMD was found at the central area of the spray and also the long traveling distance could result in the larger SMD. As could also be observed from visualization method, the concentration of droplets in the central area of spray was significantly higher.

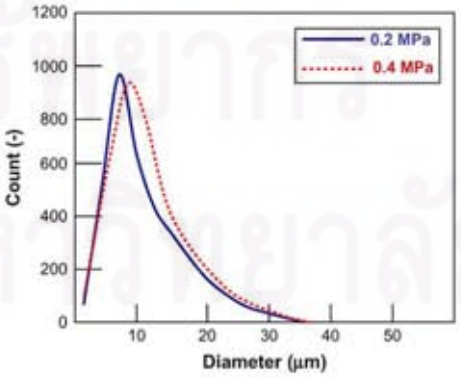

Fig. 3 – Typical droplet size distribution measured by PDA at two atomizing pressure.

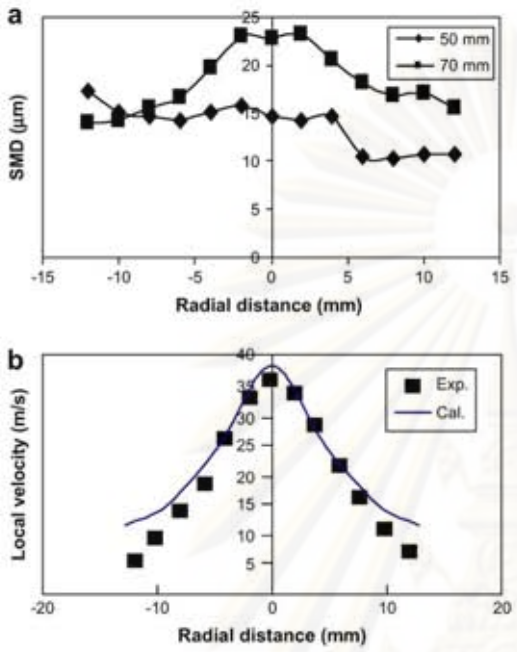

Fig. 4 – Distribution of (a) SMD and (b) local average velocity of atomized droplets within spray of P20:D80 at P_{at} = 0.4 MPa.

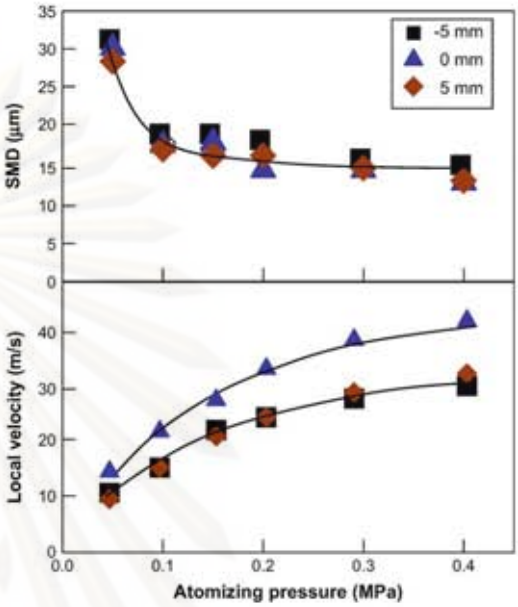

Fig. 5 – Dependence of droplet characteristics on air injection pressure for P20:D80 spray at 50 mm from nozzle tip.

The higher population of droplets at the central area would be accountable for higher opportunity of droplet collisions, resulting in the enhanced droplet coalescence [7,8,16]. With a longer traveling distance, the more diluted spray with a smaller SMD was found because the evaporation of droplets and the air entrainment induces some droplets out of the spray. In addition, the spray angle was slightly broader with increasing air injection pressure.

Meanwhile, local velocity of atomized droplets, which were induced by the air pressure of 0.4 MPa, were measured at the axial position of 70 mm away from the nozzle tip and then plotted against the spray radial distance as shown in Fig. 4(b). It could be clearly seen that the local velocity distribution was almost a parabolic function of the radial distance. The highest local velocity could be found at the center region of spray. The droplet local velocity distribution reveals its flow behavior which was controlled by the convective jet flow as described by Eq. (7) [13–16]. The analytical result also revealed that there would be energy loss during the actual atomization, leading to a lower value of measured velocity compared with that of the calculated value. The major portion of the energy loss would be due to the drag force along the traveling path of the droplets [8,15].

3.2. *Effect of atomizing air pressure*

Fig. 5 illustrates plots of SMD and local velocity of P20:D80 blended biodiesel against the atomizing air pressure at several radial distances. At a low atomizing air pressure, the increase in the atomizing pressure could lead to a decrease in the SMD of the atomized droplet. In particular, within the range of lower atomizing pressure (0.05–0.1 MPa) the generation of large droplets would be dominated, resulting in higher SMD which would occupy lower stability. A further increase in the atomizing air pressure of up to 0.4 MPa could lead to a slight decrease in the SMD. This is attributable to the fact that the balance between the shear force due to the convective air flow and the resistance due to the blended fuel viscosity would regulate the size of droplets [2,4,5]. Because of the symmetric distribution of the spray, there is no distinguishable difference in the SMD of the blended mixture. Within the uncertainty range of our measurement, the SMD of droplets at the center line or at the radial distance of 5 mm away form the center line was almost equal.

Similarly, the effect of the atomizing pressure on the local mean velocity of droplets was also examined at 3 radial distances. The local mean velocity was gradually increased with the increase in the atomizing pressure. However, the symmetric flow of cloud of droplets, which could also be confirmed as shown in Fig. 4(b), would exhibit a distribution profile along the radial distance due to momentum transfer within the convective air flow [15]. This result would suggest that droplets traveling along the center line of the atomizing nozzle would travel faster than other surrounding droplets. In order to avoid significant change in the combustion completion, suitable design review of combustion chamber would be taken into account [18].

3.3. *Effect of blending ratio*

Fig. 6(a) depicts the effect of blending ratio on the SMD of atomized droplets as a function of the radial distance. It could

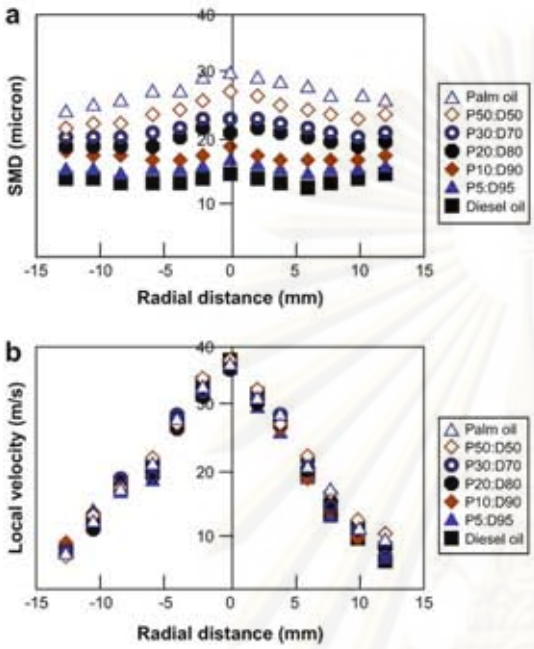

Fig. 6 – Distribution of (a) SMD and (b) local average velocity of droplets at an axial distance of 5 cm from atomizer tip (P_{at} = 0.4 MPa).

be clearly observed that when the pure diesel oil with the lowest viscosity was employed droplets with rather uniform size could be atomized with the two-fluid nozzle. However, the gradual increase in the FAME fraction would result in the value of SMD and its distribution along the radial distance. A step change of the viscosity of P50:D50 and 100% palm oil-based FAME resulted in the significantly larger SMD and broader distribution. Ali and Hanna also reported that biodiesel derived from other vegetable oils with higher viscosity could result in poorer atomization and insufficient mixing with air [1]. In this work, when 100% palm oil-based FAME was employed, more rigorous droplet coalescence could be more enhanced, resulting in a higher amount of non-vaporized liquid residue in the center of the spray. At the atomizing pressure of 0.05 MPa, liquid jets of 100% palm oil-based FAME was randomly ejected from the nozzle. These results suggested that the blending ratio of palm oil-based FAME to diesel oil which would provide uniform droplet size would be lower than 20:80. This suggestion is also in good agreement with the previous report of Lee et al. [13].

Within the uncertainty of our measurement, there was no significant tendency on the local mean velocity of atomized droplets regardless of the blending ratio. Fig. 6(b) illustrates the local mean velocity of the blended biodiesel which is also in acceptable agreement with the result of theoretical calculation using Eq. (7). With the atomizing pressure of 0.4 MPa, droplets traveling along the central region of the spray could travel 4 times faster than others in the edge of spray. This high velocity gradient is reasonably attributed to the particular characteristic of the two-fluid nozzle which provides a high air flow in its core region [7,13].

4. Conclusions

The mechanistic study of the characteristic drop size and velocity profile of blended biodiesel spray was conducted using phase Doppler Anemometry. At low air injection pressure (0.05–0.1 MPa) large droplets were generated with regards to SMD. The velocity of droplets was significantly higher when atomizing air flow rate increased. Also, the larger droplets and lower velocity were found at a longer downstream distance. The fuel properties, especially the viscosity, would significantly affect the size distribution of sprayed droplets but insignificantly affect the droplet velocity profile when compared with the effect of the air injection pressure.

Acknowledgments

The authors gratefully acknowledge financial support from the Centennial Fund of CU. Franco-Thai collaborative research project was also gratefully acknowledged. TC and K.S.K also acknowledge support from the Ministry of Education and Human Resources Development (MOE) and the Ministry of Education, Science and Technology (MEST) and the Ministry of Knowledge Economy (MKE), respectively.

REFERENCES

[1] Ali Y, Hanna MA. Alternative diesel fuels from vegetable oils. Bioresour Technol 1994;50:153–63.
[2] Goodrum JW, Eiteman MA. Physical properties of low molecular weight triglycerides for the development of biodiesel fuel models. Bioresour Technol 1996;56:55–60.
[3] Canakci M. The potential of restaurant waste lipids as biodiesel feedstocks. Bioresour Technol 2007;98:183–90.
[4] Geller DP, Goodrum JW, Siesel EA. Atmoization of short-chain triglycerides and a low molecular weight vegetable oil analogue in DI diesel engine. Am Soc Agric Engrs 2003;46(4):955–8.
[5] Ejim CE, Fleck BA, Amirfazli A. Analytical study for atomization of biodiesels and their blends in a typical injector: surface tension and viscosity effects. Fuel 2007;86:1534–44.
[6] Barata J. Modelling of biofuel droplets dispersion and evaporation. Renew Energy 2008;33:769–79.
[7] Park SW, Kim S, Lee CS. Breakup and atomization characteristics of mono-dispersed diesel droplets in a cross-flow air stream. Int J Multiphase Flow 2006;32:807–22.
[8] Hede PD, Bach P, Jensen AD. Two-fluid spray atmomization and pneumatic nozzles for fluid bed coating/agglomeration purposes. Chem Eng Sci 2008;63:3821–42.
[9] Dodge LG, Rhodes DJ, Reitz RD. Drop-size measurement techniques for sprays: comparison of Malvern laser-diffraction and aerometrics phase/Doppler. Appl Opt 1987; 26(1):2144–54.
[10] Saengkaew S, Charinpanitkul T, Vanisri H, Tanthapanichakoon W, Mees L, Gouesbet G, et al. Rainbow refractrometry: on the validity domain of Airy's and Nussenzveig's theories. Opt Coms 2006;259:7–14.

[11] Chongkhong S, Tongurai C, Chetpattananondh P, Bunyakan C. Biodiesel production by esterification of palm fatty acid distillate. Biomass Bioenergy 2007;31:563–8.
[12] Bautista LF, Vicente G, Rodrigues R, Pacheco M. Optimisation of FAME production from waste cooking oil for biodiesel use. Biomass Bioenergy 2009;33:862–72.
[13] Lee CS, Park SW, Kwon SI. An experimental study on the atomization and combustion characteristics of biodiesel-blended fuels. Energy Fuels 2005;19:2201–8.
[14] Liu Z, Reitz RD. An analysis of the dispersion and breakup mechanisms of high speed liquid drops. Int J Multiphase Flow 1997;23:631–50.
[15] Bird RB, Stewart WE, Lightfoot EN. Transport phenomena. 2nd ed. New York: John Wiley & Sons; 2000.
[16] Gong JS, Fu WB. The experimental study on the flow characteristics for swirling gas-liquid spray atomizer. Appl Thermal Eng 2007;27:2886–92.
[17] Tat ME, Van Gerpen JH. The kinematic viscosity of biodiesel and its blends with diesel fuel. J Am Oil Chem Soc 1999; 76(12):1511–3.
[18] Nascimento MAR, Lora ES, Correa PSP, Andrada RV, Rendon MA, Venturini OJ, et al. Biodiesel fuel in diesel micro-turbine engines: modelling and experimental evaluation. Energy 2008;33:233–40.

VITA

Mr. Benjapol Kongsombut was born in Lopburi, Thailand, on September 7, 1973. He entered Rangsit University, Bangkok, in June, 1997. After earning the degree of Bachelor of Engineering in Chemical Engineering in March, 2001, he gained admission to the Graduate School of Chulalongkorn University in June 2002. He continued to study in Ph.D. program under the Royal Golden Jubilee Scholarship, and he graduated in May 2010.